4. Medical Applications of Lasers

In this chapter, we will discuss principal applications of lasers in modern medicine. Due to the present boom in developing new laser techniques and due to the limitations given by the dimensions of this book, not all disciplines and procedures can be taken into account. The main intention is thus to focus on the most significant applications and to evoke a basic feeling for using certain techniques. The examples are chosen to emphasize substantial ideas and to assist the reader in grasping some technical solutions. Potential difficulties and complications arising from either method are addressed, as well. However, we should always keep in mind that any kind of laser therapy will not be indicated if alternative methods are available which offer a better rate of success, are less dangerous to the patient, and/or easier to perform.

Because of the historic sequence, the first section will be concerned with laser applications in *ophthalmology*. Even today, the majority of medical lasers sold is applied in this field. *Dentistry* was the second clinical discipline to which lasers were introduced. However, although considerable research has been done, the results were not quite as promising in most cases, and the discussion on the usefulness of dental lasers still proceeds. Today, the major effort of clinical laser research is focusing on various kinds of tumor treatments such as photodynamic therapy (PDT) and laser-induced interstitial thermotherapy (LITT). These play a significant role in many other medical disciplines like *gynecology*, *urology*, and *neurosurgery*. Due to recent advancements in instrumentation for minimally invasive surgery (MIS), e.g. the development of miniature catheters and endoscopes, novel techniques are under present investigation in *angioplasty* and *cardiology*. Very interesting laser applications were found in *dermatology* and *orthopedics*. And, recently, successful laser treatments have been reported in *gastroenterology*, *otorhinolaryngology*, and *pulmology* as discussed at the end of this chapter.

Thus, it can be concluded that – at the present time – laser medicine is a rapidly growing field of both research and application. This is not at all astonishing, since neither the development of novel laser systems nor the design of appropriate application units have yet come to stagnation. Moreover, laser medicine is not restricted to one or a few disciplines. Instead, it has meanwhile been introduced to almost all of them, and it is expected that additional clinical applications will be developed in the near future.

4.1 Lasers in Ophthalmology

In ophthalmology, various types of lasers are being applied today for either diagnostic or therapeutic purposes. In diagnostics, lasers are advantageous if conventional incoherent light sources fail. One major diagnostic tool is confocal laser microscopy which allows the detection of early stages of retinal alterations. By this means, retinal detachment and also glaucoma[1] can be recognized in time to increase the probability of successful treatment. In this book, however, our interest focuses on therapeutic laser applications. The first indications for laser treatment were given by detachments of the retina. Meanwhile, this kind of surgery has turned into a well-established tool and only represents a minor part of today's ophthalmic laser procedures. Others are, for instance, treatment of glaucoma and cataract. And, recently, refractive corneal surgery has become a major field of research, too.

The targets of all therapeutic laser treatments of the eye can be classified into front and rear segments. The front segments consist of the *cornea*, *sclera*, *trabeculum*, *iris*, and *lens*. The rear segments are given by the *vitreous body* and *retina*. A schematic illustration of a human eye is shown in Fig. 4.1. In the following paragraphs, we will discuss various treatments of these segments according to the historic sequence, i.e. from the rear to the front.
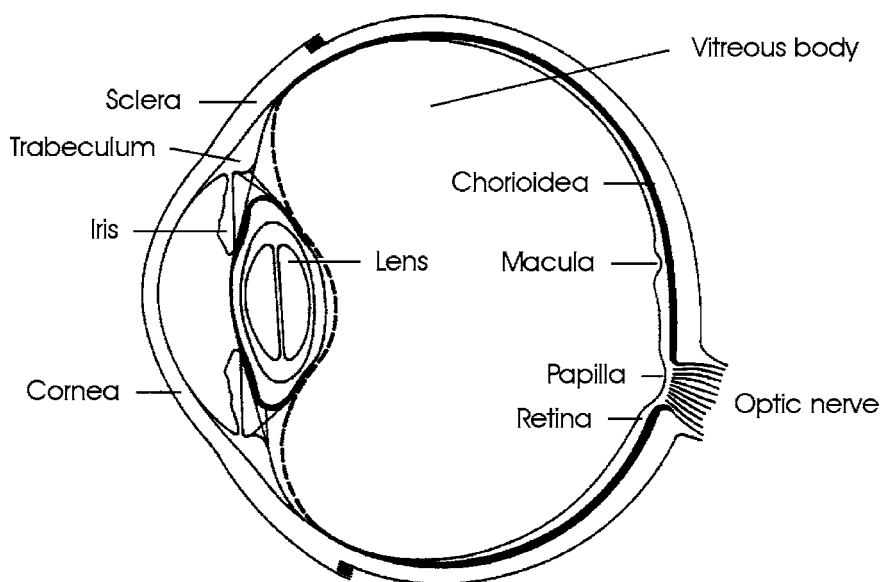
Fig. 4.1. Scheme of a human eye

---

[1] Since glaucoma is usually associated with a degeneration of the optical nerve fibers, it can be detected by measuring either the thickness of these fibers or alterations of the optic disc. Further details are given by Bille et al. (1990).

Retina

The retina is a part of the central nervous system. Its function is to convert an optical image focused on it into nerve impulses of the optic nerve emerging from it. The retina is a thin and rather transparent membrane which is permeated with blood vessels. According to Le Grand and El Hage (1980), the thickness of the retina varies from 0.5 mm near the papilla to 0.1 mm at the macula[2]. Anatomically, the retina is subdivided into several different layers, each of them having their own distinct function: pigment epithelium, receptor layer, external limiting membrane, cell layer, nerve fiber layer, and internal limiting membrane. A schematic cross-section of a human retina is shown in Fig. 4.2.
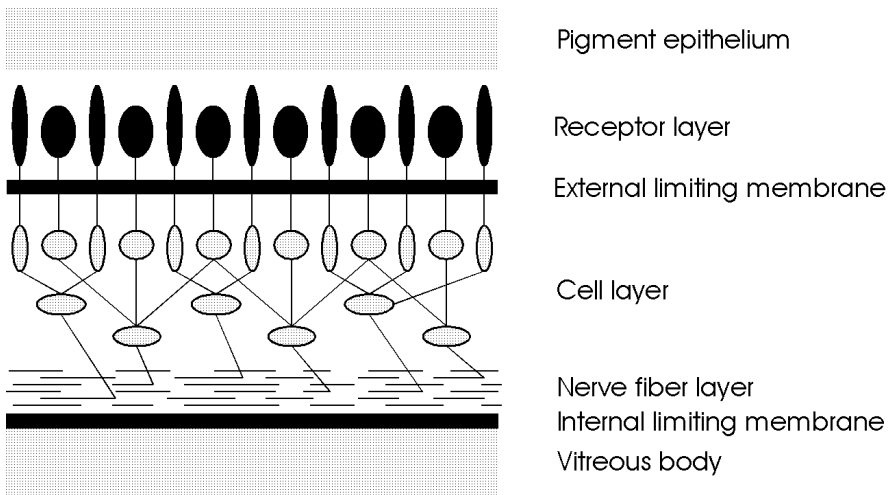
Fig. 4.2. Cross-section of a human retina

The *pigment epithelium* is strongly attached to the chorioidea. The *receptor layer* consists of two types of cells – rods and cones. Rods are used in dim light and are primarily located around the macula. Cones are recepting colors in good light and are found especially in the fovea. Obviously, light has to pass through virtually the whole retina beyond the *external limiting membrane*, before it can stimulate any receptor cells. This structural arrangement is known as the "reversed retina" and can be explained by the fact that the retina is an invagination of the embryonic cerebral wall. The *cell layer* is made up of horizontal cells, bipolar cells, amacrine cells, and ganglion cells.

---

[2] The *papilla* is a certain location where the optic nerve exits the retina. The *macula* is the region with the highest density of color receptors. An image formed on the *fovea*, the central section of the macula, is characterized by best vision. Thus, macula and fovea are the most important segments of the retina.

The main function of these cells is to serve as a first network with corresponding receptive fields. Finally, the *nerve fiber layer* contains the axons of the ganglion cells, whereas the *internal limiting membrane* forms a boundary between the retina and vitreous body.

The ophthalmologist Meyer-Schwickerath (1949) was the first to investigate the coagulation of the retina with sunlight for therapeutic purposes. Because of the inconvenient circumstances of this kind of surgery, e.g. the necessity of sunshine, he continued his studies with his famous xenon photocoagulator as reported in 1956. Shortly after the invention of the laser by Maiman (1960), first experimental studies with the ruby laser were performed by Zaret et al. (1961). The first reports on the treatment of patients were given by Campbell et al. (1963) and Zweng et al. (1964). They discovered that the ruby laser was a very suitable tool when welding detached segments of the retina to the chorioidea located underneath. However, it also became evident that the ruby laser was not able to close open blood vessels or stop bleeding. It was soon found that the argon ion laser is better suited for this aim. Its green and blue wavelengths are strongly absorbed by the hemoglobin of blood – in contrast to the red light from a ruby laser – which finally leads to the coagulation of blood and blood vessels. At typical exposure durations ranging from 0.1 s to a few seconds, applied laser powers of 0.1–1 W, and spot diameters of approximately 200–1000 µm, almost all incident laser energy is converted to heat. Thus, coagulation of retinal tissue is achieved by means of thermal interaction. As discussed in Sect. 3.2, proteins are denatured and enzymes are inactivated, thereby initiating the process of congealment.

The surgeon conducts the laser coagulation through a slit lamp and a contact glass. He approaches the necessary laser power from below threshold until the focused area just turns greyish. Coagulation of the macula is strictly forbidden, since it would be associated with a severe loss in vision. The temperatures achieved should generally remain below 80°C to prevent unnecessary vaporization and carbonization. A good localization of blood vessels, i.e. by confocal laser microscopy, and a precise application of the desired energy dose are mandatory when striving for satisfactory results.

At the beginning of the 1970s, the krypton ion laser became very significant for ophthalmic applications. Its red and yellow wavelengths at 647 nm and 568 nm, respectively, turned out to be very useful when trying to restrict the interaction zone to either the pigment epithelium or the chorioidea. Detailed histologic studies on this phenomenon were conducted by Marshall and Bird (1979). It was found that the red line is preferably absorbed by the chorioidea, whereas the yellow line is strongly absorbed by the pigment epithelium and also by the xanthophyll contained in the macula. Recently, McHugh et al. (1988) proposed the application of diode lasers, since their invisible emission at a wavelength of approximately 800 nm does not dazzle the patient's eye.

There exist six major indications for laser treatment of the retina:

– retinal holes,
– retinal detachment,
– diabetic retinopathy,
– central vein occlusion,
– senile macula degeneration,
– retinal tumors (retinoblastoma).

In the case of *retinal holes*, proper laser treatment prevents their further enlargement which could otherwise lead to retinal detachment. Laser surgery is performed by welding the retina to the underlying chorioidea within a narrow ring-shaped zone around the hole as shown in Fig. 4.3a. The attachment of the coagulated tissue is so strong that further tearing is usually suppressed. If necessary, however, the procedure can be repeated several times without severe complications.

Retinal detachment is often a consequence of undetected retinal holes or tears. It mainly occurs in myopic patients, since the vitreous body then induces an increased tensile stress to the retina. Moderate detachments are treated in a similar mode as retinal holes. In the case of a severe detachment, the treatment aims at saving the fovea or at least a small segment of the macula. This procedure is called panretinal coagulation and is illustrated in Fig. 4.3b. Unfortunately, laser treatment of retinal detachment is often associated with the formation of new membranes in the vitreous body, the retina, or beneath the retina. These complications are summarized by the clinical term *proliferative retinopathy*. A useful therapeutic technique for the dissection of such membranes was given by Machemer and Laqua (1978).
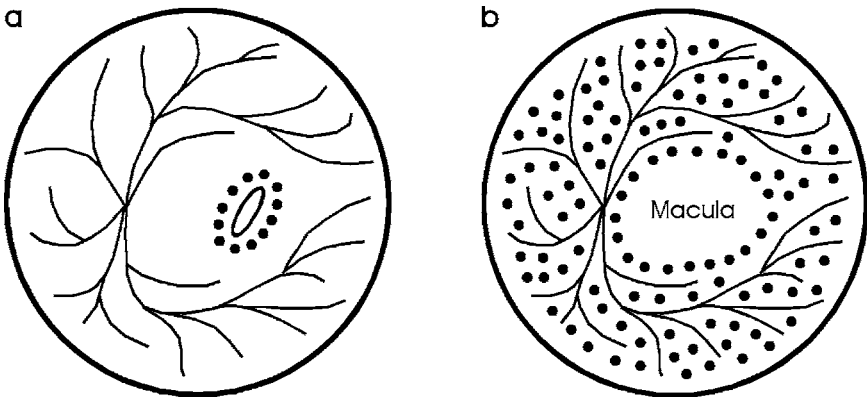
Fig. 4.3. (a) Placement of coagulation spots in the case of retinal holes or moderate detachments. **(b)** Placement of coagulation spots during panretinal coagulation
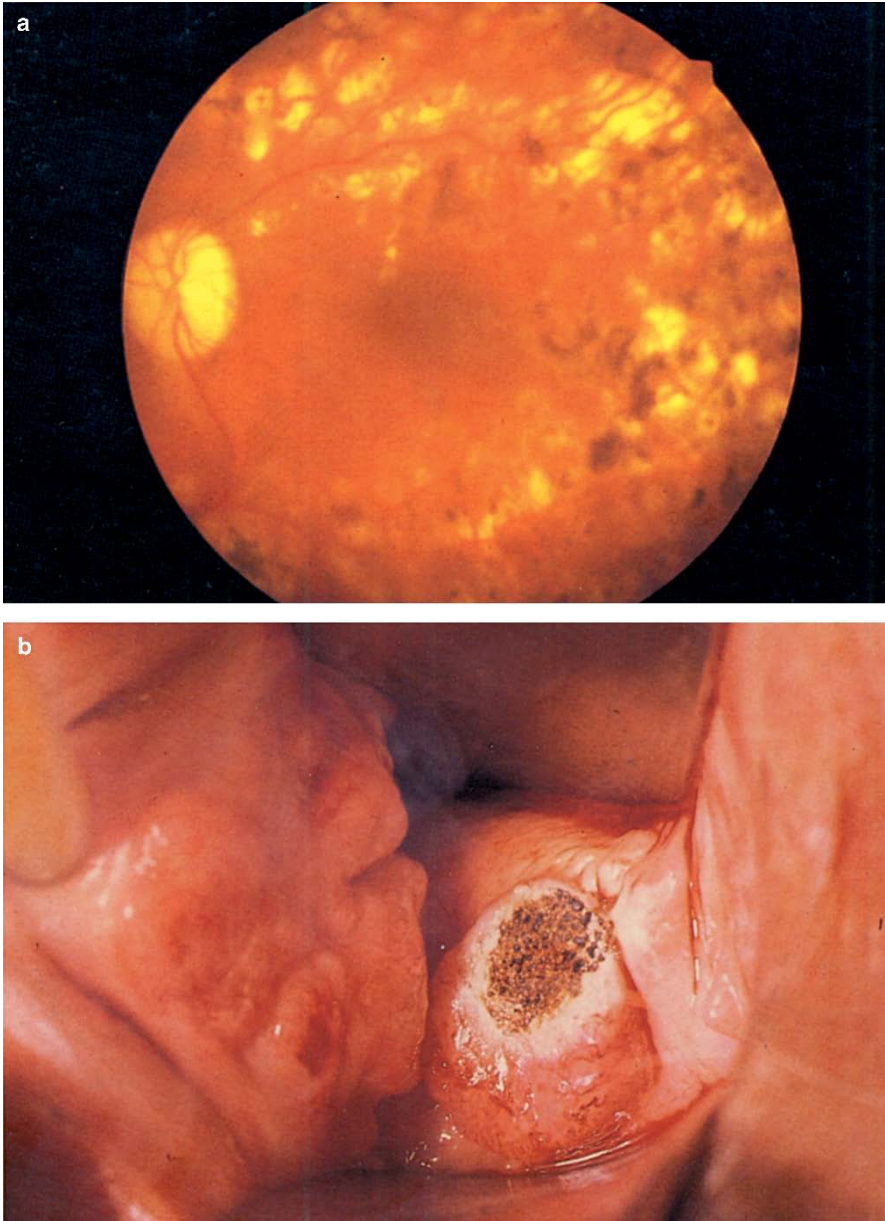
Fig. 4.4. (a) Panretinal coagulation in a diabetes patient performed with an argon ion laser (power: 200 mW). **(b)** Vaporization of cervical tissue with a CO_2 laser (power: 10 W). Photographs kindly provided by Dr. Burk (Heidelberg) and Dr. Kurek (Heidelberg)
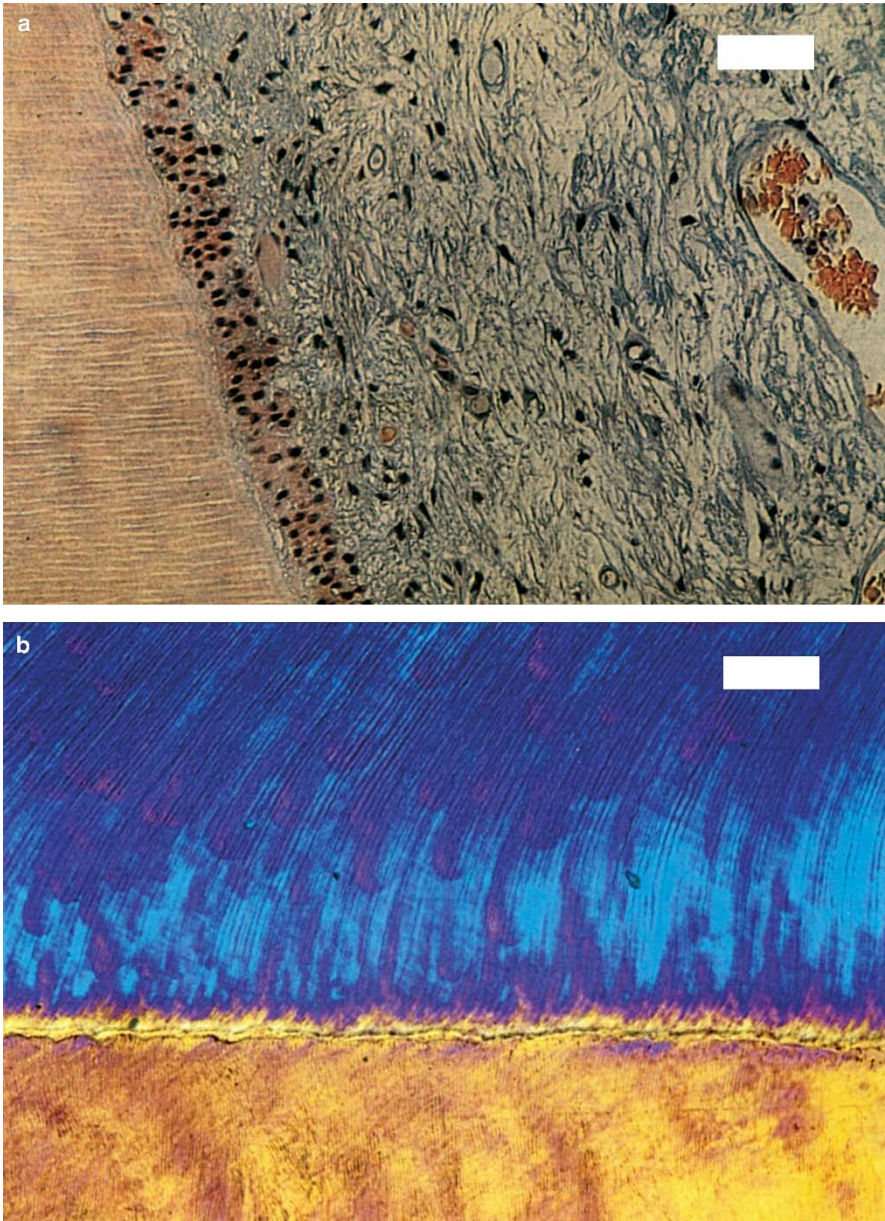
Fig. 4.5. (a) Histologic section of a human tooth after exposure to 16 000 pulses from a Nd:YLF laser (pulse duration: 30 ps, pulse energy: 500 μJ, bar: 50 μm). The junction of dentin (*left*) and pulp (*right*) is shown which was located next to the application site. **(b)** Polarized microscopy of a human tooth slice after exposure to 16 000 pulses from the same laser (bar: 50 μm). The junction of dentin (*top*) and enamel (*bottom*) is shown which was located next to the application site

When a patient is suffering from *diabetic retinopathy*, the concentration of oxygen in the blood is strongly reduced due to disturbances in the body. Because of the lack in oxygen, new blood vessels are formed which is called *neovascularization*. Hemorrhages inside the vitreous body might then lead to severe losses in vision. In order to prevent complete blindness, the whole retina is coagulated except the fovea itself, i.e. a panretinal coagulation is performed as in the case of a severe retinal detachment. By this means, it is assured that the progress of neovascularization is stopped and that at least the fovea does receive enough oxygen. The physiological mechanism of this often successful treatment is not completely understood. Probably, a significant percentage of the receptors which are consuming most of the oxygen provided is turned off. During the treatment, between 1000 and 3000 laser spots should be placed next to each other according to Schulenburg et al. (1979) and Hövener (1980). One section of a panretinal coagulation performed in a diabetes patient is captured in Fig. 4.4a.

Central vein occlusion occurs in the eyes of older patients and is usually restricted to one eye only. As an immediate consequence, retinal veins become dilated and severe edema are formed in the region of the macula. Multiple hemorrhages are associated with a strong decrease in vision. To prevent the occurrence of a secondary glaucoma, the procedure of panretinal coagulation is often performed as stated by Laatikainen et al. (1977).

Senile macula degeneration was recently increased among older patients. According to Bird (1974), it is caused by neovascular membranes being formed in the chorioidea. Subretinal fluids emerging from these membranes might lead to severe edema in the region of the macula. Further neovascularization can be prevented by coagulation with the green line of the argon ion laser or the red line of the krypton laser, respectively. These wavelengths are preferably absorbed by subretinal tissues in the pigment epithelium or the chorioidea but not by xanthophyll contained by the macula itself.

Finally, laser treatment of *retinoblastoma* has also been investigated, e.g. by Svaasand et al. (1989). Destruction of the tumor is obtained by converting laser energy to heat. In the case of malignant tumors, however, mechanical excisions or implants of radioactive substances are favored.

Vitreous Body

The vitreous body is a transparent gel that has a little greater consistency than the white of a raw egg. Its water content varies from 98 % to 99.7 % according to Le Grand and El Hage (1980), and it contains 7 g/l NaCl and 0.5 g/l soluble proteins. The vitreous body of a child is very homogeneous, whereas internal structures frequently appear in the vitreous body of an adult. Many of these inhomogeneities do not really impair the degree of vision. Most of the floating particles can be resorbed by biological mechanisms. Major pathologic alterations, however, are given by the formation of new membranes and neovascularizations extending from the retina into the

vitreous body. Their occurrence has already been described when discussing retinal detachment and diabetic retinopathy. It shall be added that only thermally acting lasers should be used for treatment due to the direct vicinity of the retina. Short pulsed lasers evoking photodisruptive effects may only be used for lens surgery and the front segments of the eye.

Lens

The lens grows during the entire human life forming an onion-like structure of adjacent shells. As a result of its continuous development and the associated decrease in water content, the lens interior progressively hardens with age. The bulk of the lens is formed by transparent lens fibers which originate from the anterior lens epithelium. The lens interior is enclosed by a homogeneous elastic membrane called the *capsule*. The capsule is connected to the *ciliary muscle* which is essential for the eye to accommodate. In a cataract, the transparency of the lens is strongly decreasing. The opaqueness is caused by either age, disease, UV radiation, food deficiencies, or trauma. The changes in the lens that lead to the formation of a cataract are not completely understood. They are somehow related to common observations of reduced amounts of potassium and soluble lens proteins which are associated with increased concentrations of calcium and insoluble lens proteins.

Beside retinal coagulation, cataract surgery of the lens is the other major laser treatment in ophthalmology. In order to achieve acceptable vision, the lens interior must be extracted. Conventional methods rely on fragmentation of the lens by phaco-emulsification followed by aspiration of the fragments. Afterwards, either an artificial lens made of silicon is inserted or the patient must wear special cataract glasses. This treatment has been proposed and documented by Kelman (1967). The posterior lens capsule is retained to prevent a collapse of the vitreous body and subsequent retinal detachment. However, new lens fibers frequently emerge from this posterior capsule forming a scattering membrane. This membrane must be removed during a second invasive surgery.

Posterior capsulotomy with a Nd:YAG laser, on the other hand, is characterized by the advantages of being both noninvasive and feasible during ambulant treatment. It was described in detail by Aron-Rosa et al. (1980) and Terry et al. (1983). Usually, a helium–neon laser is used as an aiming beam. The surgeon first focuses this laser on the posterior capsule and then adds the cutting Nd:YAG laser beam as shown in Fig. 4.6 by pressing a footpedal. Typically, pulse durations of 30 ns, pulse energies of up to 5 mJ, and focus diameters of 50–100 μm are used. With these laser parameters, local power densities exceeding 10^{10} W/cm^2 are achieved, leading to the phenomenon of optical breakdown as described in Sect. 3.4. After having placed several line cuts, the posterior membrane opens like a zipper as illustrated in Fig. 4.7. The whole procedure can be controlled through a slit lamp. The surgeon's eye is protected by a specially coated beamsplitter.
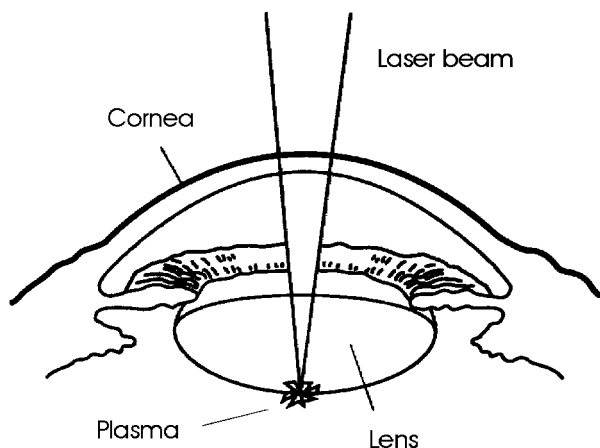
Fig. 4.6. Scheme of laser-performed posterior capsulotomy

Fig. 4.7. Lens before, during, and after posterior capsulotomy

Another laser treatment of the lens is the fragmentation of its interior rather than using ultrasonic exclusively[3]. For this kind of treatment, picosecond laser pulses are advantageous, because they are associated with a lower threshold energy for the occurrence of optical breakdown if compared with nanosecond pulses. Thus, more energy can be converted to the ionizing process itself. In Fig. 4.8, the fragmentation of a human lens is shown which was obtained by using a picosecond Nd:YLF laser. The surgeon steadily moves the focus of the laser beam without injuring the capsule. During this treatment, it is important to choose a pulse energy well above the threshold of optical breakdown, because otherwise all laser energy will be absorbed by the retina and other tissues lying underneath.

---

[3] Laser fragmentation can significantly reduce the amount of necessary phaco time.
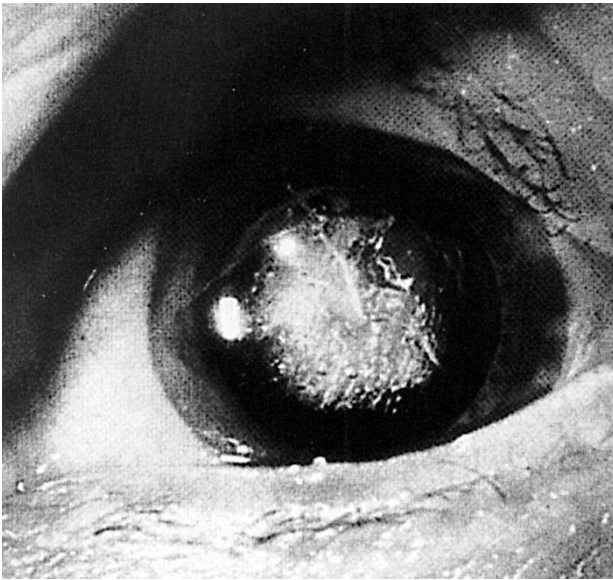
Fig. 4.8. Fragmentation of a human lens using a picosecond Nd:YLF laser (pulse duration: 30 ps, pulse energy: 1 mJ)

Iris

The iris is a tissue which is pierced by a variable circular opening called the *pupil*. Its diameter can vary from 1.5 mm to 8 mm, depending on brightness. In moderate light, the pupil diameter measures approximately 4 mm. The bulk of the iris consists of collagen fibers and pigment cells. The size of the pupil is determined by the action of two smooth muscles – the *sphincter pupillae* and the *dilatator pupillae* – which are responsible for contraction and dilatation, respectively.

In an acute block glaucoma, the drainage of aqueous humor from the rear to the front chamber is obstructed. Hence, the pressure in the rear chamber increases and shifts the iris forward. This dislocation of the iris induces a closed chamber angle which justifies the clinical term *closed-angle glaucoma*. Thereby, aqueous humor is prevented from entering the trabeculum and the canal of Schlemm. The inner eye pressure increases to values far above 20 mm Hg, thus inducing strong headaches, severe edema, degeneration of retinal nerve fibers, and a sudden loss in vision. A generally well-established procedure is called *laser iridotomy*. It provides a high immediate success rate but does not guarantee lasting cure. During this treatment, the iris is perforated as shown in Fig. 4.9 to obtain an additional passage for the aqueous humor to reach the front chamber and the trabeculum.
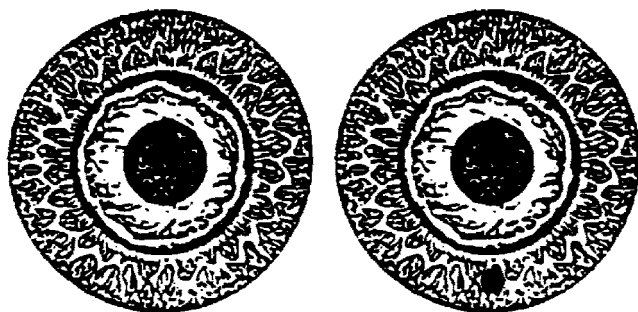
Fig. 4.9. Iris before and after laser treatment

Laser iridotomy can be performed with either argon ion lasers or pulsed neodymium lasers. Prior to laser exposure, the iris is medically narrowed. If applying the argon ion laser, typical exposure durations of 0.1–0.2 s, laser powers ranging from 700–1500 mW, and spot diameters of 50 μm are chosen according to Pollack and Patz (1976), and Schwartz and Spaeth (1980). Iridotomies induced by the argon ion laser are very successful if the iris is dark and strongly pigmented. For bright irises, neodymium lasers with pulse durations in the nanosecond or picosecond range and pulse energies up to a few millijoules are better suited. Detailed data of the procedure are given in the book by Steinert and Puliafito (1985). Perforations around the 12 o'clock position should be avoided because of rising gas bubbles disturbing the surgeon's vision. Therefore, iridotomies are usually placed between the 3 o'clock and 9 o'clock positions. The use of a proper contact glass was recommended by Roussel and Fankhauser (1983).

Laser iridotomy is a minor surgical treatment which can be performed ambulantly. Only in rare cases, complications such as severe hemorrhages or infections are induced. Prior to performing iridotomies, however, medicational treatment is provided to set an upper limit for the eye pressure.

Trabeculum

Another type of glaucoma is called *open-angle glaucoma*. It is not induced by a dislocation of the iris but a malfunction of the trabecular meshwork. The drainage of aqueous humor can be improved by a treatment called *laser trabeculotomy* during which the trabeculum is carefully perforated. First results with ruby and argon ion lasers were published by Krasnov (1973) and Worthen and Wickham (1974), respectively. Two years later, it was reported by Ticho and Zauberman (1976) that in some cases a decrease in eye pressure was obtained just by shrinking the tissue of the trabeculum instead of perforating it. These observations have been the origin for another treatment technique called *trabeculoplasty* which was described in detail by Wise and Witter (1979).

During trabeculoplasty, approximately 100 pulses from an argon ion laser are applied to the surface of the trabeculum. Focusing of the laser beam is facilitated by specially designed contact glasses. Typical focus diameters are 50–100 μm. The drop in eye pressure is assumed to arise from thermal interaction, since the heat deposited by the argon ion laser causes a shrinkage of the exposed trabecular meshwork. By this means, tensile forces are induced capable of enlarging intermediate fluid canals located in between exposed tissue areas. Moreover, these forces could possibly even widen the canal of Schlemm. Thus, the drainage of aqueous humor is improved and the eye pressure is kept at a moderate level.

Today, clinical data of follow-up periods as long as ten years are available. According to Wise (1987), trabeculoplasty has meanwhile developed to a standard type of modern laser surgery. Especially in primarily chronic glaucoma with eye pressures below 35 mm Hg, the therapy is very successful. It was pointed out, though, that ruptures of the meshwork itself should be avoided in any case.

Sclera

Among laser treatments of the sclera, external and internal sclerostomies are distinguished. In either case, surgery aims at achieving a continuous channel from the front chamber to the fluid beneath the conjunctiva. Again, this type of filtration treatment is indicated in the case of an open-angle glaucoma[4].

External sclerostomies start from the anterior sclera, thereby injuring the conjunctiva. First laser sclerostomies in glaucomateous eyes were performed by Beckman et al. (1971) using a thermally acting CO_2 laser. The main disadvantage of this method is the need for dissection of a conjunctival flap which frequently causes severe inflammation. Moreover, the low absorption of scleral tissue at visible and near infrared wavelengths makes it extremely difficult to apply neodymium lasers or other pulsed laser systems. A solution to this problem was offered by L'Esperance (1983) when using exogeneous dyes to artificially increase the absorption coefficient. By dyeing the sclera with sterile india ink at the superior limbus, some fraction of the ink also diffused deeper into the sclera. Then, when focusing an argon ion laser beam on the trabecular meshwork, L'Esperance was able to cut through the trabeculum and the sclera starting from the interior. This was the first internal sclerostomy ever performed. More recently, pulsed Nd:YAG lasers have been used to improve filtration with the method of *internal sclerostomy*. With a specially designed goniolens, the incident laser beam is redirected into an acute angle inside the eye. Scleral perforation starts just next to the trabeculum and ends beneath the conjunctiva. A schematic illustration of the surgical procedure is shown in Fig. 4.10.

---

[4] If even this procedure does not stabilize the eye pressure, the ciliary body itself must be coagulated which is the production site of the aqueous humor.
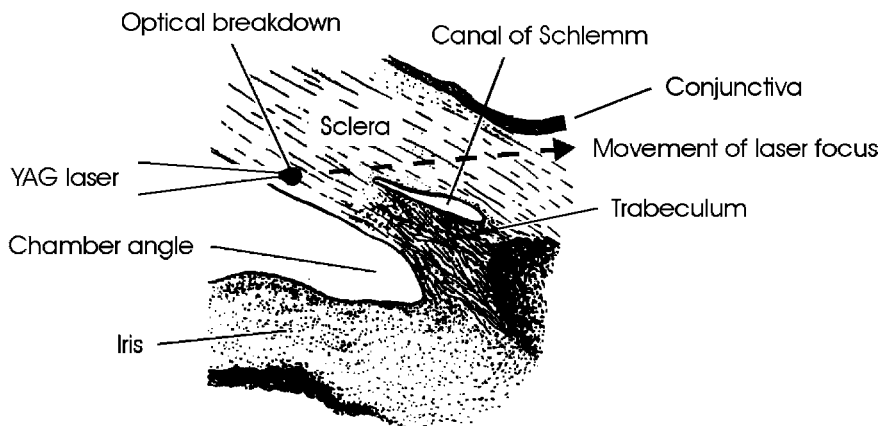
Fig. 4.10. Scheme of internal sclerostomy

First experimental and histologic results on Nd:YAG laser sclerostomy were described by March et al. (1984) and March et al. (1985). They found that approximately 250–500 pulses with pulse durations of 12 ns each and energies ranging from 16 mJ to 53 mJ were required to achieve a complete perforation of the sclera. With these laser parameters, thermal damage to adjacent tissue was limited to a few hundred μm. A few years later, visible dye lasers were also applied by again making use of different inks. The diffusion of these inks into the tissue can be accelerated by means of electrophoresis as reported by Latina et al. (1988) and Latina et al. (1990).

Cornea

Cornea and lens together account for the total refraction of the eye. However, since the anterior surface of the cornea is exposed to air with an index of refraction close to unity, refraction at the anterior surface of the cornea represents the major part. A list of refractive properties of the human eye was first provided by Gullstrand at the beginning of this century. A theoretical analysis of the refractive properties is found in the book by Le Grand and El Hage (1980). Both sets of data are given in Table 4.1 together with a third column called the *simplified eye*. In the simplified eye, the same principal planes and focal distances are assumed as for the theoretical eye. However, a round value of 8 mm is chosen for the radius of curvature of the anterior corneal surface. And, because also assuming the same indices of refraction for the cornea and aequous humor, refraction at the posterior corneal surface is neglected. From these data, it can be concluded that the power of the cornea is approximately 42 diopters, whereas the total power of the eye is roughly 59 diopters. Therefore, about 70 % of the overall refraction arises from the cornea.

Table 4.1. Parameters of the unaccommodated human eye. Data according to Le Grand and El Hage (1980)

	Gullstrand eye	Theoretical eye	Simplified eye
Index of refraction			
Cornea	1.376	1.377	1.336
Aqueous humor	1.336	1.337	1.336
Lens	1.408	1.420	1.421
Vitreous body	1.336	1.336	1.336
Radius of curvature (mm)			
Cornea (ant. surface)	7.7	7.8	8.0
Cornea (post. surface)	6.8	6.5	–
Lens (ant. surface)	10.0	10.2	10.2
Lens (post. surface)	−6.0	−6.0	−6.0
Power (diopters)			
Cornea	43.05	42.36	42.0
Lens	19.11	21.78	22.44
Total eye	58.64	59.94	59.64

The transparency of corneal tissue in the spectral region from 400 nm to 1200 nm can be attributed to its extremely regular microscopic structure as will be discussed below. The optical zone of the human cornea has typical diameters ranging from 2 mm to 4 mm and is controlled by the iris. The overall thickness of the cornea varies between 500 μm at the center of the optical axis and 700 μm at the periphery. Corneal tissue is avascular and basically consists of five distinct layers: epithelium, Bowman's membrane, stroma, Descemet's membrane, and endothelium. A schematic cross-section of the human cornea is shown in Fig. 4.11.
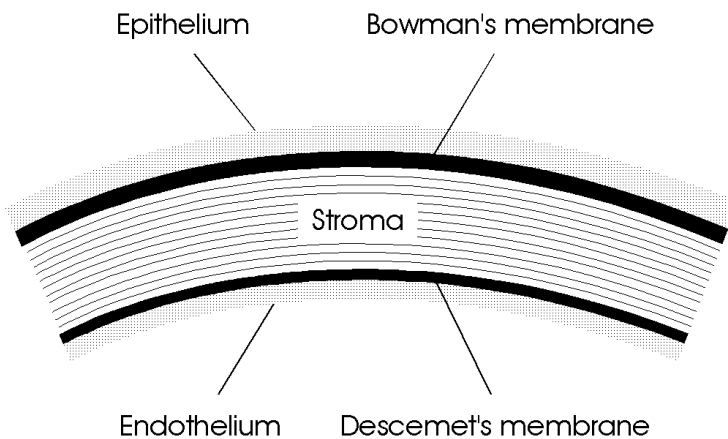
Fig. 4.11. Cross-section of a human cornea

According to Le Grand and El Hage (1980), the *epithelium* is made up of two to three layers of flat cells which – in combination with tear fluid – provide the smooth surface of the cornea. These cells are the only corneal cells capable of regenerating. *Bowman's membrane* consists of densely packed collagen fibers. All these fibers are oriented in planes parallel to the corneal surface, resulting in extremely high transparency. Due to its high density, Bowman's membrane is primarily responsible for the mechanical stability of the cornea. Almost 90 % of the corneal thickness belongs to the *stroma*. It has a structure similar to Bowman's membrane but at a lower density. Since the stroma contributes the major part of the cornea, refractive corneal surgery relies on removing stromal tissue. *Descemet's membrane* protects the cornea from its posterior side. And, finally, the *endothelium* consists of two layers of hexagonally oriented cells. Their main function is to prevent fluid of the front chamber from diffusing into the cornea.

In general, two types of corneal surgeries are distinguished: removal of any pathologic conditions and refractive corneal surgery. The first group includes treatments of irregularly shaped corneas, e.g. keratoconus, externally induced corneal injuries, and corneal transplantations. Prior to laser surgery, all these treatments had to be performed with mechanical scalpels. Today, ophthalmic lasers – among these especially the ArF excimer laser – offer a noninvasive and painless surgery. Successful circular trephinations and smoothing of irregular surfaces were, for instance, reported by Loertscher et al. (1987) and Lang et al. (1989). Very clean corneal excisions can also be obtained when using short pulsed neodymium lasers as shown in Figs. 4.12 and 4.13. The dependence of the ablation depth on pulse energy is illustrated in Figs. 4.14 and 4.15.

The other group of corneal surgeries aims at an alteration of its refractive power. Although most cases of wrongsightedness cannot be attributed to a pathologic condition of the cornea[5], it is the corneal power which is the easiest to change. First successful studies on refractive corneal surgery were reported by Fjodorov and Durnev (1979) using a diamond knife. The whole procedure is called *radial keratotomy* (from Greek: $\kappa\epsilon\rho\alpha\varsigma$ = cornea, $\tau o\mu\alpha\epsilon\iota\nu$ = to be cut). By placing radial incisions into the peripheral cornea, tensile forces are rearranged which leads to a flattening of the central anterior surface, i.e. a decrease in refractive power. Radial keratotomy has meanwhile been investigated by a variety of surgeons. Several profound reviews are available today, e.g. by Bores (1983), Sawelson and Marks (1985), and Arrowsmith and Marks (1988).

In the beginning of the 1980s, a novel method was developed which is actually removing part of the tissue with a laser. Thus, excisions are performed instead of incisions. This surgical technique is therefore called *radial keratectomy (RK)* (from Greek: $\epsilon\kappa\tau o\mu\alpha\epsilon\iota\nu$ = to be cut out). Actually, the con-

---

[5] In most myopias, the bulbus is too long. Senile hyperopia is due to a decrease in lens accommodity. Only astigmatism is frequently caused by the cornea itself.
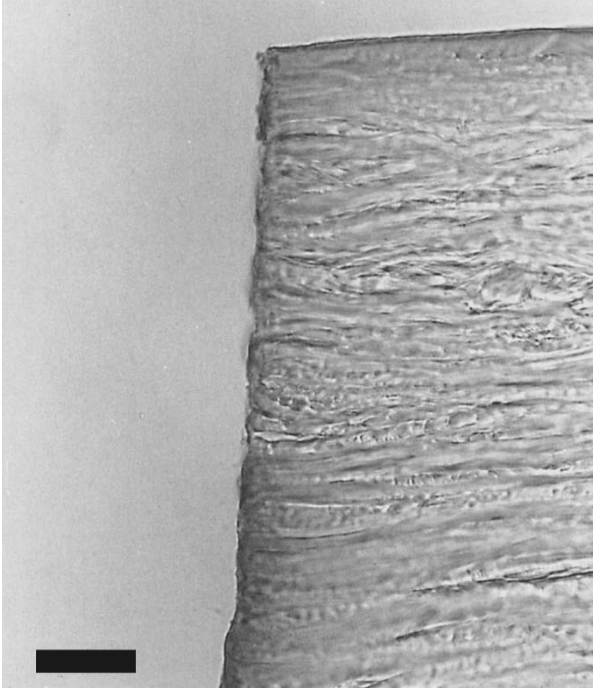
Fig. 4.12. Magnification (light microscopy) of a corneal excision achieved with a Nd:YLF laser (pulse duration: 30 ps, bar: 10 μm, original surface: *horizontal*, laser excision: *vertical*)
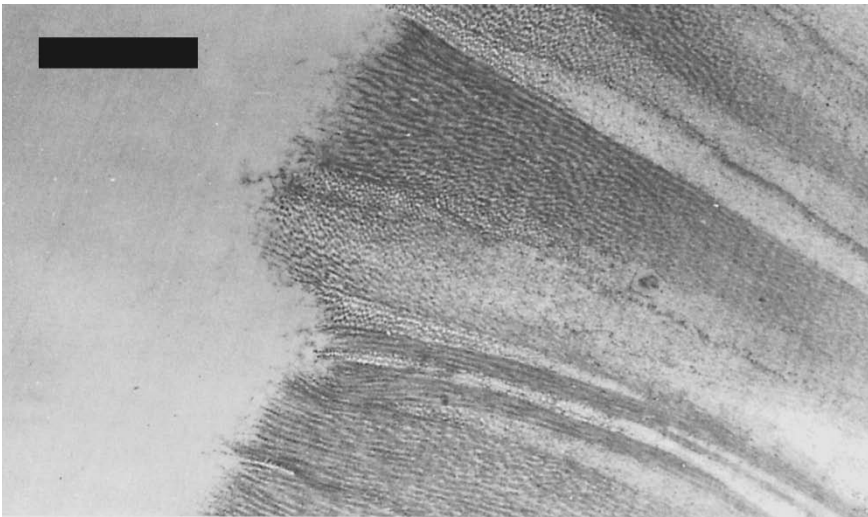
Fig. 4.13. High magnification (transmission electron microscopy) of a corneal excision achieved with a Nd:YLF laser (pulse duration: 30 ps, bar: 1 μm)
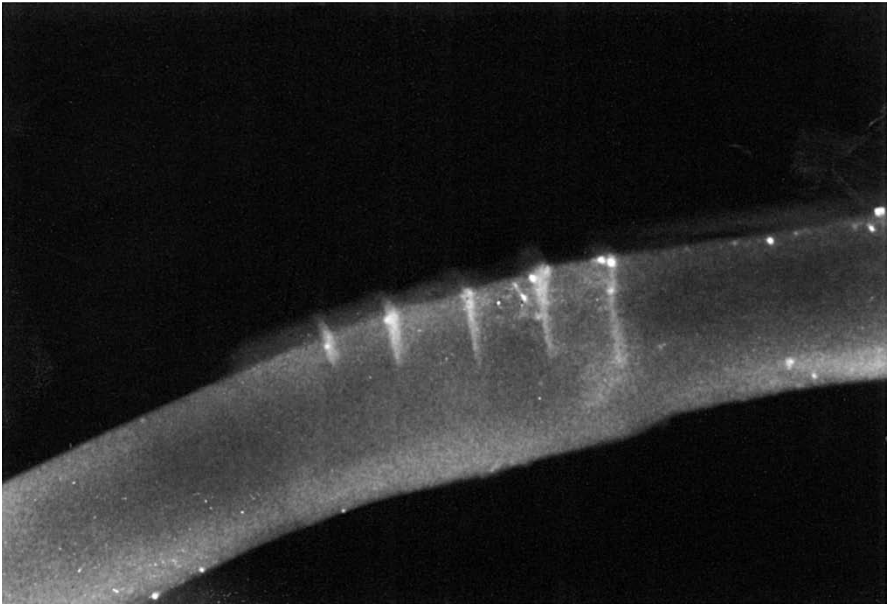
Fig. 4.14. Corneal excisions achieved with a Nd:YLF laser at different pulse energies (from *left* to *right*: 30 µJ, 50 µJ, 70 µJ, 90 µJ, and 110 µJ)
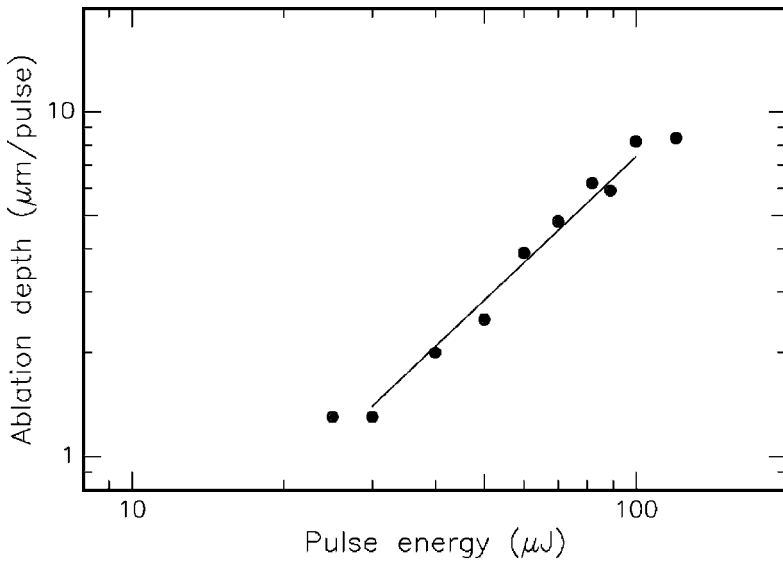
Fig. 4.15. Ablation curve of corneal stroma obtained with a Nd:YLF laser (pulse duration: 30 ps, focal spot size: 15 µm). Data according to Niemz et al. (1991)

cept of reshaping the curvature of the cornea with a laser beam was initially proposed by Keates et al. (1981). However, his original concept of applying the CO_2 laser failed, and Trokel et al. (1983) first achieved a successful keratectomy with an ArF excimer laser. Shortly afterwards, other groups also published their results, e.g. Cotlair et al. (1985), Marshall et al. (1985), and Puliafito et al. (1985). All these researchers focused on radial excisions for the purpose of correcting myopia. Moreover, astigmatism can be corrected by placing transverse excisions as reported by Seiler et al. (1988). Since excisions need to be of the order of 90 % of the corneal thickness – otherwise no significant alteration of refractive power is observed – the initial rate of corneal perforation was quite high. Today, however, perforation is usually avoidable due to improved application systems and more accurate preoperative measurements of corneal parameters. Detailed computer simulations were described by Hanna et al. (1989a).

More recently, another laser technique called *keratomileusis* (from Greek: $\lambda\upsilon\epsilon\iota\nu$ = to detach) or *photorefractive keratectomy (PRK)* has been proposed by Marshall et al. (1986). They recognized the superior quality of excimer laser ablations and investigated the direct carving of the cornea to change its optical power. During this treatment, large area ablations are performed around the optical axis rather than linear excisions in the periphery. The major advantage of keratomileusis over radial keratectomy is the ability to achieve direct optical correction rather than depending on indirect biomechanical effects of peripheral excisions. However, the basic hopes for minimal wound healing without opacification and for rapidly obtained stable refraction have not yet been supported by clinical experience. Corneal wound healing does occur in most cases, and it may take up to several months until refraction is stabilized. Radial keratectomy and keratomileusis are compared in a schematic drawing shown in Fig. 4.16.

Radial keratectomy   Keratomileusis   Keratomileusis
for myopia (only)   for myopia   for hyperopia
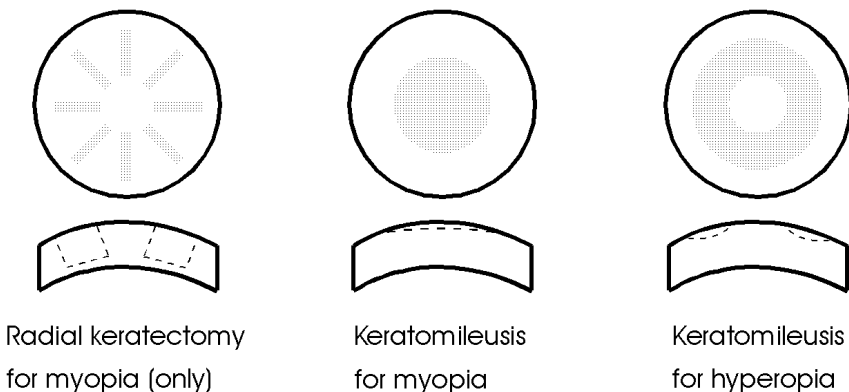
Fig. 4.16. Schemes of radial keratectomy and keratomileusis for the correction of myopia and hyperopia, respectively. Anterior view and cross-section of the cornea are shown. Dotted areas and dashed lines refer to the postoperative state

In the following paragraphs, a geometrically derived instruction is given of how the reshaping of a myopic eye has to be done. In Fig. 4.17, the pre- and postoperative anterior surfaces of the cornea are shown together with other geometrical parameters. The optical axis and an arbitrary axis perpendicular to it are labeled x and y, respectively. The curvature of the cornea is given by R, and the indices "i" and "f" refer to the initial and final states of the cornea, respectively.
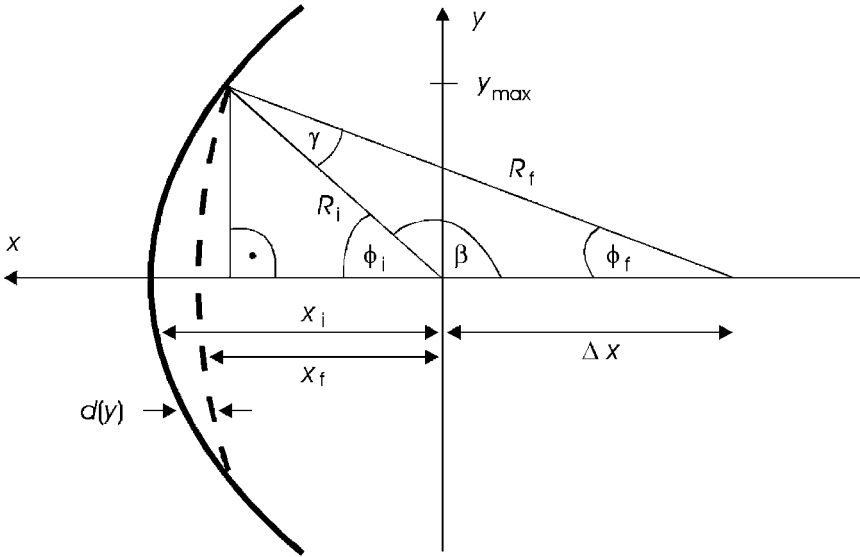
Fig. 4.17. Geometry of performing keratomileusis in a myopic eye. The pre- and postoperative anterior surfaces of the cornea are drawn as a solid curve and a dashed curve, respectively. The alteration in curvature is exaggerated

The equations for the initial and final anterior surfaces of the cornea are given by

$$x_i^2 + y^2 = R_i^2 \ , \tag{4.1}$$

$$(x_f + \Delta x)^2 + y^2 = R_f^2 \ , \tag{4.2}$$

where (x_i, y) and (x_f, y) are the coordinates of the initial and final surfaces, respectively, and Δx is the shift in the centers of curvature as shown in Fig. 4.17. We thus obtain for the depth of ablation

$$d(y) = x_i - x_f = \sqrt{R_i^2 - y^2} - \sqrt{R_f^2 - y^2} + \Delta x \ . \tag{4.3}$$

The shift Δx can be calculated from the sines of the angles β and γ and is expressed by

$$\frac{\Delta x}{\sin \gamma} = \frac{R_f}{\sin \beta} \ . \tag{4.4}$$

When using the following geometrical relations

$$\sin \beta = \sin \left(180° - \phi_i \right) = \sin \phi_i \ ,$$

$$\gamma = \phi_i - \phi_f \ ,$$

(4.4) can be turned into

$$\Delta x = R_f \ \frac{\sin \left(\phi_i - \phi_f \right)}{\sin \phi_i} \ . \tag{4.5}$$

Furthermore, we deduce from Fig. 4.17 the two expressions

$$\sin \phi_i = \frac{y_{max}}{R_i} \ ,$$

$$\sin \phi_f = \frac{y_{max}}{R_f} \ ,$$

where y_{max} is the maximum radius of the optical zone to be altered. Hence, substituting ϕ_i and ϕ_f in (4.5) leads to

$$\Delta x = \frac{R_i R_f}{y_{max}} \ \sin \left(\arcsin \frac{y_{max}}{R_i} - \arcsin \frac{y_{max}}{R_f} \right) \ . \tag{4.6}$$

From (4.3) and (4.6), we obtain

$$d(y) = \sqrt{R_i^2 - y^2} - \sqrt{R_f^2 - y^2} + \frac{R_i R_f}{y_{max}} \ \sin \left(\arcsin \frac{y_{max}}{R_i} - \arcsin \frac{y_{max}}{R_f} \right).$$

The highest ablation depth must be obtained at $y = 0$ with

$$d(0) = R_i - R_f + \frac{R_i R_f}{y_{max}} \ \sin \left(\arcsin \frac{y_{max}}{R_i} - \arcsin \frac{y_{max}}{R_f} \right) \ . \tag{4.7}$$

In (4.7), the depth $d(0)$ is given which the surgeon has to remove at the vertex of the optical axis. The unknown parameter R_f is readily obtained from the basic law of a curved refracting surface

$$\Delta D = (n_c - 1) \left(\frac{1}{R_i} - \frac{1}{R_f} \right) , \tag{4.8}$$

where ΔD is the degree of myopia expressed in units of diopters, and n_c is the refractive index of the cornea. For an attempted correction of ΔD ranging from 1 diopter to 10 diopters, the required values of R_f and $d(0)$ are listed in Table 4.2, assuming $R_i = 7.8\,\mathrm{mm}$, $n_c = 1.377$, and $y_{max} = 2.5\,\mathrm{mm}$. From these data, it can be concluded that for myopias up to 5 diopters less than one tenth of the corneal thickness needs to be ablated.

Table 4.2. Theoretical values of keratomileusis in the case of myopia. Actual data might slightly differ due to a rearrangement in mechanical stress. Assumed is an optical zone of 5 mm, i.e. $y_{max} = 2.5$ mm

ΔD (diopters)	R_f (mm)	$d(0)$ (μm)
1	7.965	9.0
2	8.137	17.9
3	8.316	26.8
4	8.504	35.7
5	8.700	44.6
6	8.906	53.4
7	9.121	62.2
8	9.347	71.0
9	9.585	79.7
10	9.835	88.4

A similar calculation applies for the correction of hyperopic eyes. However, since a peripheral ring-shaped zone needs to be ablated, the diameter of the optical zone is usually extended to 7–8 mm. It should be added that astigmatism can also be corrected by means of keratomileusis. This is achieved by simply aiming at two different values of R_f in two planes located perpendicularly to the optical axis.

In the 1980s, i.e. during the early stage of performing keratomileusis, this novel technique was further improved and corticosteroids were infrequently used. Early experiences were reported by Aron-Rosa et al. (1987) and Taylor et al. (1989). Normal reepithelialization as well as mild subepithelial haze were observed. McDonald et al. (1990) demonstrated the ability to achieve a measurable myopic refractive correction. However, they also reported on an initial regression and a poor predictability of the refractive effect. Wilson (1990) distinguished between preoperative myopias with less and more than 5.5 diopters. From his clinical observations, he concluded that good predictions can be made in the first case only. Some of his results are shown in Figs. 4.18a–b. Similar statements regarding predictability were published by Seiler and Genth (1994).

Meanwhile, several variations of PRK are being studied all over the world. The ArF excimer laser is well suited for this type of surgery because of its ablation characteristics. As we have already encountered when discussing Fig. 3.36, one pulse from this laser typically ablates 0.1–1 μm of corneal tissue which corresponds to 0.01–0.1 diopters. Usually, energy densities of 1–5 J/cm^2 are applied in order to be less dependent on energy fluctuations, since the ablation curve shown in Fig. 3.36 approaches a saturation limit. Then, the correction of one diopter is achieved with approximately 10 pulses which takes about one second at a repetition rate of 10 Hz. Although most researchers agree that the ArF laser is well suited for PRK, the choice of a proper delivery system is being controversely discussed. Most common are
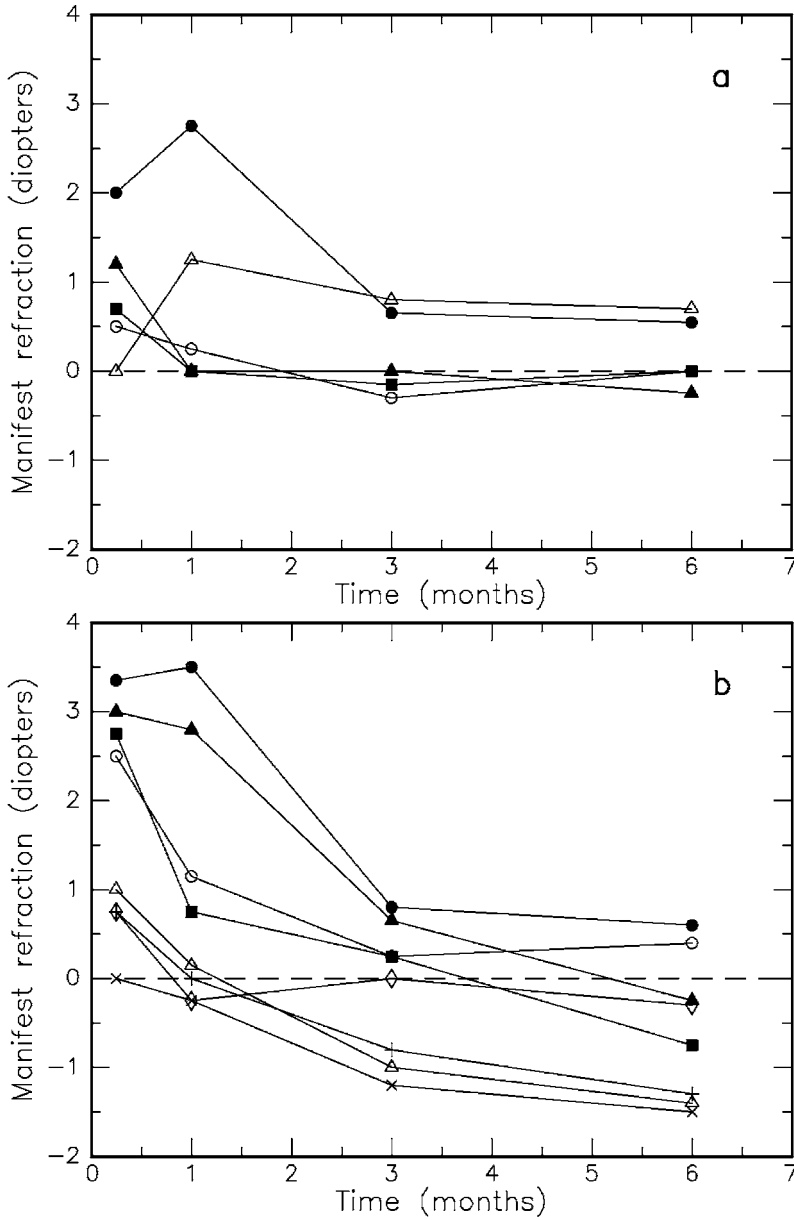
Fig. 4.18. (a) Results of ArF excimer laser keratomileusis performed in five cases of myopia with attempted corrections less than 5.5 diopters. **(b)** Results of ArF excimer laser keratomileusis performed in eight cases of myopia with attempted corrections more than 5.5 diopters. During a follow-up period of six months, eyes with more than 5.5 diopters of preoperative myopia appear to be less stable than eyes with less than 5.5 diopters. Emmetropia is indicated by a dashed line. Data according to Wilson (1990)

the methods of using a scanning slit as described by Hanna et al. (1988) and Hanna et al. (1989b), or a rotating disk mask with different apertures as used by L'Esperance et al. (1989). In the first case, the cornea is exposed to radiation from an ArF laser through a movable slit. If the slit is wider near its center, i.e. if more tissue is removed from the central cornea, it can be used for correcting myopic eyes. If the slit is wider near its ends, it is designed for treating hyperopia. The rotating disk mask, on the other hand, consists of several apertures with different diameters which are concentrically located on a wheel. The patient's eye is irradiated through one aperture at a time. In between, the wheel is turned to the next aperture. By this means, it is assured that the overall exposure gradually decreases from the center to the periphery of the cornea. Thus, tissue is removed from central areas, i.e. myopia is corrected. Hyperopias cannot be treated using the rotating disk. Either method is illustrated in Figs. 4.19a–c.
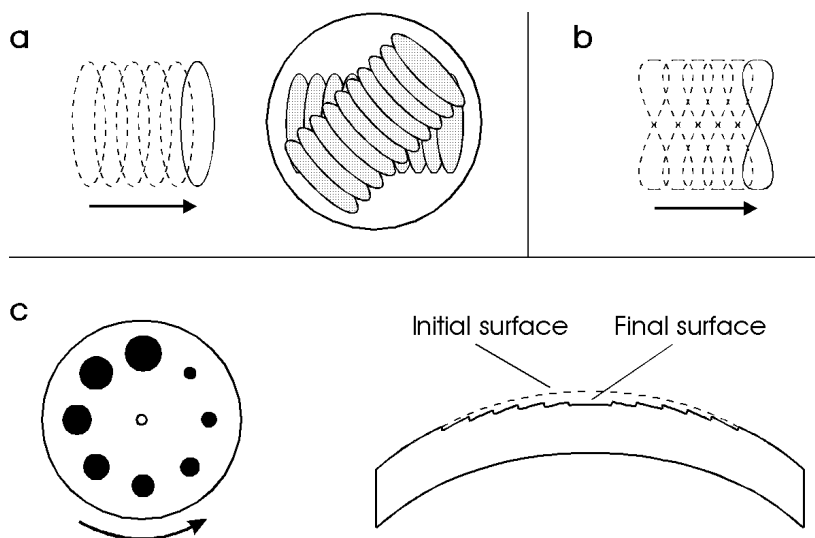
Fig. 4.19. (a) Scanning slit for correction of myopia and anterior view of cornea. **(b)** Scanning slit for correction of hyperopia. **(c)** Rotating disk mask for correction of myopia. Initial and final surfaces are shown in a corneal cross-section

In Fig. 4.20a, a photograph is shown which demonstrates the removal of corneal tissue after performance of keratomileusis. In order to visualize the stair-like ablations, a large difference in aperture diameters was chosen. The view of a treated eye through a slit lamp is captured in Fig. 4.20b. With this device, the patient's eye is illuminated by a slit which is positioned at an angle to the optical axis. From its image on the cornea, information on the corneal thickness can be derived. In the example shown in Fig. 4.20b, the cornea appears thinner at its center. Thus, a myopic eye was treated.
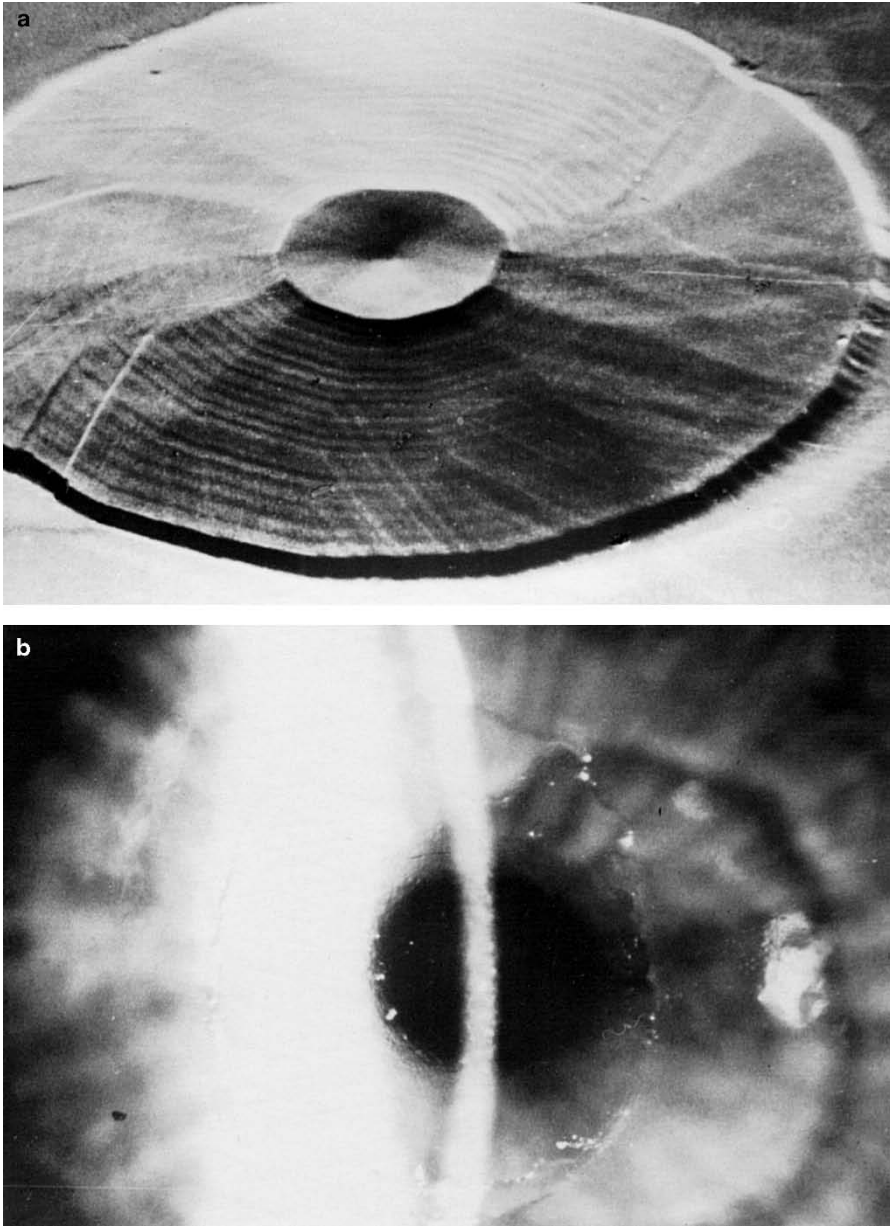
Fig. 4.20. (a) Stair-like ablations of corneal tissue after performance of keratomileusis with an ArF laser. **(b)** View of a treated eye through a slit lamp. Photographs kindly provided by Dr. Bende (Tübingen)

In a large group of keratomileusis treatments, good optical correction is obtained after approximately six months. Despite several improvements, however, two major disadvantages still remain:

− regression of the initially achieved refractive power,
− appearance of a subepithelial haze after the regression period.

The existence of a regression effect becomes obvious when looking at Figs. 4.18a–b. Within the first three months after PRK, a regression of up to three diopters has been observed. It is probably due to the processes of corneal wound healing and reepithelialization. Therefore, the patient's eye is usually transferred to a hyperopic state immediately after surgery. It is hoped that refraction stabilizes at emmetropy after the period of regression. This procedure, of course, requires a lot of patience since the patient has to use several pairs of glasses during the first months after surgery. Subepithelial haze has not been found in all patients but is a frequent consequence. It disturbs vision especially in darkness when the pupil widens. The primary cause of this haze is yet unknown. It might arise from a rearrangement of collagen fibers inside Bowman's membrane and the stroma. However, haze could also be induced by the toxic UV radiation. As stated in Sect. 3.3, cytotoxicity and mutagenicity cannot be excluded for the ArF laser wavelength at 193 nm. It is generally believed that corneal tumors do not occur. Cytotoxic effects, though, might cause a reduction in corneal transparency.

Infrared lasers have also been proposed for refractive corneal surgery, especially erbium, holmium, and neodymium lasers. When using erbium and holmium lasers, thermal degradation of corneal tissue is attempted, leading to a shrinkage of the involved collagen fibers. By this means, tensile stress is induced inside the cornea evoking a change in refractive power. Actually, this method is based on earlier studies performed by Gasset and Kaufman (1975) who used conventional heat sources in the treatment of severe keratoconus. Since thermal effects are associated with opacification, the laser energy is usually applied to a peripheral ring of the cornea. With this method, corrections of hyperopia were observed as reported by Householder et al. (1989) and Brinkmann et al. (1994).

An interesting and challenging technique for refractive corneal surgery has emerged at the beginning of the 1990s. It is called *intrastromal ablation*, and its basic principle is illustrated in Fig. 4.21. By means of focusing a laser beam inside the cornea, either a continuous disk-shaped or a ring-shaped cavity is generated, depending on the type of correction needed. When the gaseous vapor inside these cavities has diffused into the surrounding medium, the cavity collapses. It is expected that the removal of stromal tissue then induces a stable change in curvature of the anterior corneal surface. The main advantage of this technique is that the original layers of epithelium and Bowman's membrane are not injured. Thus, the stability of the cornea is less affected, and corneal haze is less likely to occur.
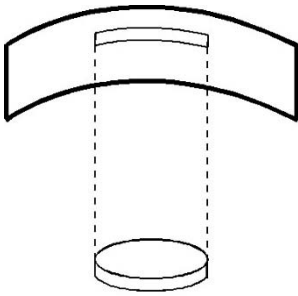
Intrastromal ablation
for myopia
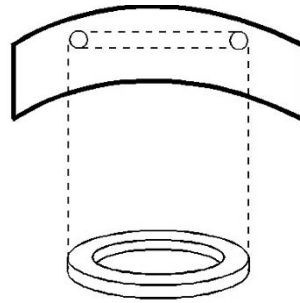
Intrastromal ablation
for hyperopia

Fig. 4.21. Schemes of intrastromal ablation

Intrastromal ablations were first reported by Höh (1990) when focusing a Q-switched Nd:YAG laser beam inside the stroma. A more detailed study followed soon after by Niemz et al. (1993a) using picosecond pulses from a two-stage Nd:YLF laser system. It was shown for the first time that a continuous intrastromal cavity can be achieved which is located approximately 150 µm beneath the epithelium. A typical example of such a laser-induced cavity inside the stroma of a human cornea is shown in Fig. 4.22. This photograph was obtained with a scanning electron microscope. Due to shrinking processes during the preparation, the cavity appears closer to the epithelium than 150 µm. The collapse of an intrastromal cavity is captured in Fig. 4.23 which was taken with a transmission electron microscope. In this case, fixation took place one hour after laser exposure. Two vacuoles are still visible which have not yet collapsed. According to Vogel et al. (1994b), endothelial damage does not occur if the focus of the laser beam is placed at least 150 µm away from the endothelium.

Meanwhile, preliminary intrastromal ablations have been performed which lead to alterations in refractive power of up to 5 diopters. In addition, extensive theoretical models have been proposed for this kind of surgery, e.g. by Hennighausen and Bille (1995). Using the algorithm of *finite elements*, certain predictions can be made concerning any changes in refraction. The method of finite elements is a very powerful tool of modern engineering science. Reshaping of the cornea by mechanical alterations is a typical problem of a special branch called *biomechanics* or *bioengineering*. Mechanical properties of the cornea have been reported by Jue and Maurice (1989). Its governing equations have been discussed by Fung (1981).

When applying the method of finite elements, the object, e.g. the cornea, is subdivided into a certain number of finite elements. The size of these elements is chosen such that each of them can be characterized by constant
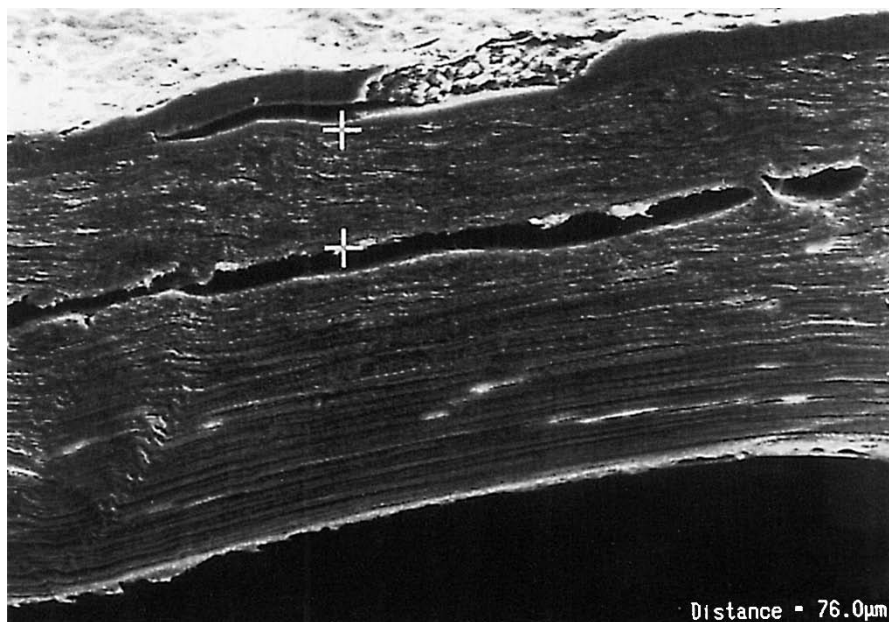
Fig. 4.22. Intrastromal cavity achieved with a Nd:YLF laser (pulse duration: 30 ps, pulse energy: 140 µJ)

Fig. 4.23. Collapse of an intrastromal cavity achieved with a Nd:YLF laser (pulse duration: 30 ps, pulse energy: 100 µJ). The two vacuoles which have not yet collapsed measure about 20 µm

physical parameters. The advantage of this procedure is that all governing equations are readily solved within each element. Then, by implementing proper boundary conditions, each element is related to its adjacent elements which finally leads to a physical description of the whole object. Any alteration of a single element consequently influences other elements, as well. In our example shown in Fig. 4.24, two intrastromal elements within the optical zone are removed. Using iterative calculations on fast processing computers, the deformed postoperative state of the cornea is simulated. In order to obtain reliable results, such a model should comprise the following properties of the cornea:

– anisotropy,
– incompressibility,
– nonlinear stress–strain behavior[6],
– nonuniform initial stress distribution.
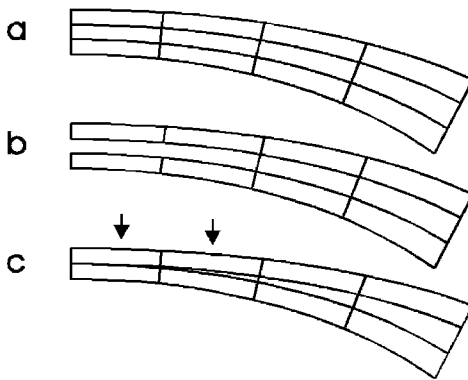
Fig. 4.24. (a–c) Simulation of an intrastromal ablation by twelve finite elements. One half of the corneal cross-section is shown. **(a)** Preoperative state. **(b)** Intrastromal ablation (immediate postoperative state). **(c)** Steady postoperative state

Today, the standard technique for refractive corneal surgery beside PRK is called *laser in situ keratomileusis (LASIK)*. This kind of treatment basically consists of three steps shown in Fig. 4.25: cutting a flap into the anterior section of the cornea with a surgical knife or a femtosecond laser, removing intrastromal tissue with an ArF laser or a femtosecond laser according to Table 4.2, and pulling the flap down again with surgical tweezers. No sewing is necessary after the treatment, since the flap immediately sticks again to the tissue underneath due to adhesive forces. The removed tissue volume causes a similar change in refraction as in the case of the intrastromal ablations described above, but LASIK provides the high precision achievable with ArF or femtosecond lasers.

---

[6] Most biological tissues do not obey *Hooke's law* of elasticity.

Step I   focused
laser beam

Step II   (a)   (b)

Step III

comea
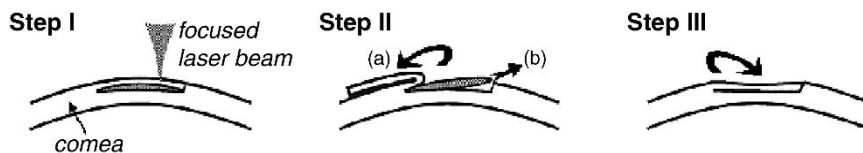
Fig. 4.25. LASIK technique based on three steps: cutting a flap into the anterior section of the cornea, removing intrastromal tissue, and pulling the flap down again

In Fig. 4.26, a high-magnification photograph of LASIK treatment is shown. With a Nd:Glass femtosecond laser, a flap was cut into the cornea and pulled upward. Furthermore, a disc-shaped volume of intrastromal tissue was excised and put aside. This fascinating photograph proves the high accuracy associated with this technique. Since LASIK has just recently been developed, of course, not much data are available so far. However, as progress with excimer laser surgery has demonstrated, research in this field continues to grow rapidly. Details are given by Pallikaris and Siganos (1994), Knorz et al. (1996), Farah et al. (1998), Patel et al. (2000), Lipshitz et al. (2001), and Rosen (2001). A reasonable judgement of this alternative for refractive corneal surgery should be possible in the near future.
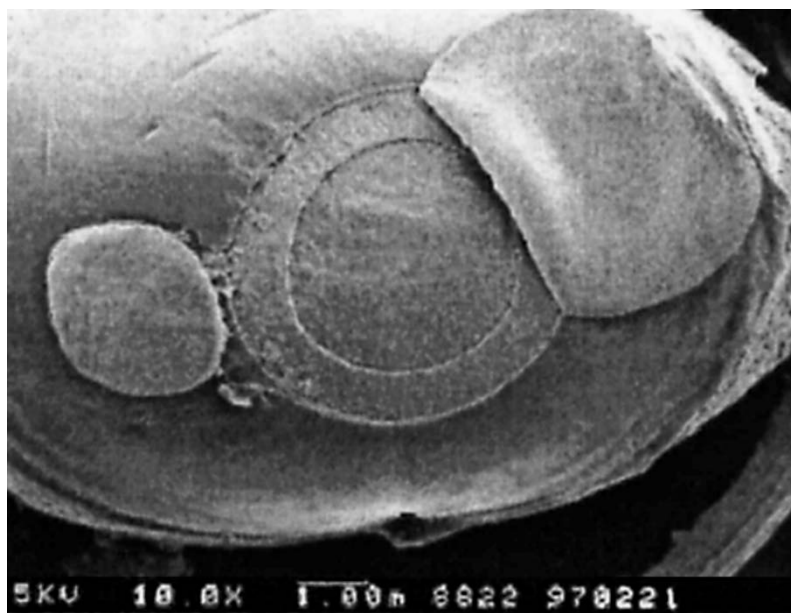
Fig. 4.26. High-magnification photograph of LASIK treatment performed with a Nd:Glass laser (pulse duration: 500 fs, pulse energy: 3 μJ)

4.2 Lasers in Dentistry

Although dentistry was the second medical discipline where lasers were applied, it basically remained a field of research. Especially in caries therapy – the most frequent dental surgery – conventional mechanical drills are still superior compared to most types of lasers, particularly CW or long-pulse lasers. Only laser systems capable of providing ultrashort pulses might be an alternative to mechanical drills as was recently shown by Niemz et al. (1993b) and Pioch et al. (1994). However, many clinical studies and extensive engineering effort still remain to be done in order to achieve satisfactory results. We should keep in mind that mechanical drills have improved over several decades until the present stage was reached, and that the development of suitable application units for laser radiation also takes time. Other topics of interest in dentistry include laser treatment of soft tissue as well as laser-welding of dental bridges and dentures. In some of these areas, research has been very successful. In this section, laser treatment of hard tooth substances, soft dental tissues, and filling materials will be addressed.

The Human Tooth

Before going into the details of laser dentistry, a brief summary of the anatomy of the human tooth as well as its physiology and pathology shall be given. In principle, the human tooth consists of mainly three distinct segments called enamel, dentin, and pulp. A schematic cross-section of a human tooth is shown in Fig. 4.27.
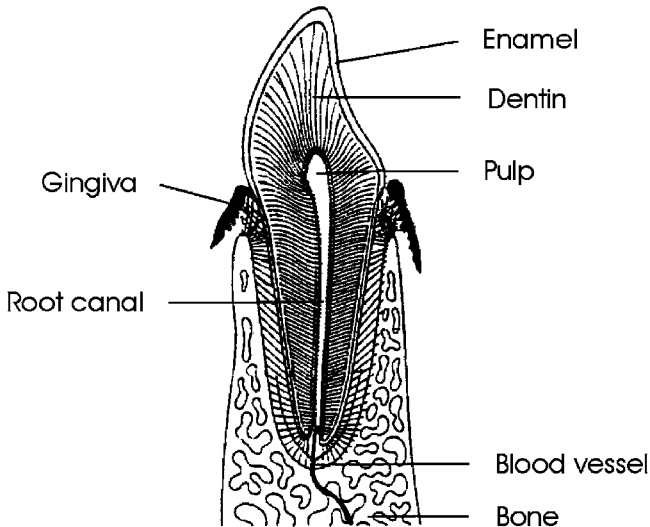
Fig. 4.27. Cross-section of a human tooth

The *enamel* is the hardest substance of the human body. It is made of approximately 95 % (by weight) hydroxyapatite, 4 % water, and 1 % organic matter. Hydroxyapatite is a mineralized compound with the chemical formula $Ca_{10}(PO_4)_6(OH)_2$. Its substructure consists of tiny crystallites which form so-called *enamel prisms* with diameters ranging from 4 µm to 6 µm. The crystal lattice itself is intruded by several impurities, especially Cl^-, F^-, Na^+, K^+, and Mg^{2+}.

The *dentin*, on the other hand, is much softer. Only 70 % of its volume consists of hydroxyapatite, whereas 20 % is organic matter – mainly collagen fibers – and 10 % is water. The internal structure of dentin is characterized by small tubuli which measure up to a few millimeters in length, and between 100 nm and 3 µm in diameter. These tubuli are essential for the growth of the tooth.

The *pulp*, finally, is not mineralized at all. It contains the supplying blood vessels, nerve fibers, and different types of cells, particularly odontoblasts and fibroblasts. Odontoblasts are in charge of producing the dentin, whereas fibroblasts contribute to both stability and regulation mechanisms. The pulp is connected to peripheral blood vessels by a small channel called the *root canal*. The tooth itself is embedded into soft tissue called the *gingiva* which keeps the tooth in place and prevents bacteria from attacking the root.

The most frequent pathologic condition of teeth is called *decay* or *caries*. Its origin lies in both cariogeneous nourishment and insufficient oral hygiene. Microorganisms multiply at the tooth surface and form a layer of *plaque*. These microorganisms produce lactic and acetic acid, thereby reducing the pH down to values of approximately 3.5. The pH and the solubility of hydroxyapatite are strongly related by

$$Ca_{10}(PO_4)_6(OH)_2 + 8\,H^+ \longleftrightarrow 10\,Ca^{2+} + 6\,HPO_4^{2-} + 2\,H_2O \ .$$
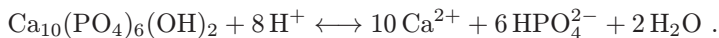
By means of this reaction, the enamel can be demineralized within a few days only. Calcium bound to the hydroxyapatite is ionized and washed out by saliva. This process turns the hard enamel into a very porous and permeable structure as shown in Fig. 4.28. Usually, this kind of decay is associated with a darkening in color. Sometimes, however, carious lesions appear bright at the surface and are thus difficult to detect. At an advanced stage, the dentin is demineralized, as well. In this case, microorganisms can even infect the pulp and its interior which often induces severe pain. Then, at the latest, must the dentist remove all infected substance and refill the tooth with suitable alloys, gold, ceramics, or composites. Among alloys, amalgam has been a very popular choice of the past. Recently, though, a new controversy has arisen concerning the toxicity of this filling material, since it contains a significant amount of mercury.

The removal of infected substance is usually accomplished with conventional mechanical drills. These drills do evoke additional pain for two reasons. First, tooth nerves are very sensitive to induced vibrations. Second,
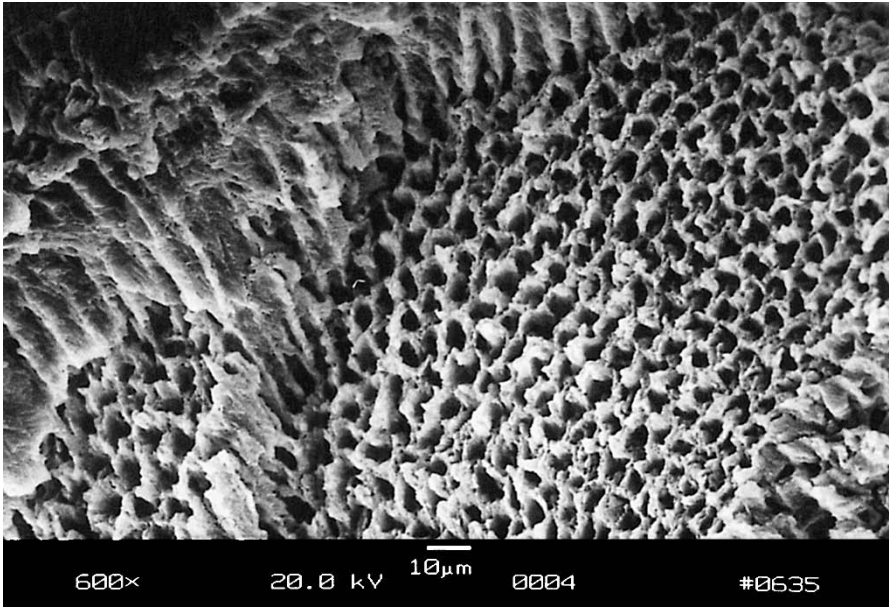
Fig. 4.28. High-magnification photograph of caries taken with a scanning electron microscope. Reproduced from Niemz (1994a). © 1994 Springer-Verlag

tooth nerves also detect sudden increases in temperature which are induced by friction during the drilling process. Pain relief without injection of an anaesthetic was the basic ulterior motive when looking for laser applications in caries therapy. However, it turned out that not all types of lasers fulfill this task. Although vibrations are avoided due to the contactless technique, thermal side effects are not always eliminated when using lasers. CW and long-pulse lasers, in particular, induce extremely high temperatures in the pulp as shown in Figs. 4.29a–b. Even air cooling does not reduce this temperature to a tolerable value. Thermal damage is negligible only when using ultrashort pulses according to the statements given in Sect. 3.2.

Meanwhile, other advantages are being discussed which could even be more significant than just pain relief[7]. Very important among these are the so-called conditioning of dental substance and a possibly more precise procedure of caries removal. Conditioning provides additional protection of the tooth by means of sealing its surface. Thereby, the occurrence of caries can be significantly delayed. Improved control of caries removal, e.g. by a spectroscopic analysis of laser-induced plasmas as shown in Figs. 3.51a–b, could minimize the amount of healthy substance to be removed. Then, indications for expensive dental crowns or bridges are effectively reduced.

---

[7] It should be kept in mind that pain relief alone would not justify the application of more expensive machines.
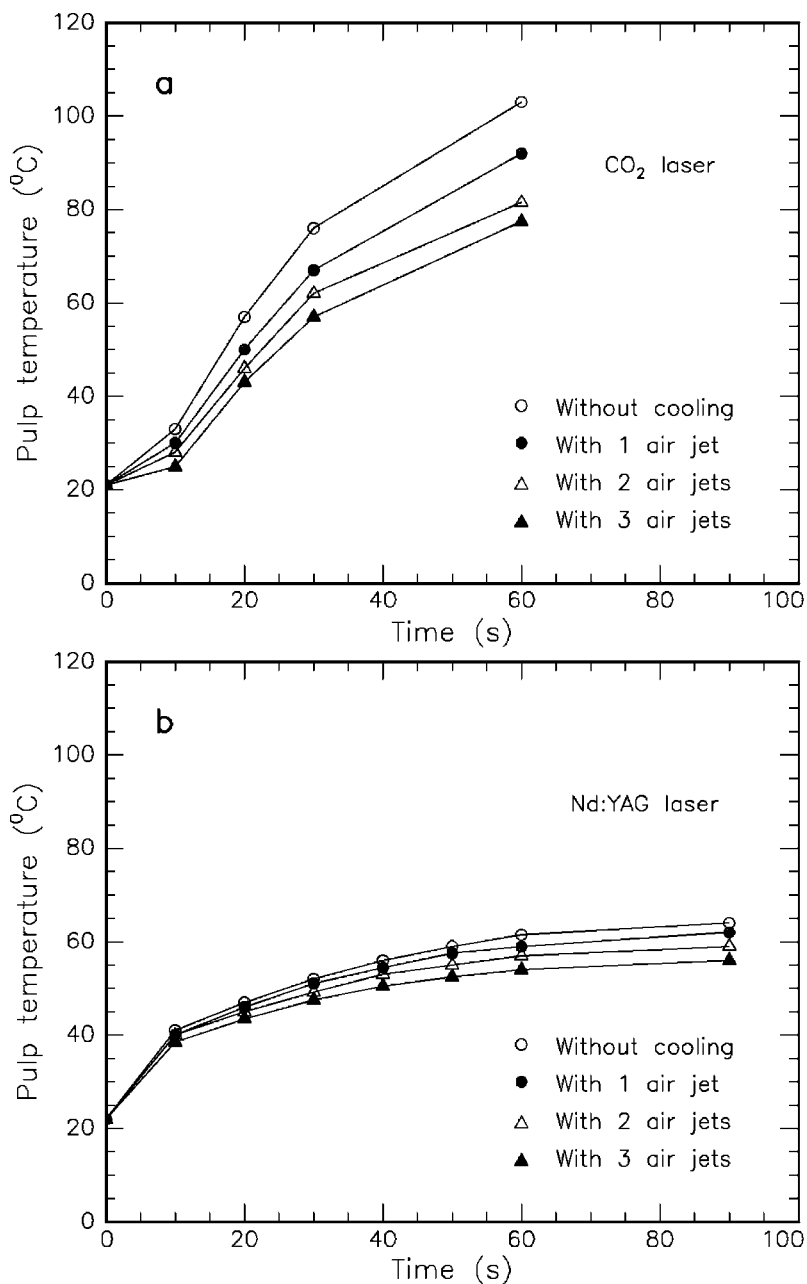
Fig. 4.29. (a) Mean temperatures in the pulp during exposure to a CW CO_2 laser (power: 5 W) without and with air cooling, respectively. **(b)** Mean temperatures in the pulp during exposure to a CW Nd:YAG laser (power: 4 W) without and with air cooling, respectively. Data according to Frentzen and Koort (1992)

Laser Treatment of Hard Tooth Substance

First experiments with teeth using the laser as a surgical tool were performed by Goldman et al. (1964) and Stern and Sognnaes (1964). Both of these groups used a pulsed ruby laser at a wavelength of 694 μm. This laser induced severe thermal side effects such as irreversible injury of nerve fibers and tooth cracking. Thus, it is not very surprising that these initial studies never gained clinical relevance. A few years later, a CO_2 laser system was investigated by Stern et al. (1972). However, the results did not improve very much compared with the ruby laser. These observations are due to the fact that both ruby and CO_2 lasers are typical representatives of thermally acting lasers. Thus, it was straightforward to conclude with Stern (1974) that without being able to eliminate these thermal effects, lasers would never turn into a suitable tool for the preparation of teeth.

Meanwhile, several experiments have been conducted using alternative laser systems. At the end of the 1980s, the Er:YAG laser was introduced to dental applications by Hibst and Keller (1989), Keller and Hibst (1989), and Kayano et al. (1989). The wavelength of the Er:YAG laser at 2.94 μm matches the resonance frequency of the vibrational oscillations of water molecules contained in the teeth as described in Sect. 3.2. Thereby, the absorption of the Er:YAG radiation is strongly enhanced, resulting in a high efficiency. However, the sudden vaporization of water is associated with a pressure gradient. Small microexplosions are responsible for the break-up of the hydroxyapatite structure. High-magnification photographs of a human tooth after Er:YAG laser exposure were shown in Sect. 3.2 in Figs. 3.11a–b. The coincidence of thermal (e.g. vaporization) and mechanical (e.g. pressure gradient) ablation effects has led to the term "thermomechanical interaction" as used by Frentzen and Koort (1991).

Initially, Er:YAG lasers seemed to be very promising because of their high efficiency in ablating dental substances. Meanwhile, though, some indication has been given that microcracks can be induced by Er:YAG laser radiation. It was found by Niemz et al. (1993b) and Frentzen et al. (1994) – using scanning electron microscopy and dye penetration tests – that these fissures can extend up to 300 μm in depth. They could thus easily serve as an origin for the development of new decay. External cooling of the tooth might help to reduce the occurrence of cracking but further research needs to be performed prior to clinical applications.

Even worse results were found with the Ho:YAG laser as reported by Niemz et al. (1993b). High-magnification photographs of a human tooth after laser exposure were shown in Figs. 3.13a–b. Severe thermal effects including melting of tooth substance were observed. Moreover, cracks up to 3 mm in depth were measured when performing dye penetration tests.

Dye penetration tests are suitable experiments for the detection of laser-induced tooth fissures. After laser exposure, the tooth is stained with a dye, e.g. neofuchsine solution, for several hours. Afterwards, the tooth is sliced

Dye penetration (μm)
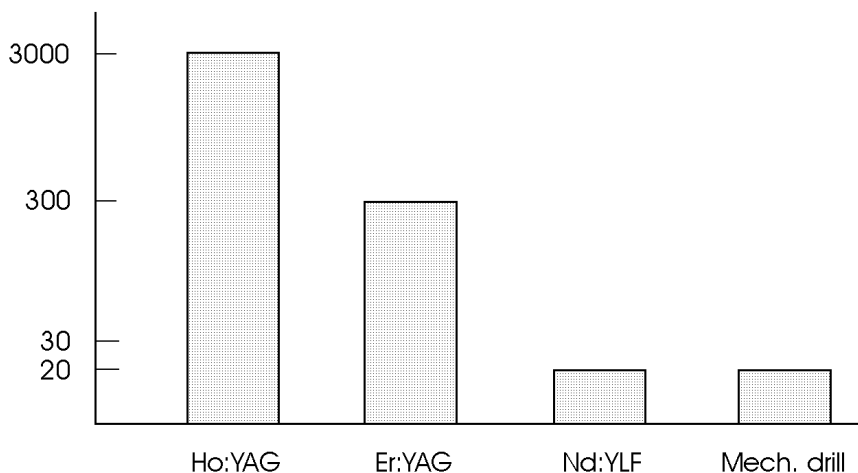
Fig. 4.30. Results of dye penetration tests for three different solid-state lasers and the mechanical drill. Listed are the maximum penetration depths inside the enamel of human teeth. Pulse durations: 250 μs (Ho:YAG), 90 μs (Er:YAG), and 30 ps (Nd:YLF). Data according to Niemz (1993b)

using a microtome, and the maximum penetration depth of the dye is determined. The results of some representative measurements are summarized in Fig. 4.30. Obviously, tooth fissures induced by Ho:YAG and Er:YAG lasers must be considered as a severe side effect.

Another laser type – the ArF excimer laser – was investigated by Frentzen et al. (1989) and Liesenhoff et al. (1989) regarding its usefulness in dentistry. Indeed, initial experiments proved that only very slight thermal effects were induced which was attributed to the shorter pulse duration of approximately 15 ns and the gentle interaction mechanism of photoablation. However, the ablation rate achieved with this laser, i.e. the ablated volume per unit time, is too low for clinical applications. Although very successful in refractive corneal surgery because of its high precision, it is exactly this accuracy with ablation depths less than 1 μm per pulse and the rather moderate repetition rates which pull the ablation rate down. This ineffectiveness and the general risks of UV radiation are the major disadvantages concerning the use of the ArF laser in dentistry.

A second UV laser – the frequency-doubled Alexandrite laser at 377 nm – was studied by Steiger et al. (1993) and Rechmann et al. (1993). It was observed that this laser offers a better selectivity for carious dentin than the Er:YAG laser, i.e. the required fluence at the ablation threshold of healthy dentin is higher when using the Alexandrite laser, whereas the thresholds for carious dentin are about the same.

Recently, a novel approach to laser caries therapy has been made by Niemz et al. (1993b) and Pioch et al. (1994) when using picosecond pulses from a Nd:YLF laser system. Although, at the early stage of experiments, uncertainty predominated concerning potential shock wave effects, it has meanwhile been verified by five independent tests that mechanical impacts are negligible. These consist of *scanning electron microscopy*, *dye penetration tests*, *hardness tests*, *histology*, and *polarized microscopy*. Latest results have been published by Niemz (1995b).

Scanning Electron Microscopy. In Figs. 4.31a–b, two SEM are shown demonstrating the ability of a picosecond Nd:YLF laser to produce extremely precise tetragonal cavities in teeth. The cavities are located in healthy and carious enamel, respectively. Both of them have lateral dimensions of $1 \times 1\,\mathrm{mm}^2$ and a depth of approximately $400\,\mu\mathrm{m}$. They were created by distributing $1\,\mathrm{mJ}$ laser pulses onto 40 lines over the tooth surface with 400 lasered spots per line, and repeating this procedure ten times for the cavity shown in Fig. 4.31a and only once for the cavity in Fig. 4.31b. Thus, a total number of 160 000 laser shots was necessary for the cavity in healthy enamel, and only one tenth of this number was needed to achieve a similar depth in carious enamel. This observation already indicates that the ablation rate of demineralized enamel is about ten times higher than that of healthy enamel, i.e. the Nd:YLF laser provides a caries-selective ablation.

In Figs. 4.32a–b, the cavity wall and bottom are shown, respectively. The cavity wall is extremely steep and is characterized by a sealed glass-like structure. This is of great significance for the prevention of further decay. The roughness of the cavity bottom is of the order of 10–$20\,\mu\mathrm{m}$ and thus facilitates the adhesion of most filling materials. The scanning ablation becomes more evident when using fewer pulses to produce a shallow cavity as shown in Fig. 4.33a. In this case, a circular ablation pattern with 2 500 pulses was selected. In Fig. 4.33b, the effect of a conventional drill on the cavity wall is demonstrated. Deep grooves and crumbled edges are clearly visible.

Dye Penetration Tests. The results of dye penetration tests after exposure to a picosecond Nd:YLF laser have already been presented in Fig. 4.30. Laser-induced fissures typically remained below $20\,\mu\mathrm{m}$. This value is of the same order as fissure depths obtained with the mechanical drill. One potential cause for the extremely small dye penetration might be the sealing effect demonstrated in Fig. 4.32a.

Hardness Tests. One obvious test for the potential influence of shock waves is the measurement of hardness of a tooth before and after laser exposure. In hardness tests according to Vickers, the impact of a diamond tip into a tooth surface is determined. Softer material is characterized by a deeper impact of the diamond tip – and thus a larger impact diameter. The hardness itself is defined as

$$H_\mathrm{V} = 1.8544\ \frac{K}{D^2}\ ,$$
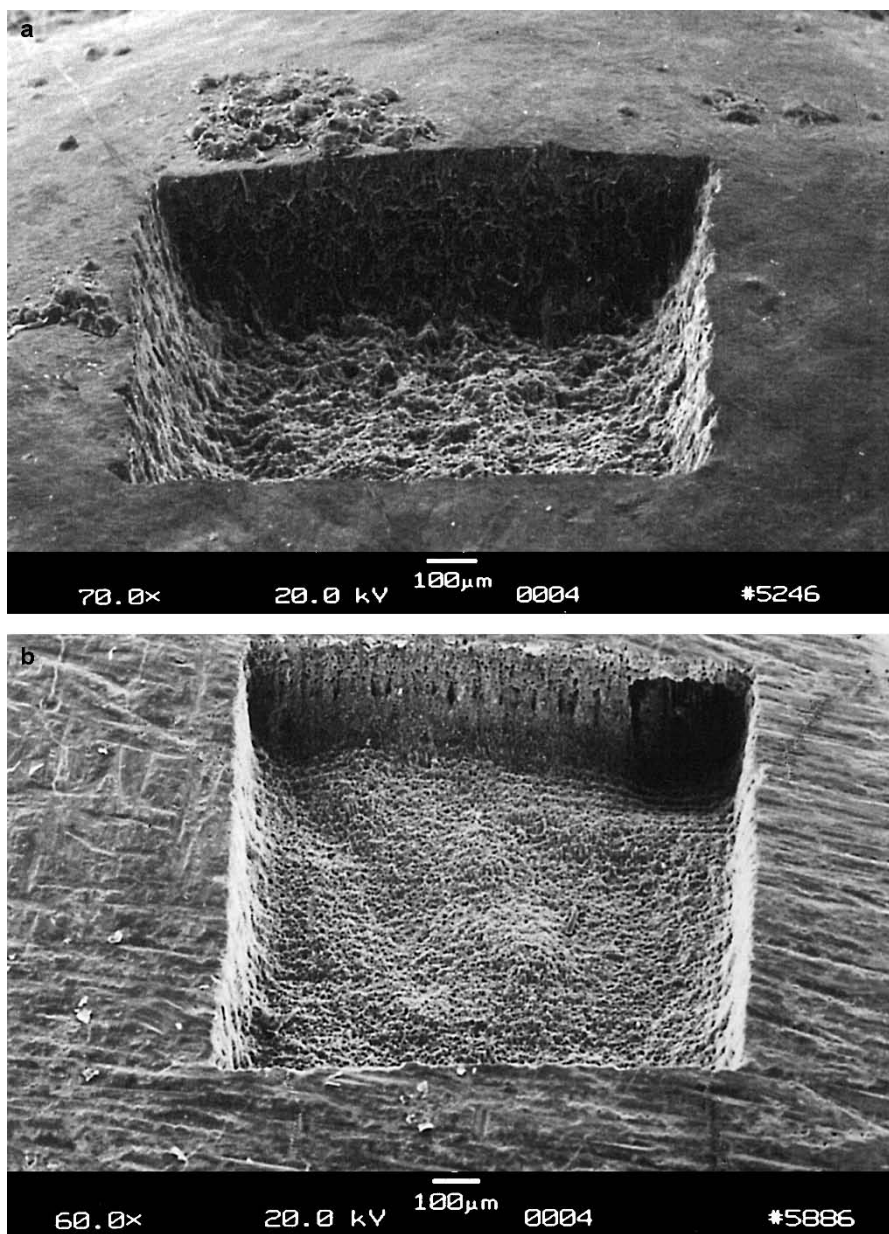
Fig. 4.31. (a) Cavity in healthy enamel achieved with 160 000 pulses from a Nd:YLF laser (pulse duration: 30 ps, pulse energy: 1 mJ). **(b)** Cavity in carious enamel achieved with 16 000 pulses from a Nd:YLF laser (pulse duration: 30 ps, pulse energy: 1 mJ)
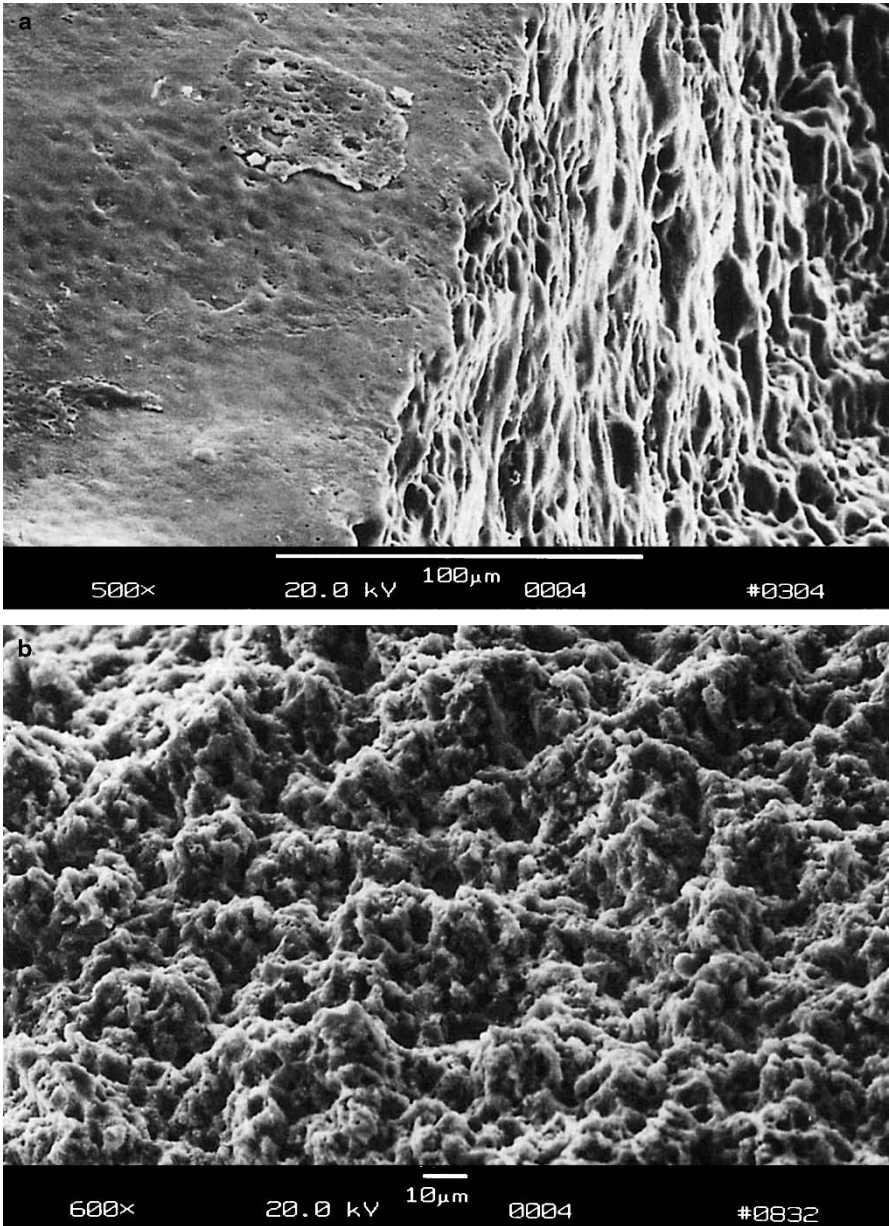
Fig. 4.32. (a) Cavity wall in healthy enamel achieved with a Nd:YLF laser (pulse duration: 30 ps, pulse energy: 1 mJ). **(b)** Cavity bottom in healthy enamel achieved with a Nd:YLF laser (pulse duration: 30 ps, pulse energy: 1 mJ)
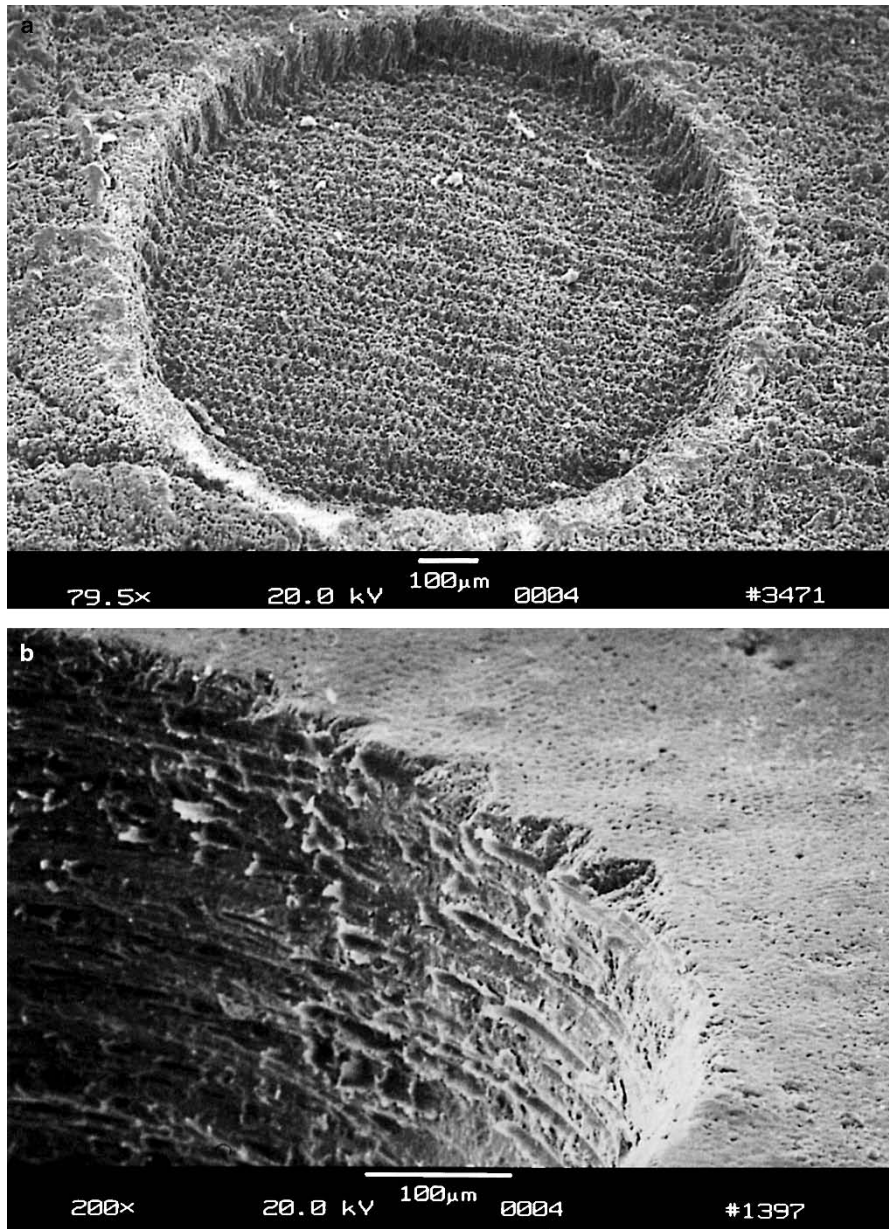
Fig. 4.33. (a) Cavity in carious enamel achieved with 2 500 pulses from a Nd:YLF laser (pulse duration: 30 ps, pulse energy: 1 mJ). **(b)** Cavity wall achieved with a conventional diamond drill

where $K = 5.0 \times 10^4$ N, and D is the impact of a diamond tip cut at an angle of $136°$ and expressed in millimeters. The results of hardness tests after exposure to picosecond Nd:YLF pulses are presented in Table 4.3. According to Niemz (1995c), no significant alteration in hardness is observed in exposed and unexposed enamel. As expected, though, dentin appears much softer due to its lower content of hydroxyapatite.

Table 4.3. Mean hardness values of teeth before and after exposure to a Nd:YLF laser (pulse duration: 30 ps, pulse energy: 1 mJ)

	D (mm)	H_V (N/mm^2)
Exposed enamel	5.9	2660
Unexposed enamel	5.8	2760
Unexposed dentin	11.5	700

Histology. The most important touchstone for the introduction of a new therapeutic technique is the biological response of the tissue, i.e. the survival of cells. Histologic sections enable specific statements concerning the condition of cells due to highly sophisticated staining techniques. In Fig. 4.5a (page 157), the dentin–pulp junction of a human tooth is shown. It was located underneath a 1×1 mm^2 area exposed to 16 000 pulses from a Nd:YLF laser. Along the junction, several odontoblasts are clearly visible. They have not intruded into the dentin and have a similar appearance as in unexposed teeth. Thus, potential shock waves do not have a detectable impact on the pulp – not even on a cellular level.

Polarized Microscopy. Polarized microscopy is an efficient tool for detecting alterations in optical density which might arise from the exposure to shock waves. If these shock waves are reflected, e.g. at the enamel–dentin junction, such alterations might even be enhanced and should thus become evident. For polarized microscopy, exposed teeth are dehydrated in an upgraded series of ethanol. Afterwards, they are kept in fluid methacrylate for at least three days. Within the following period of seven days, polymerization takes place in a heat chamber set to $43°$C. Then, the embedded samples are cut into 100 μm thick slices using a saw microtome. Finally, the slices are polished and examined with a polarized light microscope. In Fig. 4.5b (page 157), the enamel–dentin junction of a human tooth is shown. It was located underneath a 1×1 mm^2 area exposed to 16 000 pulses from a Nd:YLF laser. In the top and bottom parts of the picture, dentin tubuli and enamel prisms are found, respectively. Due to the different optical densities of dentin and enamel, these two structures appear blue and yellow in the corresponding color photograph. However, no substantial alteration in color is observed within either the dentin or the enamel. Hence, no evidence of an altered optical density due to laser-induced shock waves is given.

From the results of the above tests, i.e. the negligibility of mechanical effects, it can be concluded that the cavities shown in Figs. 4.31a–b were produced by means of plasma-induced ablation as discussed in Sect. 3.4. The main reason for these observations is that the applied pulse energies were just slightly above the threshold energy of optical breakdown. In Fig. 4.34, the ablation curves of healthy enamel, healthy dentin, and carious enamel are given, respectively. In healthy enamel, plasma sparking was already visible at approximately 0.2 mJ. Then, when taking the corresponding focal spot size of 30 μm into account, the ablation threshold is determined to be about $30 \, \text{J/cm}^2$. For carious enamel, plasma generation started at roughly 0.1 mJ, i.e. at a threshold density of $15 \, \text{J/cm}^2$. In the range of pulse energies investigated, all three ablation curves are mainly linear. Linear regression analysis yields that the corresponding slopes in Fig. 4.34 are 1 μm/0.2 mJ, 3 μm/0.2 mJ, and 8 μm/0.2 mJ, respectively. Thus, the ablation efficiency increases from healthy enamel and healthy dentin to carious enamel. From the ablation volumes, we derive that – at the given laser parameters – approximately $1.5 \, \text{mm}^3$ of carious enamel can be ablated per minute. To cope with conventional mechanical drills, a ten times higher ablation efficiency would be desirable. It can be achieved by increasing both the pulse energy and repetition rate. Then, the Nd:YLF picosecond laser might represent a considerable alternative in the preparation of hard tooth substances. The potential realization of such a clinical laser system is currently being evaluated.
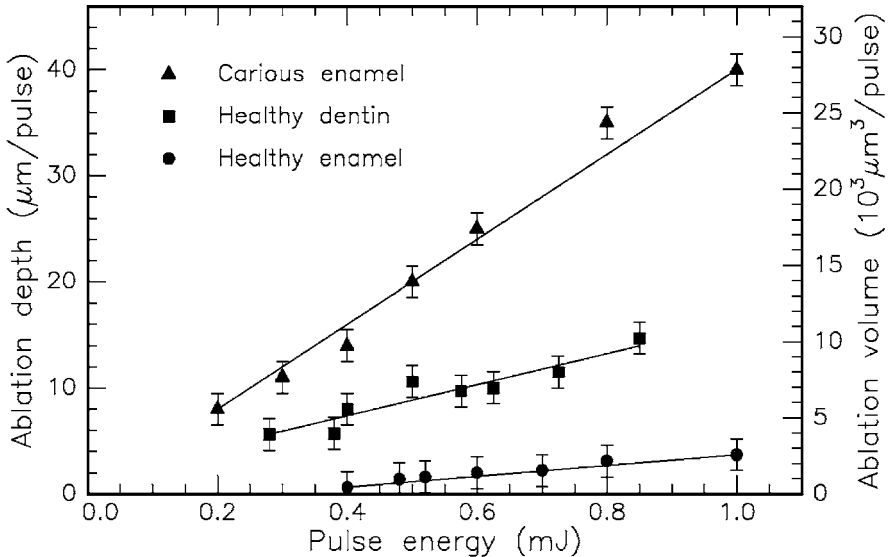
Fig. 4.34. Ablation curves of carious enamel, healthy dentin, and healthy enamel, respectively, obtained with a Nd:YLF laser (pulse duration: 30 ps, focal spot size: 30 μm). Data according to Niemz (1994a) and unpublished data

The results with the Nd:YLF picosecond laser described above have proven that ultrashort laser pulses are a considerable alternative to the mechanical drill for the removal of caries. Due to the recent progress in the generation of even shorter laser pulses, femtosecond lasers have become very promising tools, as well. First experiments with these ultrashort pulse durations have been reported by Niemz (1998). The cavity shown in Fig. 4.35 was achieved with 660 000 pulses from a Ti:Sapphire femtosecond laser at a pulse duration of 700 fs. The geometrical accuracy of the cavity and its steep walls are fascinating.
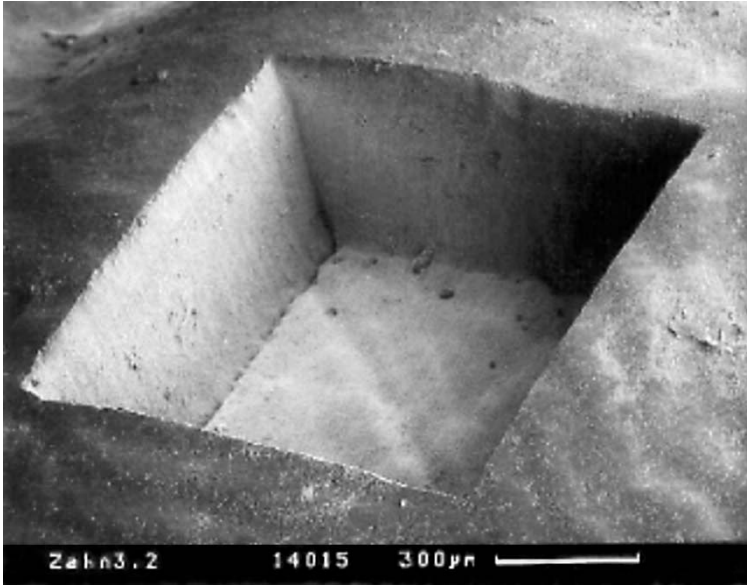
Fig. 4.35. Cavity in healthy enamel achieved with a Ti:Sapphire laser (pulse duration: 700 fs, pulse energy: 100 μJ). Photograph kindly provided by Dipl.-Ing. Bauer (Hannover), Dr. Kasenbacher (Traunstein), and Dr. Nolte (Jena)

In Fig. 4.36, a similar cavity was produced with the same laser but at a larger spacing of adjacent laser pulses. The impacts of individual line scans are clearly visible at the bottom of the cavity. The cavity itself is very clean and of superior quality, if compared to results achievable with conventional diamond drills. Finally, Fig. 4.37 demonstrates the extremely high precision provided by femtosecond lasers. In between exposed areas, unexposed bars remain with a width of less than 10 μm. No mechanical drill is able to achieve similar results. Furthermore, Fig. 4.37 provides the ultimate proof that mechanical shock waves are negligible when applying femtosecond laser pulses at a suitable energy.
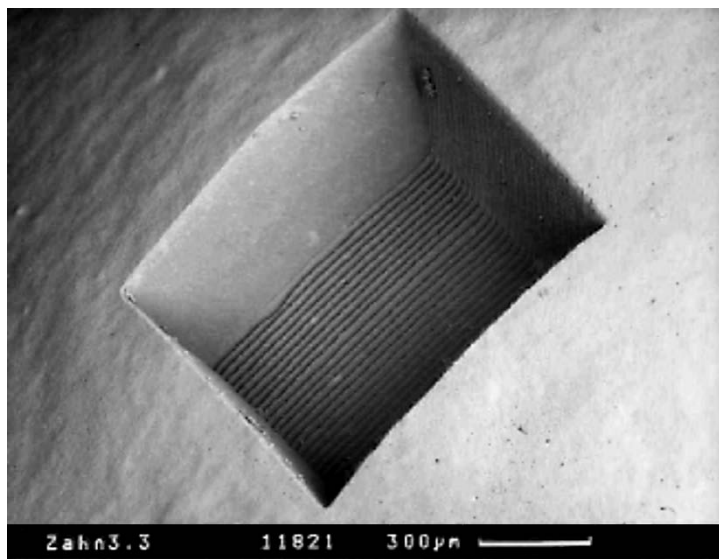
Fig. 4.36. Cavity in healthy enamel achieved with a Ti:Sapphire laser (pulse duration: 700 fs, pulse energy: 100 μJ). Photograph kindly provided by Dipl.-Ing. Bauer (Hannover), Dr. Kasenbacher (Traunstein), and Dr. Nolte (Jena)
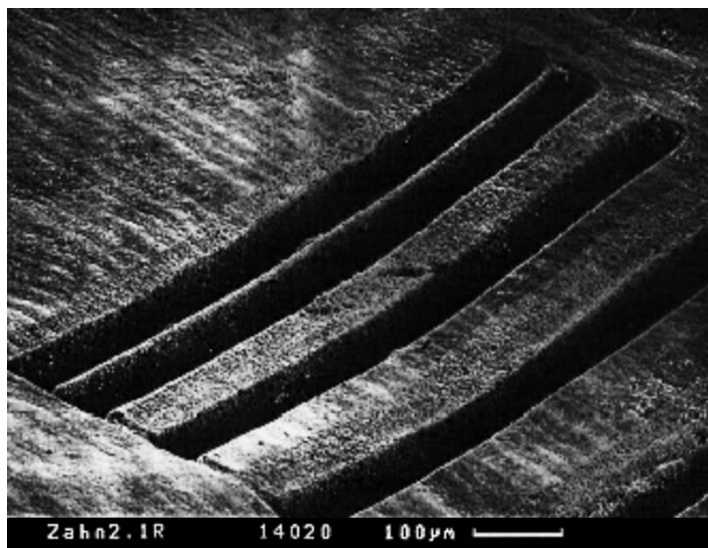
Fig. 4.37. Cavities in healthy enamel achieved with a Ti:Sapphire laser (pulse duration: 700 fs, pulse energy: 100 μJ). Photograph kindly provided by Dipl.-Ing. Bauer (Hannover), Dr. Kasenbacher (Traunstein), and Dr. Nolte (Jena)

One very important issue associated with dental laser systems is the temperature increase inside the pulp where odontoblasts, blood vessels, and tooth nerves are located. Only increments below 5°C are tolerable, otherwise thermal side effects might occur as discussed in Sect. 3.2. Moreover, the feeling of pain is induced at pulp temperatures which exceed approximately 45°C. It is thus very important to remain below these temperatures when striving for clinical applicability. In Fig. 4.38, the temperature increments induced by a picosecond Nd:YLF laser at a repetition rate of 1 kHz are summarized. For this experiment, human teeth were cut into 1 mm thick slices. On one surface of these slices, the laser beam was scanned over a $1 \times 1\,\mathrm{mm}^2$ area, while the temperature was measured at the opposite surface by means of a thermocouple. The observed temperature increments depend on the number of consecutive pulses as well as on the total duration of exposure. We have already stated in Sect. 3.2 that high repetition rates can also induce an increase in temperature even when using picosecond pulses. Hence, a higher temperature is obtained when applying 30 instead of only 10 consecutive pulses before moving the focal spot to the next position. The total duration of exposure also affects the final temperature, although the increase during the first minute is most significant. From these results, we can conclude that up to approximately 10 consecutive pulses may be applied to a tooth at a repetition rate of 1 kHz if the temperature in the pulp shall not increase by more than 5°C.
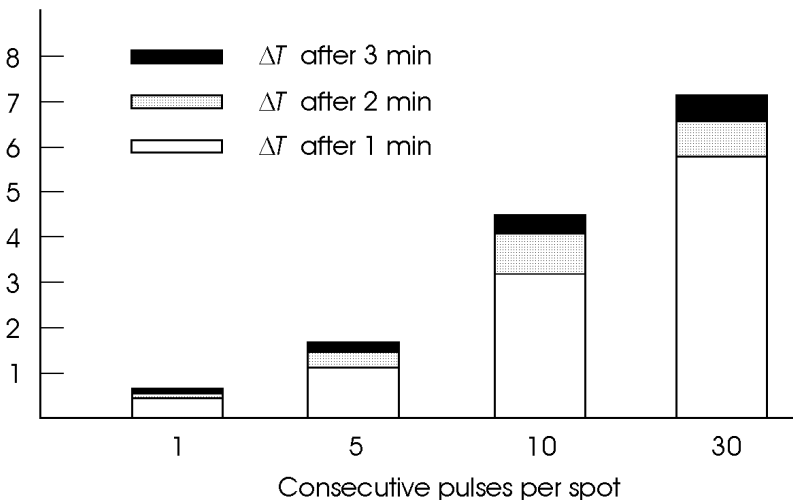
Fig. 4.38. Increase in temperature in a distance of 1 mm from cavities achieved with a Nd:YLF laser (pulse duration: 30 ps, pulse energy: 1 mJ, repetition rate: 1 kHz). Unpublished data

A novel dental application of lasers has recently been proposed by Niemz (1995d). Using a confocal laser scanning microscope, the space to be occupied by dental fillings can be very precisely determined. The confocal principle requires that only light reflected within the focal pane is detected. Thereby, very high axial resolutions can be obtained compared to conventional microscopy. With the confocal microscope, several layers of the cavity to be filled are scanned. From the reflected intensities, a three-dimensional plot of the cavity is calculated as shown in Fig. 4.39a. These data can be inverted to form a direct pattern for the milling of inlays or crowns with a CNC-machine as demonstrated in Fig. 4.39b.
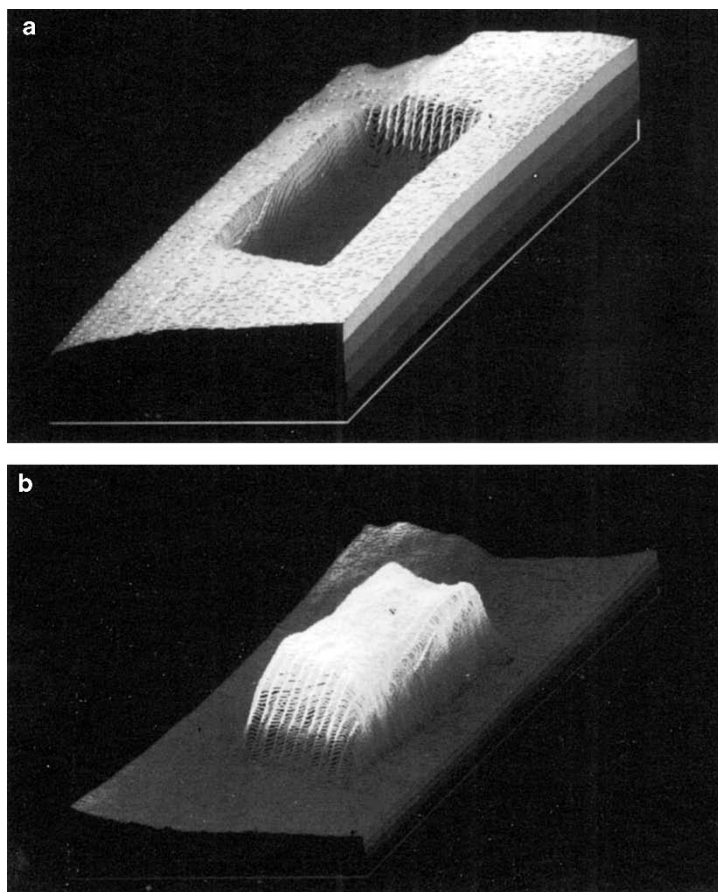
Fig. 4.39. (a) Three-dimensional plot of a laser-induced cavity captured with a confocal laser scanning microscope. The cavity was achieved with a Nd:YLF laser (pulse duration: 30 ps). **(b)** Inverted image of the same cavity as calculated with a computer. Reproduced from Niemz et al. (1995d). © 1995 Springer-Verlag

Laser Treatment of Soft Dental Tissue

Several studies have been reported on the use of a CO_2 laser in the management of malignant, premalignant, and benign lesions of the oral mucosa, e.g. by Strong et al. (1979), Horch and Gerlach (1982), Frame et al. (1984), and Frame (1985). Since the oral environment is very moist, radiation from the CO_2 laser is predestined for such purposes because of its high absorption. When treating a soft tissue lesion inside the mouth, the surgeon has a choice of two techniques – either excision or vaporization. It is usually preferable to excise the lesion because this provides histologic evidence of its complete removal and confirmation of the preceding diagnosis. During vaporization, a risk always remains that not all altered tissue is eliminated. Hence, if a pathologic lesion is vaporized, a biopsy should be obtained from the adjacent tissue after the treatment.

The CO_2 laser is particularly useful for small mucosal lesions. Most of them can be vaporized at a power of 5–10 W in pulsed or CW mode. After laser treatment, the wound is sterile and only minimal inflammatory reactions of the surrounding tissue occur. One major advantage is that there is no need to suture the wound, since small blood vessels are coagulated and bleeding is thus stopped. The wound edges can even be smoothed with a defocused beam. Wound healing usually occurs within a period of two weeks, and the process of reepithelialization is complete after about 4–6 weeks. Frame (1985) states that patients tolerate the procedure well and initially complain of little pain. However, the treated area may become uncomfortable for approximately 2–3 weeks.

Cases of leukoplakia are difficult to treat by conventional surgery, since they are frequently widespread inside the mouth. The lesion is usually outlined with a focused CO_2 laser beam for easy visualization. Afterwards, it is vaporized with a defocused beam at a power of about 15–20 W. According to Horch (1992), laser-treated leukoplakias heal very well, and there is only little evidence of recurrence. Even leukoplakias on the tongue and lips can be treated without losses in performance of these organs.

Malignant lesions require a higher laser power of approximately 20–30 W to deal with the bulk of the tumor. Lanzafame et al. (1986) state that the recurrence of local tumors is reduced when using the CO_2 laser rather than a mechanical scalpel. The thermal effect of the radiation is made responsible for this observation. However, it is questionable whether laser treatments of malignant oral tumors are successful during a longer follow-up period, since metastases have often already spread to other parts of the body. In these cases, laser application is restricted to a palliative treatment. A specimen, for biopsy can also be excised with a CO_2 laser as one would do with a conventional scalpel. More recently, Patel (1988) reported on the application of a Nd:YAG laser in the treatment of oral cancer. However, in the treatment of soft dental tissues, this laser has not gained clinical relevance so far.

Lasers in Endodontics

Endodontics is concerned with the treatment of infections of the root canal. These arise from either a breakthrough of decay into the pulp or from plaque accumulation beneath the gingiva and subsequent bacterial attacks of the root. In either case, once the pulp or the root canal are infected by bacteria, the only treatment is to sterilize both pulp and root, thereby taking into account the associated death of the tooth. However, even a dead tooth may reside in place for years.

The mechanical removal of bacteria, plaque, infected root cementum, and inflammated soft tissues is regarded as an essential part of systematic periodontal treatment. The excavation of the root itself is a very complicated and time-consuming procedure, since roots are very thin and special tools are required. The procedure can be supported by antimicrobial chemicals to ensure sterility which is a mandatory condition for success of the treatment. Along with the rapid development of medical laser systems, it has been discussed whether lasers could improve conventional techniques of endodontics, especially in removal of plaques and sterilization. First experimental results using CO_2 and Nd:YAG lasers in endodontics were published by Weichmann and Johnson (1971) and Weichmann et al. (1972). By means of melting the dentin next to the root, the canal wall appears to be sealed and thus less permeable for bacteria. Indeed, Melcer et al. (1987) and Frentzen and Koort (1990) stated that lasers may have a sterilizing effect. Sievers et al. (1993) observed very clean surfaces of the root canal after application of an ArF excimer laser. However, both the CO_2 laser and the ArF laser will not gain clinical relevance in endodontics, since their radiation cannot be applied through flexible fibers. Even other laser systems will not be applicable exclusively, since suitable fiber diameters of 400 µm are still too large for unprepared roots. Thinner fibers are very likely to break inside the root causing severe complications and additional mechanical operation.

Laser Treatment of Filling Materials

In dental practice, not only tooth substance needs to be ablated but also old fillings have to be removed, e.g. when a secondary decay is located underneath. For the removal of metallic fillings, infrared lasers cannot be used, since the reflectivity of these materials is too high in that spectral range. Amalgam should never be ablated with lasers at all. In Figs. 4.40a–b, two samples of amalgam are shown which were exposed to a Nd:YLF laser and an Er:YAG laser, respectively. During irradiation, the amalgam has melted and a significant amount of mercury has been released which is extremely toxic for both patient and dentist. For other filling materials, e.g. composites, little data are available. Hibst and Keller (1991) have shown that the Er:YAG laser removes certain kinds of composites very efficiently. However, it is quite uncertain whether lasers will ever be clinically used for such purposes.
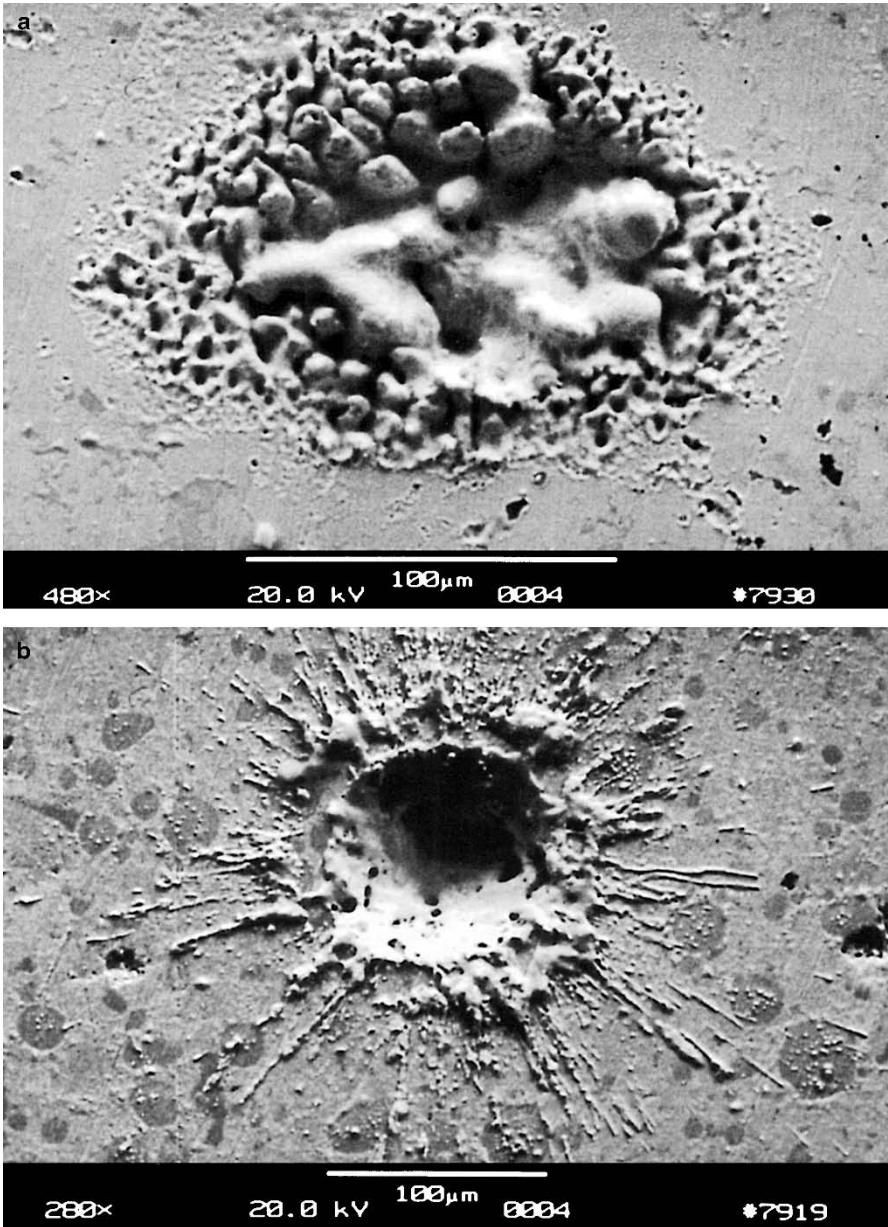
Fig. 4.40. (a) Removal of amalgam with a Nd:YLF laser (pulse duration: 30 ps, pulse energy: 0.5 mJ). **(b)** Removal of amalgam with an Er:YAG laser (pulse duration: 90 μs, pulse energy: 100 mJ)

Another very interesting topic in dental technology is laser-welding of dental bridges and dentures. It can be regarded as an alternative to conventional soldering. During soldering, the parts to be joined are not melted themselves but are attached by melting an additional substance which, in general, is meant to form an alloy between them. Laser-welding, on the other hand, attaches two parts to each other by means of transferring them to a plastic or fluid state. This is achieved with high power densities in the range 10^2–10^9 W/cm^2. According to van Benthem (1992), CO$_2$ lasers and Nd:YAG lasers are preferably used. Since the reflectivity of metals is very high in the infrared spectrum, it must be assured that either a laser plasma is induced at the surface of the target or that the target is coated with a highly absorbing layer prior to laser exposure. Dobberstein et al. (1991) state that some laser-welded alloys are characterized by a higher tear threshold than soldered samples as shown in Fig. 4.41. However, van Benthem (1992) argues that such behavior cannot be observed in all alloys, but tear thresholds in laser-welded alloys can definitely reach the same values as the original cast. According to his studies, the major advantages of laser-welding are: higher resistence against corrosion, the ability to weld different metals, the ability to weld coated alloys, and lower heat load. Moreover, the reproducibility of laser-welded alloys is significantly higher than during soldering. For further results, the interested reader should consult the excellent review given by van Benthem (1992).
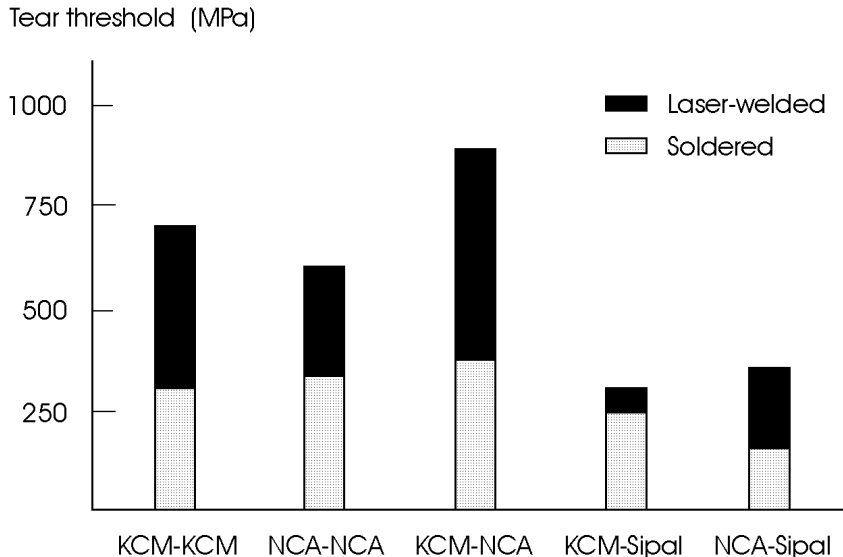
Fig. 4.41. Tear thresholds of laser-welded and soldered dental alloys (KCM: cobalt-based alloy, NCA: nickel-based alloy, Sipal: silver-palladium-based alloy). Data according to Dobberstein et al. (1991)

4.3 Lasers in Gynecology

Beside ophthalmology, gynecology is one of the most significant disciplines for laser applications. This is mainly due to the high success rate of about 93–97 % in treating *cervical intraepithelial neoplasia (CIN)*, i.e. uncommon growth of new cervical tissue, with the CO_2 laser. CIN is the most frequent alteration of the *cervix* and should be treated as soon as possible. Otherwise, cervical cancer is very likely to develop. The cervix represents the connective channel between the *vagina* and *uterus*. The locations of the cervix and adjacent organs are illustrated in Fig. 4.42.
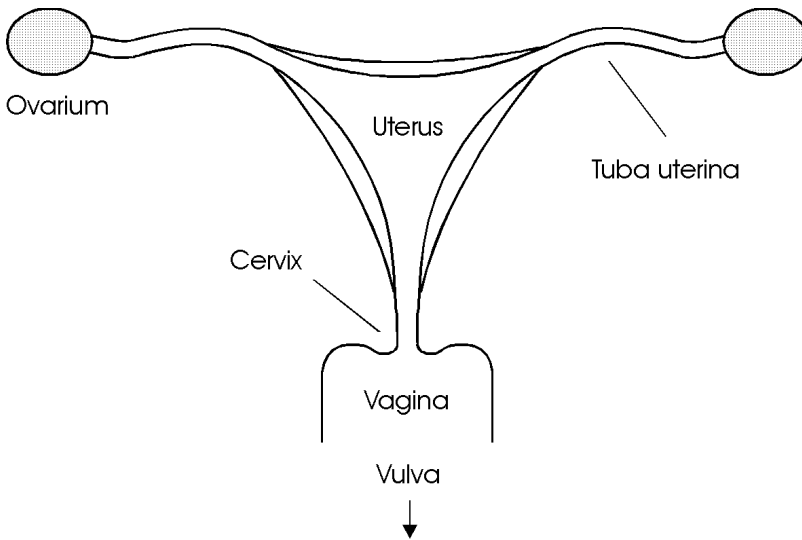
Fig. 4.42. Scheme of female reproduction organs

The CO_2 laser is the standard laser in gynecology. Beside treating CIN, it is applied in vulvar intraepithelial neoplasia (VIN) and vaginal intraepithelial neoplasia (VAIN). Depending on the type of treatment, CO_2 lasers can be operated in three different modes – CW radiation, chopped pulse, and superpulse – as shown in Fig. 4.43. Chopped pulses with durations in the millisecond range are obtained from CW lasers when using rotating apertures. Superpulses are achieved by modulation of the high voltage discharge. Thereby, pulse durations less than 1 ms can be generated. The peak power is inversely related to the pulse duration. The mean powers of CW radiation and chopped pulses are nearly the same, whereas it decreases in the case of superpulses. As discussed in Sect. 3.2, shorter pulse durations are associated with a reduction of thermal effects. Hence, by choosing an appropriate mode of the laser, the best surgical result can be obtained.

Peak power (W)
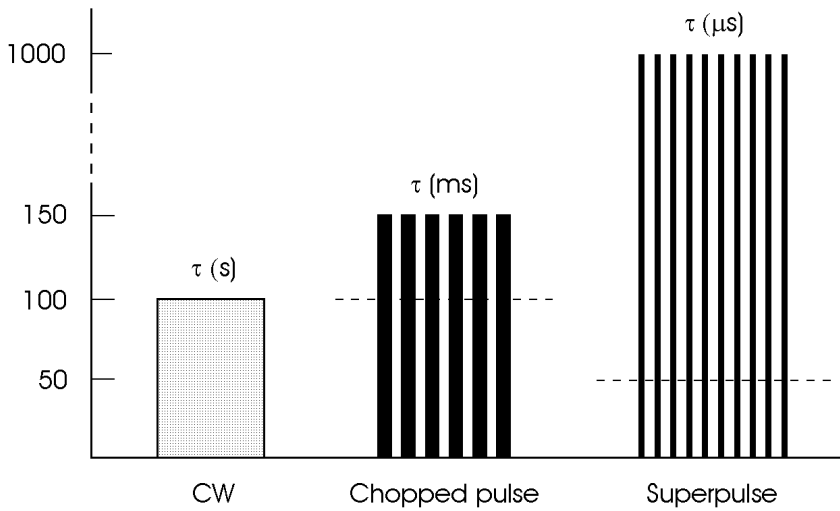
Fig. 4.43. CW, chopped pulse, and superpulse modes of a CO_2 laser. Dashed lines denote mean powers

Beside selecting the temporal mode, the surgeon has to decide whether he applies a focused or defocused mode as shown in Fig. 4.44. Only in tightly focused mode are deep excisions achieved. In partially focused mode, less depth but a larger surface is vaporized. In defocused mode, the power density decreases below the threshold of vaporization, and tissue is coagulated only.
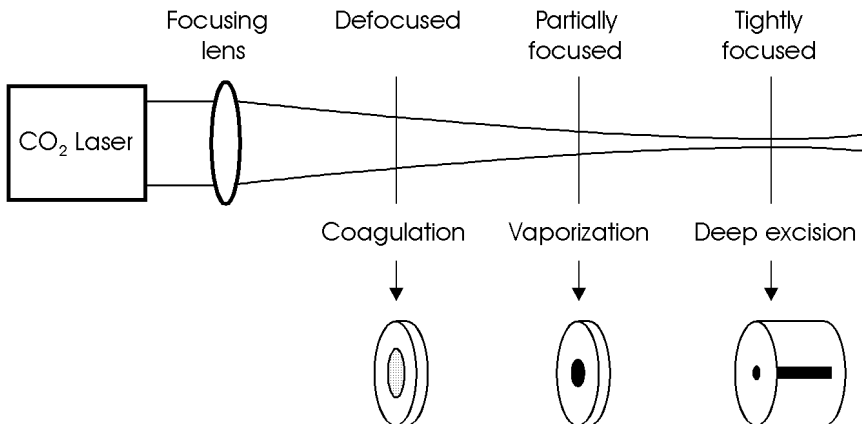
Fig. 4.44. Coagulation, vaporization, and excision modes of a CO_2 laser, depending on a defocused, partially focused, or tightly focused beam

In gynecology, there exist several indications for laser treatment:

- vulvar intraepithelial neoplasia (VIN),
- vaginal intraepithelial neoplasia (VAIN),
- cervical intraepithelial neoplasia (CIN),
- endometriosis,
- obstruction of the uterine tube,
- sterilization,
- twin-twin transfusion syndrome.

Vulvar Intraepithelial Neoplasia (VIN). As already mentioned above, neoplasia generally describes uncommon growth of new tissue. In the case of VIN, intraepithelial tissue of the vulva is significantly proliferated. After histologic examination, the altered tissue is usually vaporized with a CW CO_2 laser in a partially focused mode. According to Baggish and Dorsey (1981), typical power densities of $100\,W/cm^2$ are applied to achieve vaporization depths of about 3–4 mm. In the event of bleeding, the laser beam is immediately switched to a defocused mode.

Vaginal Intraepithelial Neoplasia (VAIN). VAIN is a similar diagnosis as VIN, except that it occurs inside the vagina. Initial studies using the CO_2 laser were reported by Stafl et al. (1977). Due to the thinner and more sensitive vaginal tissue, slightly lower power densities are applied. The use of a proper surgical microscope is indicated.

Cervical Intraepithelial Neoplasia (CIN). The tissue at risk for the development of cervical cancer is the columnar epithelium which is located in the transformation zone. This type of epithelium can migrate up and down the endocervical channel. Therefore, it is very important to determine its exact location prior to any treatment. This is usually achieved with a colposcope which essentially is an endoscope specially designed for gynecologic purposes. The extent of columnar epithelium is relatively constant. Thus, the more it is exposed at the ektocervix, the less likely is the existence of diseased tissue inside the channel. In order to exclude any potential inflammation, a biopsy specimen is obtained and a second or third control examination is performed after 3–6 months. According to the histologic evaluation of the biopsy, three grades of CIN (I–III) and cervical carcinoma are distinguished, depending on the progress of neoplasia. If the biopsy reveals the presence of cervical carcinoma, a complete resection of the cervix is indicated. At a late stage of cancer, adjacent organs such as the uterus or vagina might have to be removed, as well.

In the case of CIN I, the columnar epithelium is usually located at the ektocervix as shown in Fig. 4.45a. The ablated epithelium is vaporized in a similar fashion as in VIN or VAIN. According to Wright et al. (1983), the procedure should aim at a treated depth of approximately 6 mm. Fast movements of the laser beam cause a more homogeneous distribution of heat and thus reduce the probability of carbonization. Scanning mirror devices are

available to assist the surgeon in steadily moving the beam. In Fig. 4.4b (page 156), a vaporization of cervical tissue is shown as achieved with a CO_2 laser at a power of 10 W. Escape of smoke is usually inevitable during surgery, but can be managed with specially designed suction tubes.
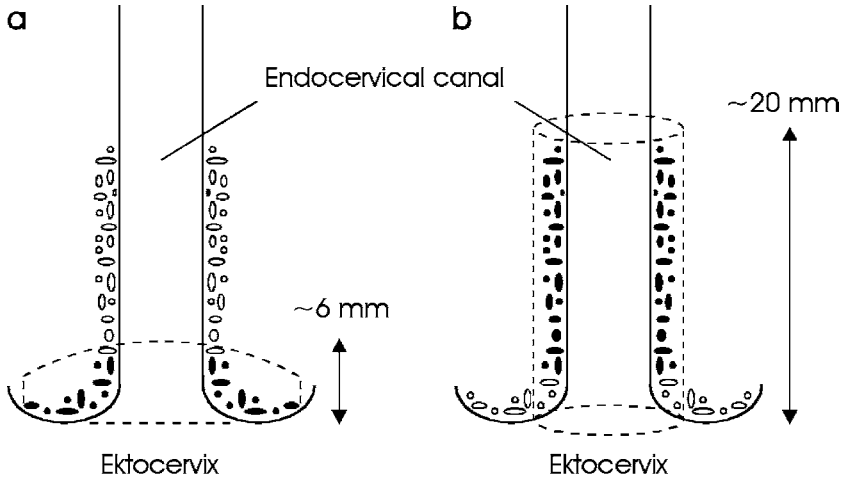
Fig. 4.45. (a) CO_2 laser treatment in the case of CIN I. Diseased epithelium is illustrated by filled ovals. Dashed lines indicate the dome-shaped volume to be vaporized. **(b)** CO_2 laser treatment in the case of CIN II or CIN III. Dashed lines indicate the cylindrical volume to be excised
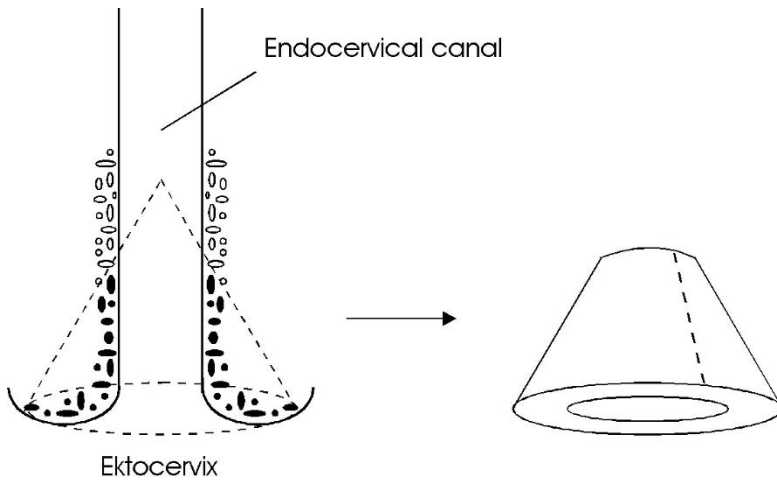
Fig. 4.46. Alternative CO_2 laser treatment in the case of CIN II or CIN III. Diseased epithelium is illustrated by filled ovals. Dashed lines indicate the cone-shaped volume to be excised (*left*). The excised cone is unzipped for histologic examination (*right*)

If CIN II or CIN III is diagnosed, parts of the cervix must be removed to reduce the probability of recurrence. Two different treatment techniques were proposed by Dorsey and Diggs (1979) and Wright et al. (1983). Either surgery is performed only after careful evaluation of the obtained biopsy and determination of the cervical length with a micrometer probe. Dorsey and Diggs (1979) suggest excising a cone-shaped volume out of the cervix with a focused CO_2 laser as demonstrated in Fig. 4.46. The angle of the cone can be adjusted to individual extents of neoplasia. The procedure itself is called *laser conization*. The excised cone is then unzipped for histologic examination as shown in Fig. 4.46. By this means, it can be determined whether all altered tissue has been removed.

An alternative method was proposed by Wright et al. (1983) which is illustrated in Fig. 4.45b. Instead of a cone-shaped volume, a cylindrical volume is removed. The vertical cylindrical excisions are achieved with a focused CW CO_2 laser, whereas the horizontal excision inside the cervix is performed with either a mechanical scalpel or the same CO_2 laser in superpulse mode. After excision of the complete cylinder, the remaining surface is coagulated by defocusing the CW laser beam to achieve local hemostasis. According to Heckmann (1992), cylindrical excisions are better adjusted to individual cases than cone-shaped excisions. In either case, most of the cervical tissue regenerates after being removed. A ten-year review on the treatment of CIN with the CO_2 laser was published by Baggish et al. (1989). In Table 4.4, typical cure rates after one laser treatment are summarized.

Table 4.4. Results of CIN treatment with the CO_2 laser. Data according to Baggish et al. (1989)

	Vaporization	Conization
Number of patients	3070 (100 %)	954 (100 %)
Cured	2881 (93.8 %)	925 (97.0 %)
Persistent	189 (6.2 %)	29 (3.0 %)

According to Wright et al. (1983), laser surgery is an excellent modality for treating CIN when compared to conventional techniques, e.g. cryotherapy. Recently, however, it has been demonstrated by Baggish et al. (1992) that high-frequency electric currents can do the same job as CO_2 lasers. When using thin loops of 10–15 mm in height, similar thermal damage was observed as with a 40 W CO_2 laser. Profound studies with low voltage loop diathermy have already been reported by Prendeville et al. (1986) for the purpose of taking cervical biopsies. Since electrically induced excisions are faster and less expensive equipment is required, they probably represent the preferred choice in the near future. This is one of the few applications, where lasers can – and should – be replaced by simpler surgical tools.

Endometriosis. The cyclic growth of uterine-like mucosa outside the uterus is called *endometriosis*. It appears as dark burns, deep nodules, or vesicles. Endometriosis can be either coagulated, vaporized, or excised. In the 1980s, Keye and Dixon (1983) reported on the use of an argon ion laser in coagulating endometriosis. Further studies soon followed by Feste (1985) and Lomano (1985) using CO_2 and Nd:YAG lasers, respectively. However, treatment of endometriosis with the Nd:YAG laser involves the risk of injuring deeper structures because of the low absorption coefficient at this wavelength. Nevertheless, this laser is being clinically applied in cases of endometriosis which are associated with infertility, and reasonable success rates have been reported, e.g. by Corson et al. (1989) and Shirk (1989). Deeply located endometriosis is usually excised rather than vaporized. A scalpel is still necessary to cut off the distal end.

Obstruction of the Uterine Tube. Tubal obstructions can be caused by either adhesions, proliferated growth of tissue, or tubal pregnancies. In the case of adhesions, *salpingolysis* is performed, i.e. the recanalization of the *salpinx* (from Greek: $\sigma\alpha\lambda\pi\iota\gamma\xi$ = trumpet). By means of CO_2 or Nd:YAG laser radiation, the adhesions are vaporized to obtain a free tubal lumen. Care should be taken not to traumatize the endothelium of the tube, since this can cause troublesome bleeding as well as damage to the tube. In the presence of proliferated growth of tissue, additional openings of the tube can be generated in a treatment called *salpingostomy*. Tubal pregnancies can usually be managed by either salpingostomy or *salpingectomy*. Salpingectomy denotes the complete removal of one tube. Successful laser treatment of tubal pregnancies was reported by Huber et al. (1989).

Sterilization. A sure way to achieve sterilization is to artifically occlude both uterine tubes. This is performed by either suturing the tube or by coagulating it with a Nd:YAG laser. According to Bailer (1983), safe sterilization is obtained when coagulating both tubes on a length of about 1 cm.

Twin-Twin Transfusion Syndrome. This syndrome is caused by a misplaced shunt vessel between the twins. It usually leads to an unbalanced blood supply and is often lethal to both twins. In pilot studies, De Lia et al. (1995) and Ville et al. (1995) have just recently demonstrated that occlusion of this vessel by means of coagulation with a Nd:YAG laser is technically feasible.

Gynecology comprises a wide range of potential laser applications. An excellent review is found in the book by Bastert and Wallwiener (1992). Several minimally invasive techniques have already been described above, but others are yet to be developed. Very promising is the recently established method of laser-induced interstitial thermotherapy (LITT) which can be used to coagulate malformations inside the uterus by means of thin optical fibers. Initial studies have already been reported by Wallwiener et al. (1994). Thus, lasers might turn into irreplaceable gynecologic tools, especially in the presence of pregnancies where conventional surgery is often lethal to the fetus.

4.4 Lasers in Urology

The workhorse lasers of urology are primarily CO_2, argon ion, Nd:YAG, and dye lasers. CO_2 lasers are best in precise cutting of tissue as already discussed in Sect. 3.2. Argon ion lasers and Nd:YAG lasers are used for the coagulation of highly vascularized tumors or malformations. Among these two lasers, the Nd:YAG laser is preferably applied for the coagulation of large tissue volumes because its radiation deeply penetrates into tissues. Moreover, Q-switched Nd:YAG lasers which interact in the photodisruptive mode have become a standard tool in lithotripsy beside ultrasound fragmentation. Dye lasers have not been investigated until recently in lithotripsy and in photo-dynamic therapy.

After the development of the first fiberoptic endoscope by Nath et al. (1973), Staehler et al. (1976) performed initial experimental studies with the argon ion laser in urology. Meanwhile, the indications for urologic laser treatments have significantly increased. They extend from the *external genital*, the *lower urinary tract (urethra)*, the *bladder*, the *upper urinary tract (ureter)*, all the way up to the *kidneys* as shown in Fig. 4.47. In addition, very promising results have already been achieved in treating benign hyperplasia of the *prostate* which embraces the urethra. Various laser therapies for all these different organs require specific strategies and parameters. They shall now be discussed in the above order.
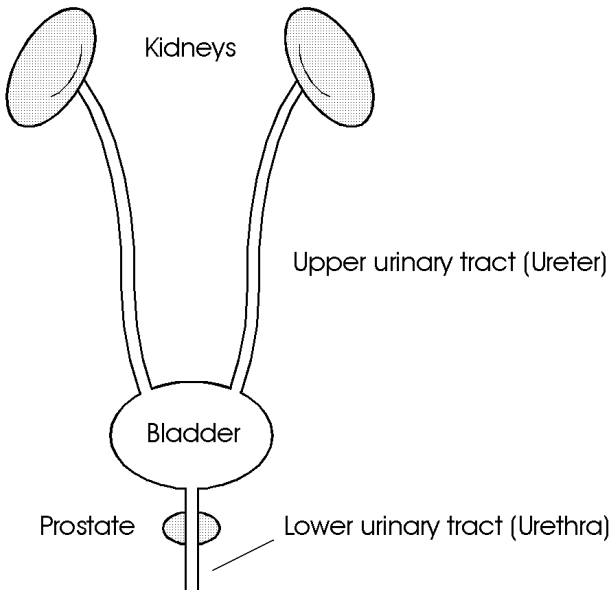
Fig. 4.47. Scheme of male urinary tract

The most frequent malformations of the external genital are called *condylomata acuminata*. These benign warts must be treated as early as possible, because they tend to be very infectious and degenerating. After circumcision and application of 4 % acetic acid to suspected areas, they are coagulated with either Nd:YAG or CO_2 lasers. Occasional recurrences cannot be excluded, especially in the treatment of intraurethral condylomata. With both laser types, however, the rate of recurrence is less than 10 % as reported by Baggish (1980) and Rosemberg (1983). Hemangiomas of the external genital should be treated with radiation from Nd:YAG lasers because of its higher penetration depth. Hofstetter and Pensel (1993) stated that additional cooling of the tissue surface may even improve the procedure. Carcinoma of the external genital are best treated with a Nd:YAG laser if they are at an early stage. This significantly reduces the risk of having to perform a partial amputation. According to Eichler and Seiler (1991), powers of 40 W and focal spot sizes of 600 μm are usually applied. At an advanced stage, the tumor is first mechanically extirpated. Afterwards, the remaining tissue surface should be additionally coagulated.

Frequent diseases of the lower urinary tract are stenoses induced by either inflammation, tumor growth, or unknown origins. In these cases, *urethrotomy* by endoscopic control is usually performed as proposed by Sachse (1974). During this conventional technique, stenotic material is removed with a cold scalpel. Unfortunately, restenoses often occur due to scarring of the tissue. Further urethrotomies are not of great help, since they only enhance additional scarring. The first recanalizations of urethral stenoses with an argon ion laser were performed by Rothauge (1980). However, the results obtained were not as promising as initially expected. Then, no further progress was made until Wieland et al. (1993) recently published first results using a Ho:YAG laser. Meanwhile, follow-up periods of 20 months after Ho:YAG laser treatment were reported by Nicolai et al. (1995). They concluded that this technique is a considerable alternative to mechanical urethrotomy in virgin stenoses as well as restenoses. The probability for the occurrence of laser-induced restenoses is approximately 10 % only. In Figs. 4.48a–b, the effects of the Ho:YAG laser on the urethra and ureter are shown, respectively. In both samples, thirty pulses with an energy of 370 mJ and an approximate duration of 1 ms were applied.

Tumors of the bladder are very difficult to treat, since they tend to recur after therapy. It is yet unknown whether this is due to metastasation induced either prior to or by the treatment. Unfortunately, bladder tumors also easily break through the bladder wall. Thus, a treatment is successful only if it completely removes the tumor, does not perforate the bladder wall, and does not damage the adjacent intestine. Frank et al. (1982) have compared the effects of CO_2, Nd:YAG, and argon ion lasers on bladder tissue. Among these, the Nd:YAG laser has proven to be best suited in coagulating bladder tumors. Argon ion lasers are applicable only in superficial bladder tumors.
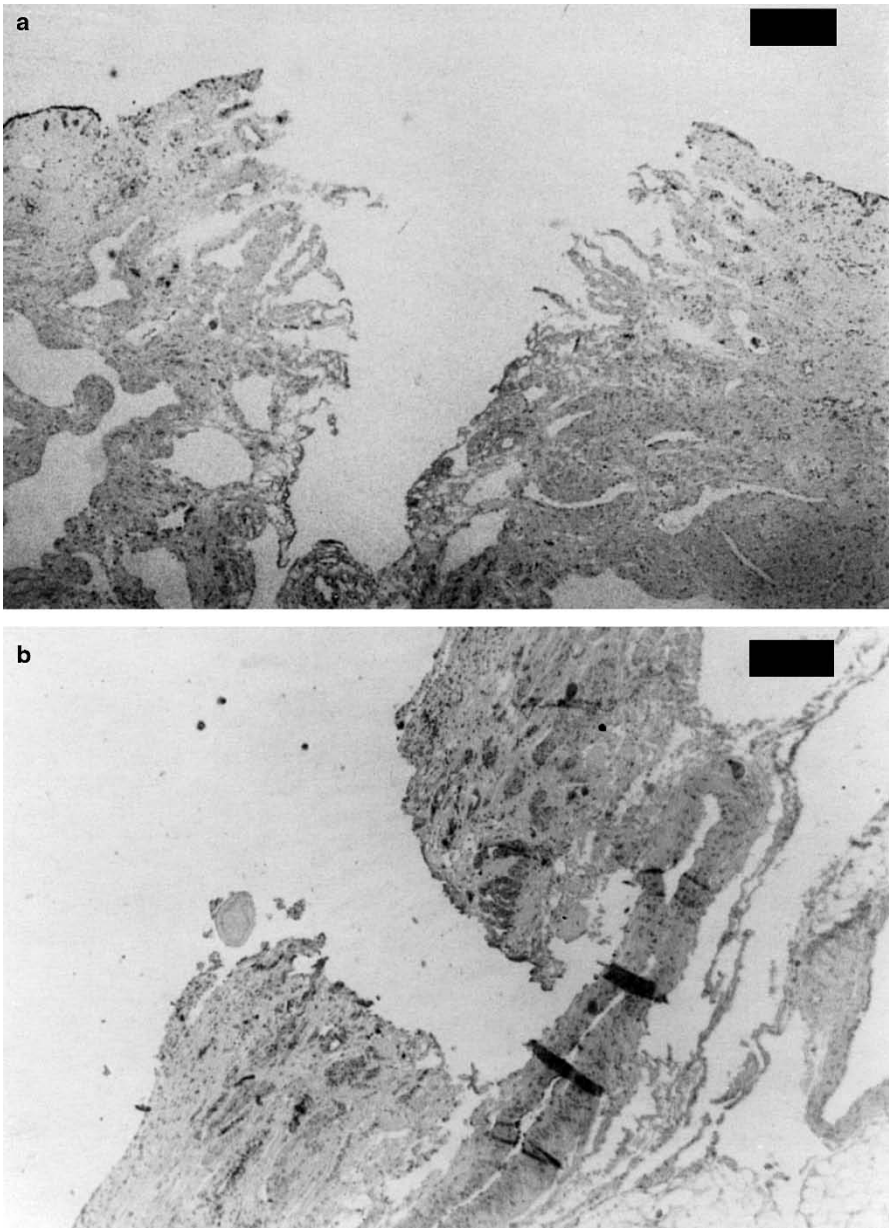
Fig. 4.48. (a) Effect of thirty pulses from a Ho:YAG laser (pulse duration: 1 ms, pulse energy: 370 mJ, bar: 250 μm) on the urethra. **(b)** Effect of thirty pulses from a Ho:YAG laser (pulse duration: 1 ms, pulse energy: 370 mJ, bar: 250 μm) on the ureter. Photographs kindly provided by Dr. Nicolai (Regensburg)

According to Hofstetter et al. (1980), the rate of recurrence after laser treatment is approximately 1–5 %, whereas it ranges from 40–60 % if conventional transurethral resection (TUR) is performed. Even advanced tumors can be efficiently removed with Nd:YAG lasers, since the hemostatic treatment guarantees best vision. Pensel (1986) suggests the application of 30–40 W of laser power and a working distance between 1 mm and 2 mm. The tumor should be irradiated until it visibly pales. Afterwards, coagulated necrotic tissue is mechanically removed. For safety reasons, the remaining tissue surface should be coagulated, as well.

It was emphasized by Hofstetter and Pensel (1993) that tumors can still be graded and staged by biopsies after coagulation. Usually, control biopsies should be obtained within the next 3–6 months. The laser treatment itself is extremely safe, since perforations of the bladder wall are very unlikely, and the function of the bladder remains unaffected. All transurethral treatments are performed with a rigid cytoscope and a flexible fiber. In most cases, local anesthetization is sufficient.

Recently, photodynamic therapy (PDT) has gained increasing significance in the treatment of bladder tumors. First endoscopic applications of HpD have already been investigated by Kelly and Snell (1976). Several clinical reports on PDT are available, e.g. by Benson (1985), Nseyo et al. (1985), and Shumaker and Hetzel (1987). A complete treatment system including in vivo monitoring and dose control was decribed by Marynissen et al. (1989). A list of potential complications arising when using dihematoporphyrin ether was given by Harty et al. (1989). Today, photodynamic therapy is considered as a useful supplement to other techniques, since it enables the resection of tumors which are not visible otherwise. The ability of simultaneous diagnosis – by means of laser-induced fluorescence – and the treatment of tumors is thus one of the key advantages of photodynamic therapy. So far, red dye lasers at 630 nm and energy densities between 10–50 J/cm^2 are usually applied. In most cases, laser treatment is still restricted to superficial tumors due to the limited penetration depth at the specific wavelength. However, the recent discovery of novel photosensitizers like 5-aminolaevulinic acid (ALA) – as already discussed in Sect. 3.1 – will certainly improve photodynamic therapy in urology during the next few years.

Lithotripsy of urinary calculi is often based on ultrasound techniques. However, not all calculi are equally indicated for such an external therapy. In particular, those calculi which are stuck inside the ureter are in an extremely inconvenient location. In these cases, laser-induced lithotripsy offers the advantage of directly applying energy to the vicinity of the calculus by means of a flexible fiber. First experiments regarding laser lithotripsy have already been performed by Mulvaney and Beck (1968) using a ruby laser. From today's perspective, though, it is quite obvious that these initial studies had to be restricted to basic research, since they were associated with severe thermal side effects. Watson et al. (1983) first proposed the application of a Q-

switched Nd:YAG laser. Shortly after, pulsed dye lasers were investigated by Watson et al. (1987). With the decrease in pulse durations, additional complications arose concerning induced damage of the fiber. Extensive calculations of the limits of fiber transmission were published by Hering (1987). The advantages of different approaches like bare fibers or focusing fiber tips were studied by Dörschel et al. (1987) and Hofmann and Hartung (1987). Furthermore, a review of 20 years of laser lithotripsy experience was given by Dretler (1988).

Today, dye lasers and Nd:YAG lasers are preferably used for lithotripsy of urinary calculi inside the ureter. A detailed description of the procedure was given by Hofstetter et al. (1986). Typically, pulse energies of 50–200 mJ and pulse durations between 10 ns and 1 μs are applied. The diameter of the optical fiber varies between 200 μm and 600 μm. With these parameters, optical breakdown is achieved close to the target. As described in Sect. 3.5, plasma formation at high pulse energies is associated with shock waves, cavitations, and jets. This photodisruptive interaction finally leads to the fragmentation of urinary calculi.

Since the 1980s, research in urology has increasingly focused on various treatments of the prostate. This very sensitive organ embraces the urethra. Diseases of the prostate, e.g. benign hyperplasias or carcinoma, thus often tend to handicap the discharge of urine. A profound analysis of the development of benign prostatic hyperplasia (BPH) was given by Berry et al. (1984). Several conventional therapies are available, e.g. the initial application of phytopharmaka or transurethral resection in severe cases. Other techniques such as cryotherapy or photodynamic therapy have also been investigated, e.g. by Bonney et al. (1982) and Camps et al. (1985). A complete list of potential treatment methods was provided by Mebust (1993). During the first few years, research was restricted to the treatment of prostatic carcinoma. Böwering et al. (1979) were the first to investigate the effect of Nd:YAG laser radiation on tumors of the prostate. Shortly after, several detailed reports followed, e.g. by Sander et al. (1982) and Beisland and Stranden (1984). The latter study pointed out the extreme importance of temperature monitoring of the adjacent rectum. Extensive clinical results were reported by McNicholas et al. (1988). Usually, indication for laser treatment is given only if the tumor cannot be completely resected otherwise.

At the beginning of the 1990s, the demand for minimally invasive techniques significantly increased. In the treatment of BPH, two milestones were achieved with the development of improved surgical techniques called *transurethral ultrasound-guided laser-induced prostatectomy (TULIP)* and *laser-induced interstitial thermotherapy (LITT)*. The idea of TULIP was proposed by Roth and Aretz (1991) and Johnson et al. (1992). Detailed clinical results were published by McCullough et al. (1993). The key element of TULIP is to position a 90° prism inside the urethra by ultrasound control. Thereby, the precision in aiming at the target is strongly enhanced.

In other studies, Siegel et al. (1991) have shown that hyperthermia alone, i.e. temperatures up to 45°C, is not sufficient in treating BPH. This has led to the idea of LITT as already described in Sect. 3.2. During LITT, the tissue is completely coagulated, i.e. temperatures above 60°C are obtained. The technical realization of suitable ITT fibers was discussed by Hessel and Frank (1990). In urology, initial experimental results with LITT were published by McNicholas et al. (1991) and Muschter et al. (1992). With typical laser powers of 1–5 W, coagulation volumes with diameters of up to 40 mm are achieved. Meanwhile, Muschter et al. (1994) have reported on clinical studies with approximately 200 patients. Roggan et al. (1994) have determined the optical parameters of prostatic tissue for diode lasers at 850 nm and Nd:YAG lasers at 1064 nm, respectively. Their data are found in Table 2.3. Moreover, they observed that the scattering coefficient of prostatic tissue increases during coagulation by an appoximate factor of two. With these data and appropriate computer simulations, they were able to optimize the parameters for an efficient procedure.

In Fig. 4.49, the most significant postoperative results of LITT in the treatment of BPH are summarized. According to Muschter et al. (1993), the peak urinary flow rate increased from 6.6 ml/s to 15.2 ml/s two months after treatment, whereas the residual urinary volume decreased from 206 ml to 38 ml. The mean weight of the prostate dropped from 63 g to 44 g during the same period. These data are based on mean values obtained from 15 patients. Severe complications were not observed. From these results, it can be concluded that LITT is an excellent therapy for BPH.
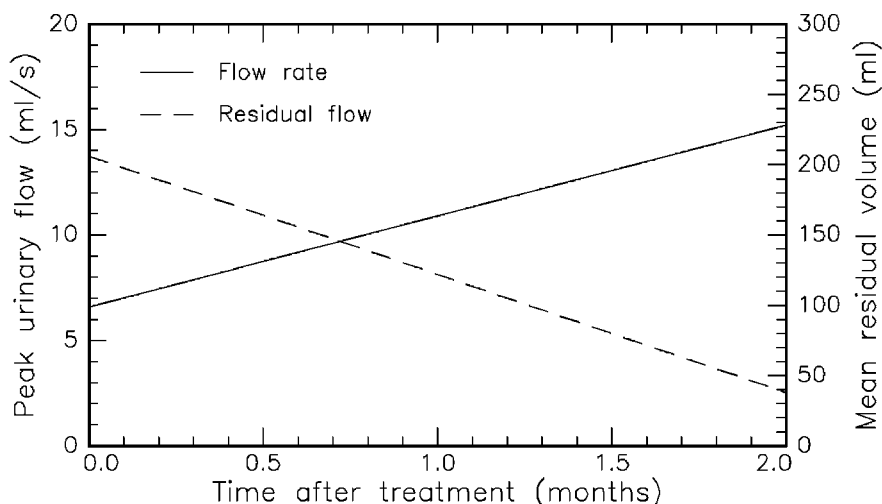
Fig. 4.49. Peak urinary flow and mean residual urinary volume after LITT of benign prostatic hyperplasia. The data represent mean values from 15 patients. Data according to Muschter et al. (1993)

4.5 Lasers in Neurosurgery

Neurosurgery deals with diseases of the central nervous system (CNS), i.e. the brain and the spine. Surgery of brain tumors is very difficult, since extremely localized operations are necessary due to the complicated structure and fragility of the brain. Moreover, the tumor itself is often not easily accessible, and very important vital centers are situated beside it. Therefore, it is not surprising that a considerable amount of research funds is currently being spent in this field, especially since any kind of brain tumor – even benign tumors – are extremely life-threatening. This is because space inside the skull is very limited. Hence, growth of new tissue increases the pressure inside the brain which leads to mechanical damage of other neurons. A schematic cross-section of the brain is shown in Fig. 4.50.
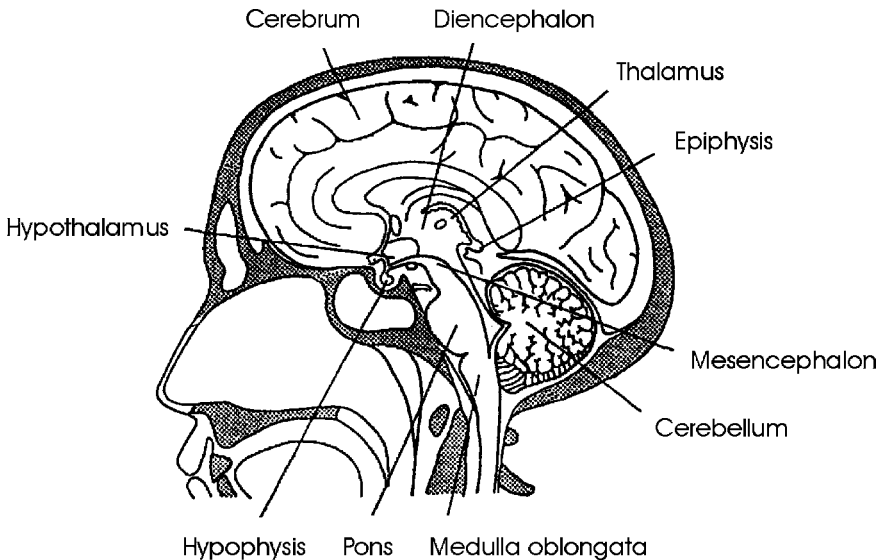
Fig. 4.50. Scheme of a human brain

The major parts of the brain are the cerebrum, diencephalon, cerebellum, and brainstem. The diencephalon can be further divided into the hypothalamus, hypophysis, thalamus, and epiphysis, whereas the brainstem consists of the mesencephalon, pons, and medulla oblongata. Usually, tumors of the brainstem are highly malignant and, unfortunately, they reside in an inaccessible location. In general, brain tissue can be divided into *gray matter* and *white matter* which are made up of cell nuclei and axons, respectively. Blood perfusion of gray and white matter differs remarkably. The corresponding ratio is about five to one.

The application of lasers in neurosurgery has been extremely slow compared with other medical fields, e.g. ophthalmology. This was mainly due to two reasons. First, studies by Rosomoff and Caroll (1966) revealed that the ruby laser was not of great help in neurosurgery. Second, initial experiments with the CO_2 laser were performed at too high energy levels, e.g. by Stellar et al. (1970), which was dangerous and completely unnecessary. It then took some time until Ascher (1979), Beck (1980), and Jain (1983) reawakened interest in neurosurgical lasers, especially moderate CO_2 lasers and Nd:YAG lasers. The principal advantages of lasers in neurosurgery are evident. Lasers are able to cut, vaporize, and coagulate tissue without mechanical contact. This is of great significance when dealing with very sensitive tissues. Simultaneous coagulation of blood vessels eliminates dangerous hemorrhages which are extremely life-threatening when occurring inside the brain. Moreover, the area of operation is sterilized as lasing takes place, thereby reducing the probability of potential infections.

According to Ascher and Heppner (1984) and Stellar (1984), the main advantage of the CO_2 laser is that its radiation at a wavelength of $10.6\,\mu m$ is strongly absorbed by brain tissue. By this means, very precise cuts can be performed. However, CO_2 lasers are not appropriate for the coagulation of all blood vessels. In particular, arteries and veins with diameters $> 0.5\,mm$ tend to bleed after being hit by the laser beam. Nd:YAG lasers, on the other hand, are effective in coagulating blood vessels as stated by Fasano et al. (1982) and Wharen and Anderson (1984b). Ulrich et al. (1986) even observed very good results on both ablation and coagulation when combining a Nd:YAG laser emitting at $1.319\,\mu m$ and a $200\,\mu m$ fiber. The biological response of brain tissue to radiation from Nd:YAG lasers was extensively studied by Wharen and Anderson (1984a). A preliminary report on the clinical use of a Nd:YAG laser was given by Ascher et al. (1991). Moreover, neurosurgical applications of argon ion lasers had been investigated by Fasano (1981) and Boggan et al. (1982), but they seem to be rather limited, since radiation from these lasers is strongly scattered inside brain tissue.

The main problem with CW lasers is that they do not remove brain tumors but only coagulate them. Necrotic tissue remains inside the brain and can thus lead to the occurrence of severe edema. Moreover, adjacent healthy tissue might be damaged due to heat diffusion, as well. Recently, two alternative lasers have been investigated concerning their applicability to neurosurgery: Er:YAG and Nd:YLF lasers. Cubeddu et al. (1994) and Fischer et al. (1994) have studied the ablation of brain tissue using free-running and Q-switched Er:YAG lasers. They observed limited thermal alterations of adjacent tissue. However, mechanical damage was very pronounced. Since the Er:YAG laser emits at a wavelength of $2.94\,\mu m$, its radiation is strongly absorbed in water as already discussed in Sect. 3.2. Thus, soft brain tissue – having a high water content – is suddenly vaporized which leads to vacuoles inside the tissue with diameters ranging up to a few millimeters. In Fig. 4.51a, mechanical damage
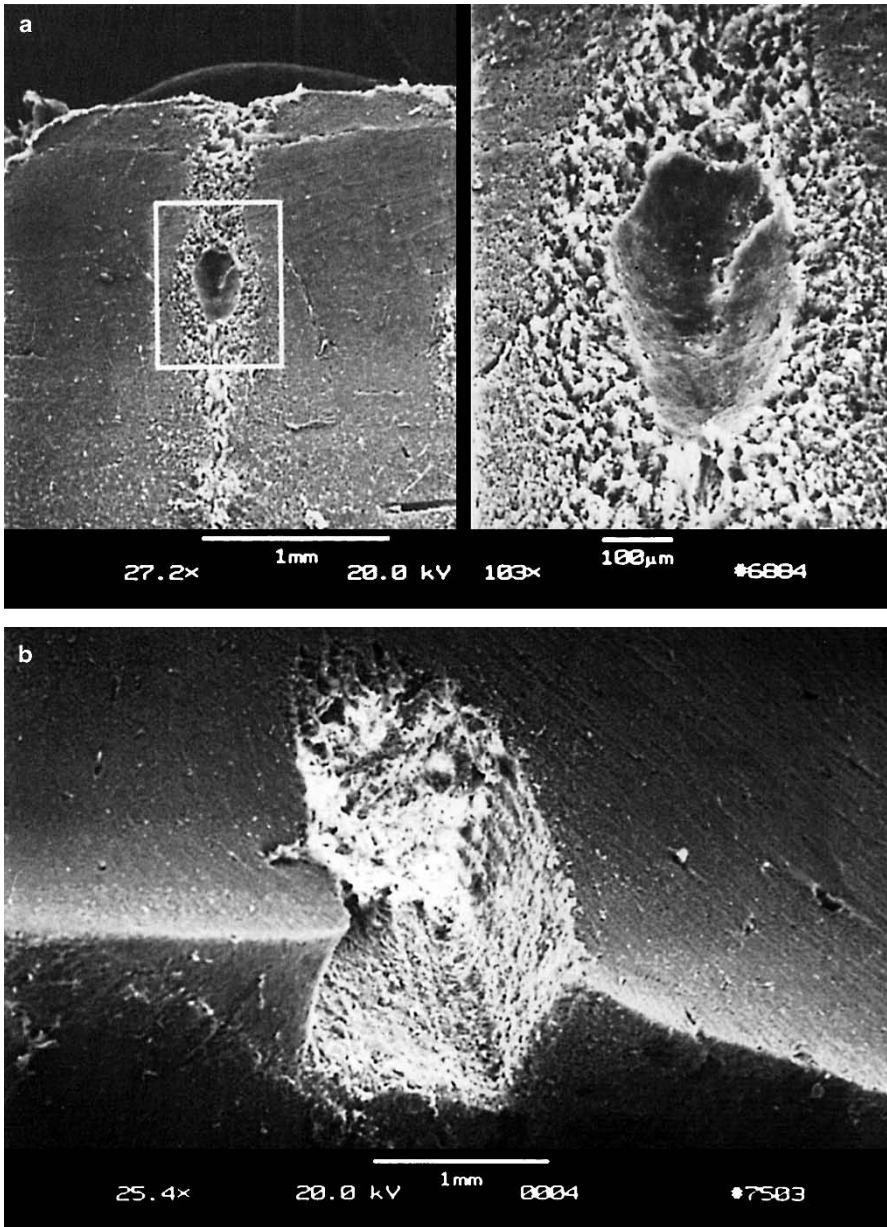
Fig. 4.51. (a) Brain tissue after exposure to an Er:YAG laser (pulse duration: 90 μs, pulse energy: 60 mJ). Mechanical damage is evident. **(b)** Voluminous ablation of brain tissue achieved with the same laser. Reproduced from Fischer et al. (1994) by permission. © 1994 Springer-Verlag

up to a depth of at least 1.5 mm is clearly visible. Therefore, it is not very helpful that even large volumes of brain tissue can be ablated with Er:YAG lasers as shown in Fig. 4.51b.

The ablation of brain tissue with a picosecond Nd:YLF laser system was investigated by Fischer et al. (1994). In Fig. 4.52, the ablation depths of white and gray brain matter are given, respectively. Obviously, there is no significant difference in ablating either substance. It is interesting to observe, though, that there is no saturation in ablation depth even at energy densities as high as $125\,\mathrm{J/cm^2}$. Thus, higher laser powers will probably enable ablation depths $> 200\,\mathrm{\mu m}$. Fischer et al. (1994) state that the corresponding ablation threshold is at approximately $20\,\mathrm{J/cm^2}$.
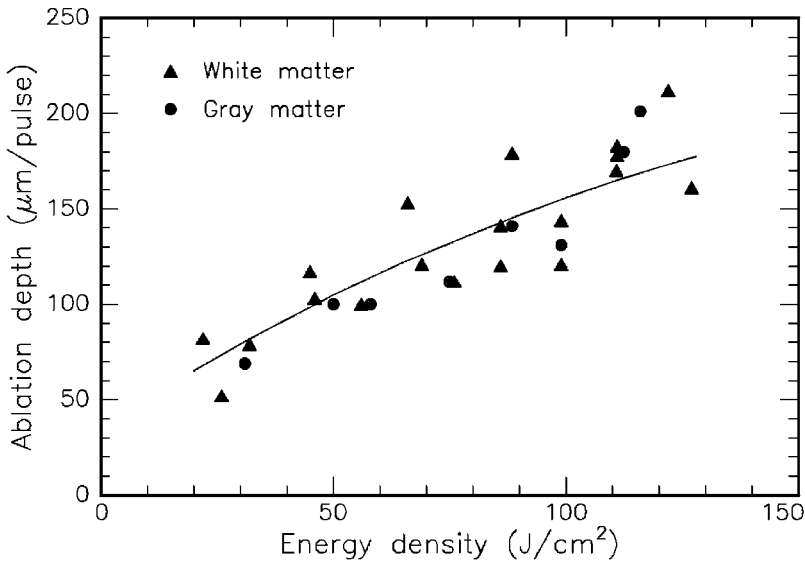
Fig. 4.52. Ablation curve of white and gray brain matter obtained with a Nd:YLF laser (pulse duration: 30 ps, focal spot size: $30\,\mathrm{\mu m}$). Data according to Fischer et al. (1994)

Two samples of brain tissue which were exposed to the Nd:YLF laser are shown in Figs. 4.53a–b. A rectangular ablation geometry was achieved by scanning the laser beam. The lesion in Fig. 4.53a is characterized by steep walls and is approximately $600\,\mathrm{\mu m}$ deep. In Fig. 4.53b, a histologic section of an ablation edge is shown as obtained with the Nd:YLF laser. The tissue was stained with cluever barrera to visualize any thermal effects. There is no evidence of either thermal or mechanical damage to adjacent tissue. Hence, removal of tissue can be attributed to the process of plasma-induced ablation as described in Sect. 3.4. Nonthermal ablation of tissue is a mandatory requirement for precise functional surgery of the brain.
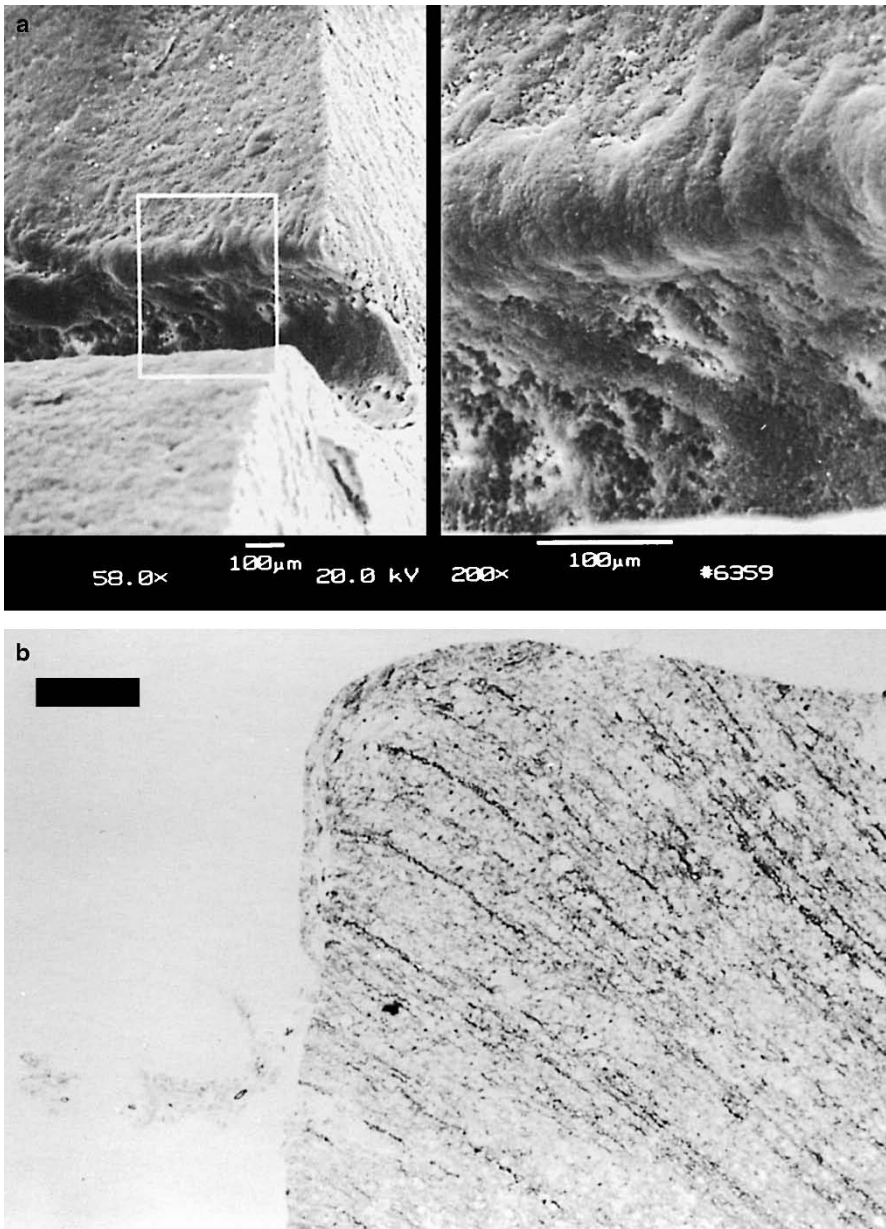
Fig. 4.53. (a) Brain tissue after exposure to a picosecond Nd:YLF laser (pulse duration: 30 ps, pulse energy: 0.5 mJ). **(b)** Histologic section of brain tissue after exposure to the same laser (bar: 50 μm). Reproduced from Fischer et al. (1994) by permission. © 1994 Springer-Verlag

A very precise technique is called *stereotactic neurosurgery* which was
described in detail by Kelly et al. (1982). It requires a so-called stereotactic
head ring made of steel or carbon fibers which is tightly fastened to the pa-
tient's skull by several screws. This ring defines a coordinate system which
serves as a valuable means of orientation during surgery. The head ring ap-
pears on CT or magnetic resonance images (MRI) and thus determines the
coordinates of the tumor. Various kinds of aiming devices can be mounted
to the ring allowing for precise operation in all three dimensions. The main
goal of stereotactic neurosurgery is to plan a suitable penetration channel
in advance of surgery, set its coordinates with respect to the head ring, and
then keep this channel during surgery. By this procedure, the risk of hitting
a vital center within the brain can be significantly reduced, and the success
of a treatment becomes more predictable.

The concept of stereotactic laser–neurosurgery according to Bille et al.
(1993) is illustrated in Fig. 4.54. By means of a stereotactic head ring, a laser
probe is inserted into the brain. CT and NMR data are used to correctly
position the distal end of the probe inside the tumor. A schematic drawing
of the laser probe is given in Fig. 4.55. It basically consists of a conical tube
which contains a rotating mirror at its distal end, a movable focusing lens,
and additional channels for aspiration and rinsing. Aspiration is necessary to
maintain a constant pressure at the site of operation. The laser probe is rinsed
to remove debris from the rotating mirror and to increase the efficiency of the
ablation process. The rotating mirror deflects the laser beam perpendicularly
to the axis of rotation. Tissue is thus ablated in cylindrical layers as shown
in Fig. 4.55. Furthermore, it is planned to integrate a confocal laser scanning
microscope into this system for the automatic detection of blood vessels as
illustrated in Fig. 4.56.
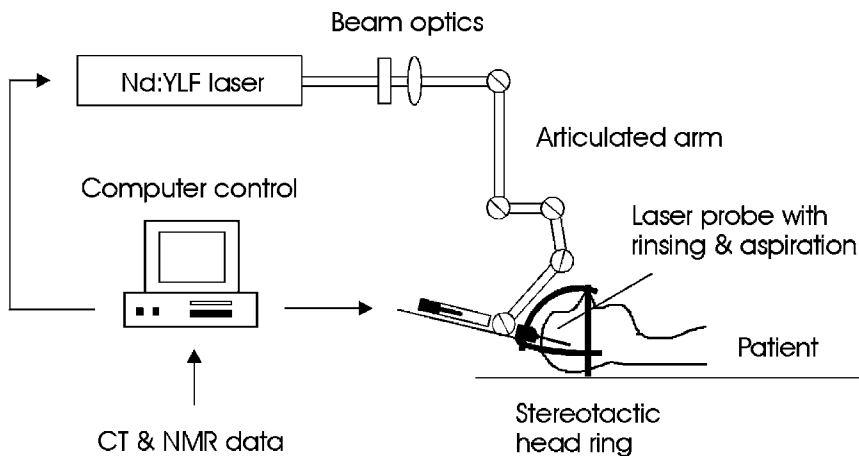
Fig. 4.54. Concept of stereotactic laser–neurosurgery

Rotation

Laser probe

Focusing lens

Geometry of ablation

Up and down
movement

Optical
breakdown
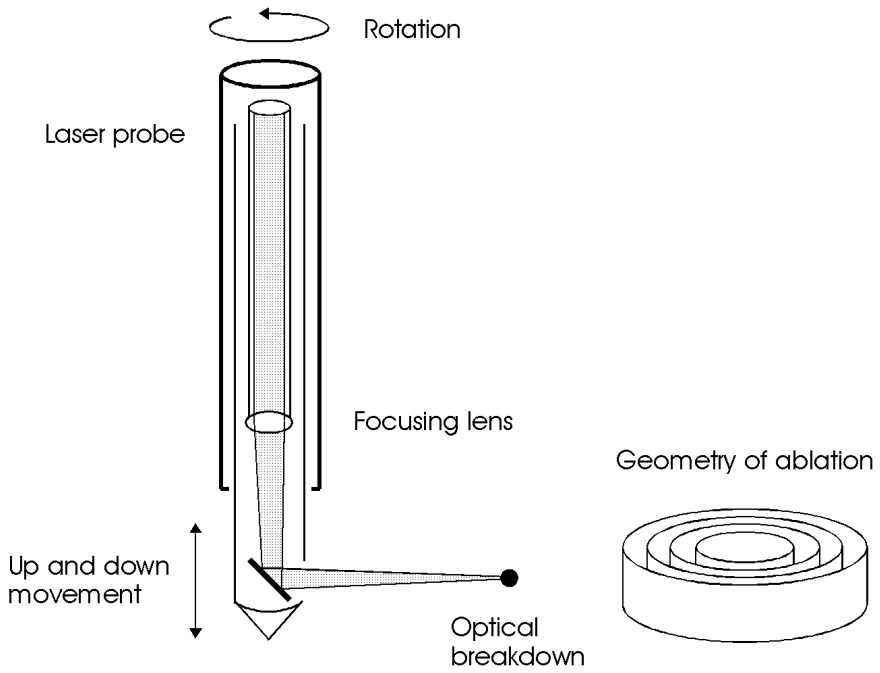
Fig. 4.55. Schematic drawing of laser probe

Laser probe

Blood
vessel

Plasma-induced
ablation

Detection and
coagulation of
blood vessels

50 mm
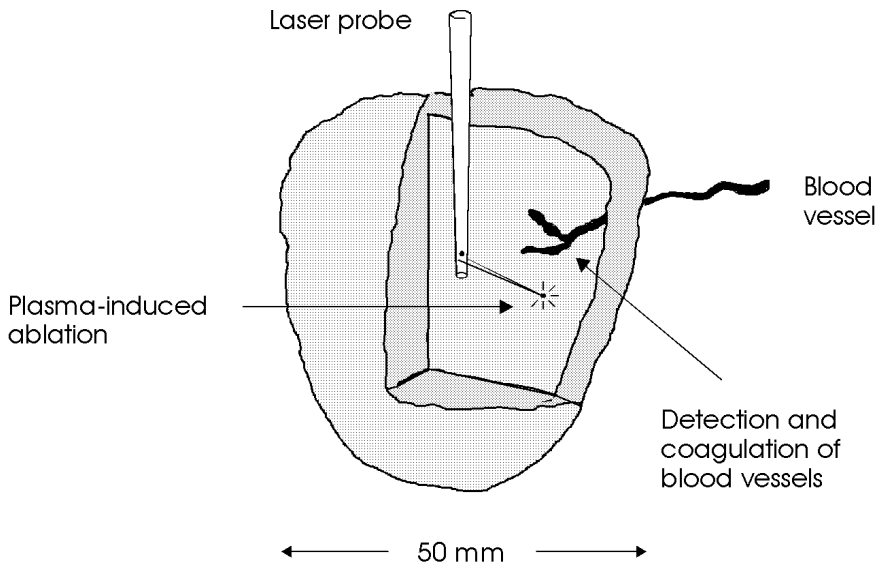
Fig. 4.56. Topology of tumor ablation

It should be mentioned that stereotactic neurosurgery is already a well-established clinical discipline. Stereotactic techniques are not only applied in combination with lasers but with alternative therapies, e.g. insertion of radioactive seeds (^{60}Co or ^{125}J) and high-frequency coagulation, as well. In general, any of these procedures alone might not lead to a complete necrosis of all tumor cells. In these cases, however, the stereotactic concept provides a useful combination of several treatment techniques by simply exchanging the surgical equipment mounted to the head ring of the patient. The principal advantages of stereotactic surgery, of course, are its high precision – within tenths of a millimeter – in aiming at the tumor and the ability to manage surgery with a tiny hole in the skull of less than 1 cm in diameter[8]. Stereotactic surgery thus certainly belongs to the favored treatments of minimally invasive surgery (MIS).

An exciting technique of sutureless microvascular anastomosis using the Nd:YAG laser was developed by Jain (1980). It is performed in some cases of cerebrovascular occlusive disease. During anastomosis, a branch of the superficial temporal artery is connected to a cortical branch of the middle cerebral artery. Typical laser parameters are powers of 18 W, focal spot sizes of 0.3 mm, and single exposure durations of 0.1 s. This method is considerably faster than conventional suture techniques, it does not induce damage to the endothelium of the vessel, and it can be performed on relatively small and/or deeply located blood vessels, as well. The mechanism of vessel welding is not completely understood but is believed to rely on heat-induced alterations in collagen of the vessel. First clinical results had already been reported by Jain (1984a), but a high rate of associated complications soon slowed down the initial euphoria. Later, Neblett et al. (1986) and Ulrich et al. (1988) combined the application of a Nd:YAG laser with conventional techniques of anastomosis, and they achieved more promising results. In blood vessels with diameters of 0.8–1.2 mm, neither short-term nor long-term complications occurred.

Spinal surgery is the other principal field of neurosurgical treatments. According to Jain (1984b), the CO_2 laser has proven to be useful in treating tumors of the spinal cord. Such tumors can be coagulated without severe complications. Ascher and Heppner (1984) have reported on the successful dissection of intramedullary gliomas of the spinal cord with a pulsed CO_2 laser. Moreover, some basic procedures concerning pain relief of the spinal cord can be performed with this laser. Spinal laser surgery is still in its infancy, and considerable progress is expected within the next few years when miniaturized surgical instruments become available, e.g. in the technique of laser-assisted nerve repair as already proposed by Bailes et al. (1989). The combination of highly sophisticated endoscopes and appropriate laser systems might then turn into a powerful joint venture.

---

[8] Conventional craniotomies usually require openings in the skull of at least 5 cm in diameter.

4.6 Lasers in Angioplasty and Cardiology

Angioplasty is concerned with the treatment of blood vessels which are narrowed by atherosclerosis[9]. The obstructions stem from the formation of an anorganic plaque inside the vessels which reduces or even completely suppresses the blood flow. The degree of a so-called *stenosis* is determined by

$$\% \text{ stenosis} = 100 \ \frac{\text{intimal area}}{\text{intimal area} + \text{lumen area}} \ ,$$

where the areas are obtained from a cross-sectional view of the vessel, the intima is the interior wall of the vessel, and the lumen is the space available for blood flow.

The promotion factors of plaques are not completely understood. The formation of a plaque might be favored at sites of a local vessel injury where cells capable of repairing the vessel wall tend to gather. If some of the secreted products of these cells are not carried away, a plaque is formed. After the cells have died, primarily anorganic concrements with a high content of calcium are left behind.

The non-surgical treatment of atherosclerosis was introduced by Dotter and Judkins (1964) when performing angioplasty of femoral arterial stenoses with a specially designed dilatation catheter. In the 1970s, Grüntzig (1978) and Grüntzig et al. (1979) modified this technique to enable its application in coronary arteries, i.e. the blood vessels supplying the heart itself. Atherosclerotic plaques inside these vessels are extremely life-threatening, since their obstruction necessarily induces myocardial infarction. *Percutaneous transluminal coronary angioplasty (PTCA)* has since been used in many patients with angina or acute myocardial infarction, and a large variety of balloon catheters is available today. In general, the method of PTCA has been widely accepted, and several reviews have already been published, e.g. by Grüntzig and Meier (1983) and Landau et al. (1994).

The main mechanisms by which PTCA increases the size of the vessel lumen are cracking, splitting, and disruption of the atherosclerotic plaque. Resorption of plaque material is also initiated by simply pushing it into the vessel wall. All these effects are evoked by inflation of a balloon placed inside the blood vessel. According to Waller (1983), balloon inflation may be deleterious, however, causing plaque hemorrhage, extensive dissection of the vessel wall, and thrombus formation. Therefore, the treatment needs to be performed extremely carefully and by X-ray control. Aspirin and heparin are usually administered to reduce the incidence of thrombosis.

Although PTCA is generally safe, some short-term and long-term complications do occur. Among the first, arterial dissection and intracoronary thrombosis are most severe. On the other hand, a recurrence of the original stenosis may take place even months after the treatment. This process of

---

[9] The term *arteriosclerosis* applies in arteries only.

so-called *restenosis* has been extensively studied by Lange et al. (1993) who also considered it as the "Achilles' heel" of coronary angioplasty. Serruys et al. (1988) reported on the occurrence of restenoses in 30 % of patients treated with PTCA. Restenoses are believed to be initiated by accidental injury of the vessel wall, resulting in the subsequent release of thrombogenic, vasoactive, and mitogenic factors. Endothelial damage, in particular, leads to the activation of macrophages and smooth muscle cells as stated by Austin et al. (1985). Thereby, growth factors are released which in turn may promote their own synthesis. Thus, a self-perpetuating process is initiated which is associated with a thickening of the intima, i.e. the interior part of the vessel wall. Finally, the vessel is obstructed again. Since the occurrence of these restenoses is not predictable, extensive follow-up studies are usually performed. According to Hombach et al. (1995), there is a slight decrease in the probability of restenoses when implanting specially designed mechanical stents inside the vessel wall immediately after balloon dilatation.

Beside PTCA, other surgical treatments are available in cases of coronary arteriosclerosis. These are *bypass surgery*, *atherectomy*, and *high-frequency rotational coronary angioplasty (HFRCA)*. Among these, only bypass surgery is performed during complete anesthetization. It is a very complicated type of surgery, since the chest must be opened and the heart beat is interrupted. Atherectomy is a more rigorous version of PTCA, where the plaque is additionally planed away by means of mechanical abrasion. Finally, in HFRCA, a miniaturized mechanical drill called a rotablator is used for vessel recanalization as described by Tierstein et al. (1991).

First experiments regarding laser angioplasty were performed by Macruz et al. (1980), Lee et al. (1981), Abela et al. (1982), and Choy et al. (1982). While these in vitro studies left no doubt that laser light could ablate atherosclerotic plaque, it was quite uncertain whether such a treatment could be transferred to in vivo surgery. Choy et al. (1984) and Ginsburg et al. (1985) were the first to try clinical laser angioplasties. Laser light was applied to the plaque by means of optical fibers. However, only thermally acting lasers – i.e. argon ion, CO_2, and Nd:YAG lasers – were investigated at that time which induced severe thermal injuries such as extensive coagulation, necrosis of vascular tissue, and perforation of the vessel wall. In addition, mechanical perforations often occurred due to the bare distal end of the optical fibers. All these complications turned out to be extremely critical when applying laser angioplasty to coronary arteries as initially suggested by Selzer et al. (1985) and Sanborn et al. (1986).

It was Hussein (1986) who developed a novel tip design, the so-called *hot tip*. It consists of a simple metal cap which completely encloses the distal end of the fiber, thereby converting all laser energy to heat by means of absorption. Instead of using a tightly focused laser beam, plaques are removed by homogeneously distributed heat as shown in Fig. 4.57. Usually, CW argon ion lasers and Nd:YAG lasers are applied, although any kind of laser radiation

could be used which is absorbed by the metal cap. Detailed measurements of
the temperature distribution associated with various parameters were per-
formed by Labs et al. (1987). According to Cumberland et al. (1986), the
concept of using a hot tip diminishes the incidence of thermal perforations
to a degree that makes it acceptable for many cases of peripheral angio-
plasty. However, the method of thermal angioplasty has led to considerable
controversy, as well. Other groups, e.g. Diethrich et al. (1988), observed the
occurrence of so-called vasospasm – i.e. thermally induced shrinkage of the
vessel wall – when using a hot tip applicator. In general, these vasospasms
are not predictable, and they can induce severe secondary obstructions.
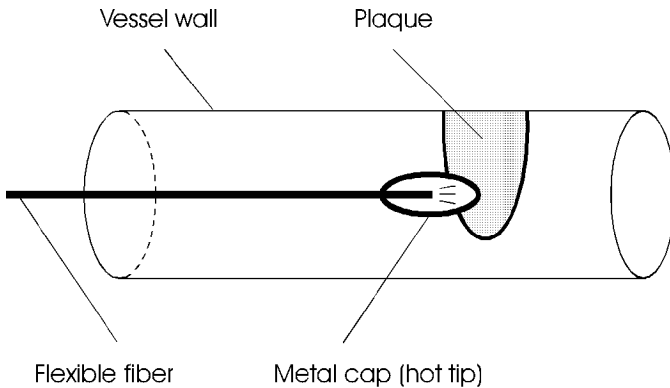
Fig. 4.57. Scheme of a laser-driven hot tip for vessel recanalization

The common denominator of the above concerns is that laser-induced
thermal injury is a virtually unavoidable by-product of CW lasers. Basic
improvement could not be achieved until moving from one laser–tissue in-
teraction to another. As discussed in Sect. 3.2, only pulsed lasers with pulse
durations shorter than $1\,\mu s$ provide nonthermal ablation.

Grundfest et al. (1985) first demonstrated that pulsed XeCl excimer
lasers are capable of performing efficient plaque ablations with only mini-
mal thermal injury of adjacent tissue. These studies were done shortly after
the description of the photoablative interaction mechanism by Srinivasan
and Mayne-Banton (1982). Thus, it was straightforward that researchers
also focused on other applications for excimer laser radiation. Unfortunately,
though, an unpredictable type of complication occurred as discussed below
which soon slowed down initial enthusiasm. Karsch et al. (1989) were the
first to report on clinical results of percutaneous coronary excimer laser angio-
plasty. In this study, thirty patients were treated with a 1.3 mm laser catheter
consisting of twenty $100\,\mu m$ quartz fibers. These fibers were located concen-
trically around a 0.35 mm thick flexible guide wire as shown in Fig. 4.58.
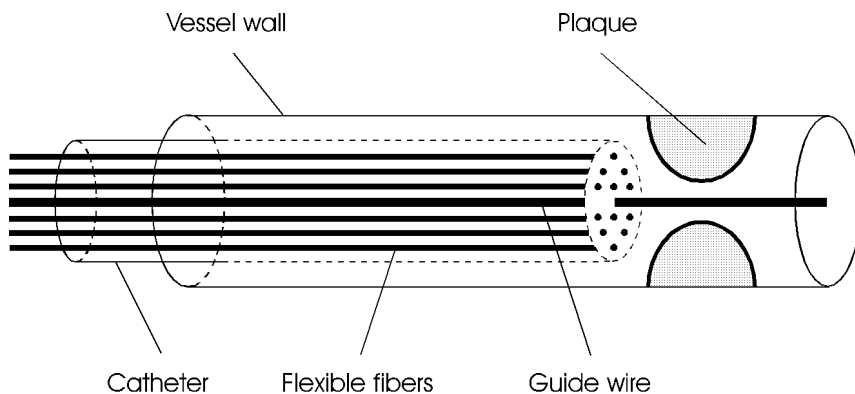
Fig. 4.58. Scheme of laser angioplasty for vessel recanalization

After moving the guide wire into the coronary artery, the catheter was guided into the correct position. The fibers were coupled to a XeCl excimer laser emitting at a wavelength of 308 nm and pulse durations of 60 ns. Typical energy densities of up to 5 J/cm^2 were applied. The mean percentage of stenosis fell from 85 % initially to 41 % immediately after laser treatment, and the primary success rate was as high as 90 %. In twenty patients, subsequent balloon dilatation was additionally performed. Perforations of the vessel wall did not occur in any of the patients. However, it was only shortly after when Karsch et al. (1991) published a second report admitting that one patient suddenly died two months after laser treatment. Postmortem histologic examination proved that a severe restenosis had occurred which had led to an acute myocardial infarction.

In Figs. 4.59a–b, two photographs are shown demonstrating the removal of atherosclerotic plaque with a XeCl excimer laser. For this ablation, Hanke et al. (1991) have applied pulse durations of 60 ns at a repetition rate of 20 Hz. An enlargement of the plaque itself is captured in Fig. 4.59a. On the right half of the picture shown in Fig. 4.59b, parts of the plaque have already been removed without injuring the vessel wall.

Today, it is well accepted that restenoses are extremely pronounced following excimer laser angioplasty. Their occurrence can be attributed to an enhanced proliferation of smooth muscle cells as has been demonstrated by Hanke et al. (1991). Most of these cells undergo DNA synthesis during two weeks after laser treatment, resulting in intimal thickening within the first four weeks. Obviously, the mechanism of photoablation is more stimulating than only mechanical cracking or abrasion. Thus, even though photoablation is a rather gentle technique for removing plaques, its long-term effects forbid its use for the purpose of vessel recanalization. Therefore, excimer laser angioplasty is generally being rejected today, and it is rather doubtful whether it will ever gain clinical relevance.
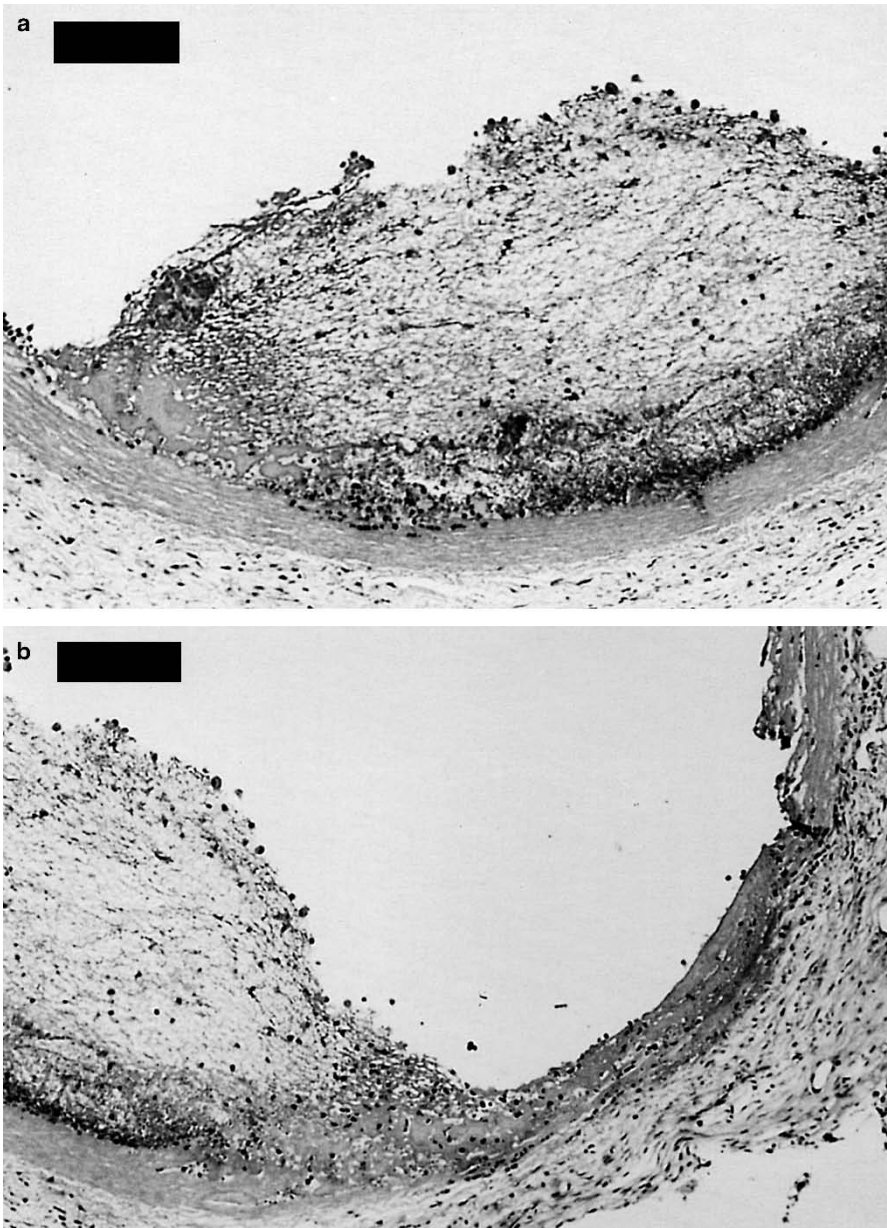
Fig. 4.59. (a) Histologic section of atherosclerotic plaque inside a blood vessel (bar: 150 µm). The vessel wall is located at the *bottom* of the picture. **(b)** Ablation of atherosclerotic plaque with a XeCl excimer laser (pulse duration: 60 ns, repetition rate: 20 Hz, bar: 150 µm, plaque: *left*, ablation: *right*). Photographs kindly provided by Dr. Hanke (Tübingen)

Meanwhile, other laser types have also been investigated concerning their application in angioplasty and cardiology. One of them is the Ho:YAG laser which has been studied in detail by Hassenstein et al. (1992). However, an extensive increase in intimal thickening was observed within the first six weeks after laser treatment. And, again, the proliferation of smooth muscle cells seems to be responsible for this effect. Thus, the clinical use of holmium laser angioplasty appears to be extremely limited.

More promising are CO_2 laser systems which can be used to create additional channels for the blood supply of the heart. These channels originate from the epicardium, i.e. the periphery of the heart, and remain open after laser treatment. This technique is called *transmyocardial laser revascularization (TMLR)* and was initially proposed by Mirohseini et al. (1982). Shortly after, first clinical experiences were reported by Mirohseini et al. (1986). Yano et al. (1993) have confirmed the effect of revascularization. Other investigators, though, could not verify their results, e.g. Whittaker et al. (1993). Recently, Horvath et al. (1995) were able to judge treatment effects by measuring the local contractility of the heart muscle. They concluded that acute infarcts treated by TMLR show improved contractility both in the short- and long-term. Moreover, they observed diminished areas of necrosis. However, further studies regarding blood flow and recovery need to be performed prior to the general acceptance of TMLR.

Even if therapeutic laser treatments of blood vessels should never become a safe procedure, laser diagnostics will always play a significant role in angioplasty and cardiology. Apart from X-ray and ultrasound angiography, Doppler angiography and laser endoscopy are very sensitive techniques. A typical example of a laser endoscope is shown in Fig. 4.60. Visible laser radiation is emitted from the distal end of a flexible fiber and illuminates the area of interest. Modern engineering science has meanwhile enabled the design of extremely miniaturized and highly sophisticated laser endoscopes.
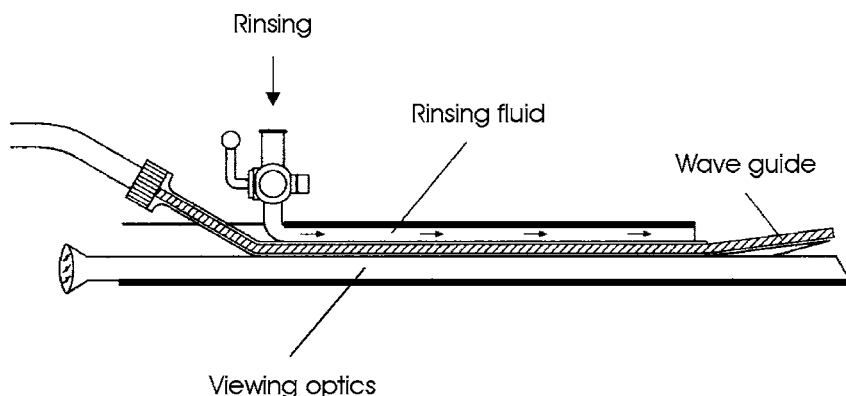
Fig. 4.60. Scheme of laser endoscope for angioplasty

4.7 Lasers in Dermatology

In dermatology, thermal effects of laser radiation are commonly used, especially coagulation and vaporization. Since the optical parameters of skin, i.e. absorption and scattering, are strongly wavelength-dependent, various kinds of tissue reaction can be evoked by different laser systems. In clinical practice, mainly five types of lasers are currently being used: argon ion lasers, dye lasers, CO_2 lasers, Nd:YAG lasers, and ruby lasers.

A schematic cross-section of the human skin is given in Fig. 4.61. The skin grossly consists of three layers: *epidermis*, *dermis*, and *subcutis*. The outer two layers – epidermis and dermis – together form the *cutis*. The epidermis contains so-called keratocytes and melanocytes which produce keratin and melanin, respectively. Both keratin and melanin are important protective proteins of the skin. Most of the dermis is a semi-solid mixture of collagen fibers, water, and a highly viscous gel called ground substance. The complex nature of the skin creates a remarkable tissue with a very high tensile strength which can resist external compression but remains pliable at the same time. Blood vessels, nerves, and receptors are primarily located within the subcutis and the dermis.
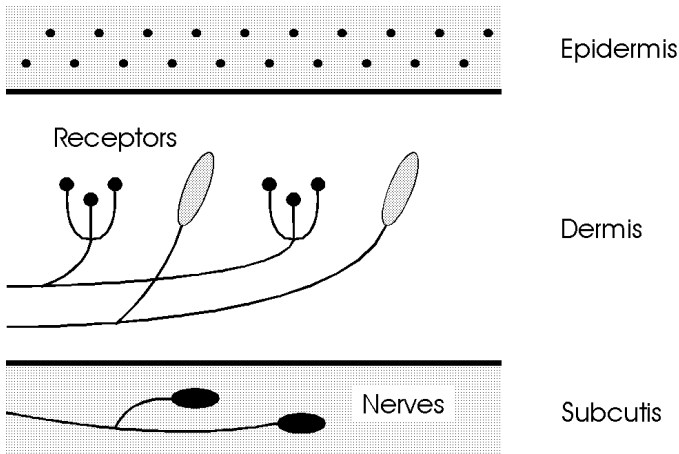
Fig. 4.61. Cross-section of human skin

On a microscopic scale, the air–skin interface is quite rough and therefore scatters incident radiation. Absorption of light by chromophores such as hemoglobin or melanin give skin its unique color. Optical scattering by collagen fibers in the ground substance largely determines which fraction of incident light penetrates into connective tissues. Detailed studies regarding the optical parameters of skin were performed by Graaff et al. (1993b).

Radiation from the argon ion laser is strongly absorbed by hemoglobin and melanin as already illustrated in Fig. 2.4. This laser is thus predestined for superficial treatments of highly vascularized skin. Apfelberg et al. (1978) and Apfelberg et al. (1979a) investigated laser-induced effects on various abnormalities of the skin. The most frequent indications for the application of argon ion lasers are given by port wine stains (*naevi flammei*). Earlier methods of treating these malformations – e.g. cryotherapy, X-ray, or chemical treatment – had failed, and patients were advised to accept their misery. The idea of removing port wine stains with argon ion lasers has led to the most significant progress of lasers in dermatology so far. The treatment itself requires a lot of patience, since several sessions are necessary over a period of up to a few years. The faster the treatment is to come to an end, the higher is the probability for the occurrence of scarring. However, "patient" patients are usually rewarded with an acceptable outcome. In Figs. 4.62a–b, two photographs of the pre- and postoperative states of a laser-treated port wine stain are shown.

Treatment of port wine stains with argon ion lasers is usually performed in several sessions. First, a small test area of approximately $4\,\mathrm{mm}^2$ is irradiated. During this test, a suitable laser power is determined by gradually increasing it until the skin visibly pales. According to Dixon and Gilbertson (1986) and Philipp et al. (1992), laser powers of 2–5 W are applied during an exposure time of 0.02–0.1s. Immediately after laser exposure, inflammation of the skin frequently occurs. After four weeks, the test area is checked for recanalization and scarring. And after another four weeks, a second test area is treated. If both tests lead to acceptable results, the whole stain is exposed. Multiple exposures of the same area should be avoided in any case. Laser treatment may be repeated after a few years, but it is advisable to choose pulsed dye lasers for the second time. Haina et al. (1988) did not recommend treatment of patients up to 16 years of age, since otherwise severe scarring might occur. Laser radiation is usually applied by means of a flexible handpiece. In the treatment of facial stains, the eyes of both patient and surgeon must be properly protected. One disadvantage of treating port wine stains with argon ion lasers is that it is rather painful to the patient. Depending on the location and spatial extent of the stain, treatment is performed during either local or complete anesthetization.

Less painful and probably even more efficient is the treatment of port wine stains with dye lasers. Although quite expensive, these machines have recently gained increasing significance in dermatology, especially in the treatment of port wine stains and capillary hemangiomas. Detailed studies were reported by Morelli et al. (1986), Garden et al. (1988), and Tan et al. (1989). Frequently, Rhodamine dye lasers are used which emit radiation at wavelengths in the range 570–590 nm. Typical pulse durations of 0.5 ms and energy densities of 4–$10\,\mathrm{J/cm}^2$ have been recommended. About 20–60s after laser exposure, the color of the treated skin turns red, and after another few

Fig. 4.62. (a) Preoperative state of a port wine stain. (b) Postoperative state of the same stain after several treatments with an argon ion laser (pulse duration: 0.3 s, power: 2.5 W, focal spot size: 2 mm). Photographs kindly provided by Dr. Seipp (Darmstadt)

minutes livid blue. Although pain is less pronounced as with argon ion lasers, patients frequently talk of triple pain perception: mechanical impact during the light flash, stabbing pain shortly afterwards, and finally a longer lasting heat wave within the skin. The irradiated area itself might be irritating for several days. One major advantage of treating port wine stains with dye lasers is that this procedure can be successfully performed among children as reported by Tan et al. (1989).

The basic mechanism by which pulsed laser radiation can cause selective damage to pigmented structures in vivo has been termed *selective photothermolysis* and was thoroughly described by Anderson and Parrish (1983). It requires the presence of highly absorbing particles, e.g. pigments of the skin. Extensive experimental and theoretical studies were recently performed by Kimel et al. (1994) and van Gemert et al. (1995). With their results, treatment of port wine stains will be further improved in the near future.

In dermatology, the CO_2 laser is used for tissue vaporization. Compared to the conventional scalpel, it offers the possibility of precise tissue removal without touching the tissue. Thus, feeling of pain is significantly reduced. External ulcers and refractory warts are common indications. In warts, however, deep lesions should be performed to reduce the probability of recurrence.

Recently, argon ion and CO_2 lasers have also gained attention in efficiently removing tattoos. Clinical studies were reported by Apfelberg et al. (1979b) and Reid and Muller (1980). Today, ruby lasers are commonly used for tattoo removal as stated by Scheibner et al. (1990) and Taylor et al. (1990). Indeed, good results can be obtained, although they do depend on the dyes used in the tattoo. It is extremely important that all dye particles are removed during the same session. In Figs. 4.63a–b, two photographs are shown which prove the efficiency of laser-induced tattoo removal.

Radiation from the Nd:YAG laser is significantly less scattered and absorbed in skin than radiation from the argon ion laser. The optical penetration depth of Nd:YAG laser radiation is thus much larger. According to Seipp et al. (1989), major indications for Nd:YAG laser treatments in dermatology are given by deeply located hemangiomas or semimalignant skin tumors. However, argon ion and CO_2 lasers should never be replaced by Nd:YAG lasers when treating skin surfaces.

Dermatology is one of the few medical disciplines where biostimulative effects of laser radiation have been reported. Positive stimulation on wound healing is one of the current topics of controversy as discussed in Sect. 3.1. A considerable number of papers has been published, but most of the results could not be reproduced, and initial claims could thus not be verified. Moreover, the principal mechanisms of biostimulation have not yet been understood. In general, one should be very careful when using laser radiation for such purposes, especially when applying so-called "soft lasers" with extremely low output powers which most probably do not evoke any effect at all other than additional expenses according to Alora and Anderson (2000).

Fig. 4.63. (a) Preoperative state of a tattoo. **(b)** Postoperative state of the same tattoo after six complete treatments with an argon ion laser (pulse duration: 0.3 s, power: 3 W, focal spot size: 0.5 mm). Photographs kindly provided by Dr. Seipp (Darmstadt)

4.8 Lasers in Orthopedics

Progress in surgical medicine is often related to an improved technique of performing *osteotomies*, i.e. bone excisions. Standard tools in orthopedics are saws, milling-machines and mechanical drills. All of them operate in contact mode and possibly induce severe mechanical vibrations and hemorrhage. It is thus straightforward to ask whether lasers might represent a considerable alternative in orthopedic surgery.

Bone fulfills three major functions: mechanical support of the body, protection of soft tissues, and supply of minerals and blood cells. The hardness of bone results from a complex structure of hydroxyapatite, water, soluble agents, collagen, and proteins. The chemical composition of bone is listed in Table 4.5. The high water content is responsible for strong absorption of infrared radiation. Therefore, CO_2, Er:YAG, and Ho:YAG lasers are predestined for the efficient treatment of bone.

Table 4.5. Mean composition of human bone

Matter	Percentage	Constituent
Anorganic	$50-60\,\%$	Hydroxyapatite
	$15-20\,\%$	Water
	$5\,\%$	Carbonates
	$1\,\%$	Phosphates
Organic	$20\,\%$	Collagen
	$1-2\,\%$	Proteins

In the 1970s, Moore (1973), Verschueren and Oldhoff (1975), and Clayman et al. (1978) reported on osteotomies performed with CO_2 lasers. Extensive studies on bone healing were published by Gertzbein et al. (1981) and Pao-Chang et al. (1981). All researchers agreed on a delayed healing process compared with conventional osteotomies. Thermal damage of the bone rim is exclusively made responsible for this time delay. Detailed data on the ablation characteristics were given by Kaplan and Giler (1984) and Forrer et al. (1993). The ablation curves of fresh and dried bone obtained with the CO_2 laser are illustrated in Fig. 4.64a. From the above, we could conclude that CO_2 lasers always evoke severe thermal side effects in bone. This statement, however, is not generally true. Forrer et al. (1993) have also demonstrated the potential of CO_2 lasers for bone ablation with very little thermal damage. When selecting the laser transition at $9.6\,\mu m$, a pulse duration of $1.8\,\mu s$, and an energy density of $15\,J/cm^2$, they found thermally altered damage zones of 10–$15\,\mu m$ only. In this case, both wavelength and pulse duration play a significant role. First, the absorbance of bone at $9.6\,\mu m$ is higher than at $10.6\,\mu m$. Second, shorter pulse durations tend to be associated with less thermal damage as already discussed in Sect. 3.2.
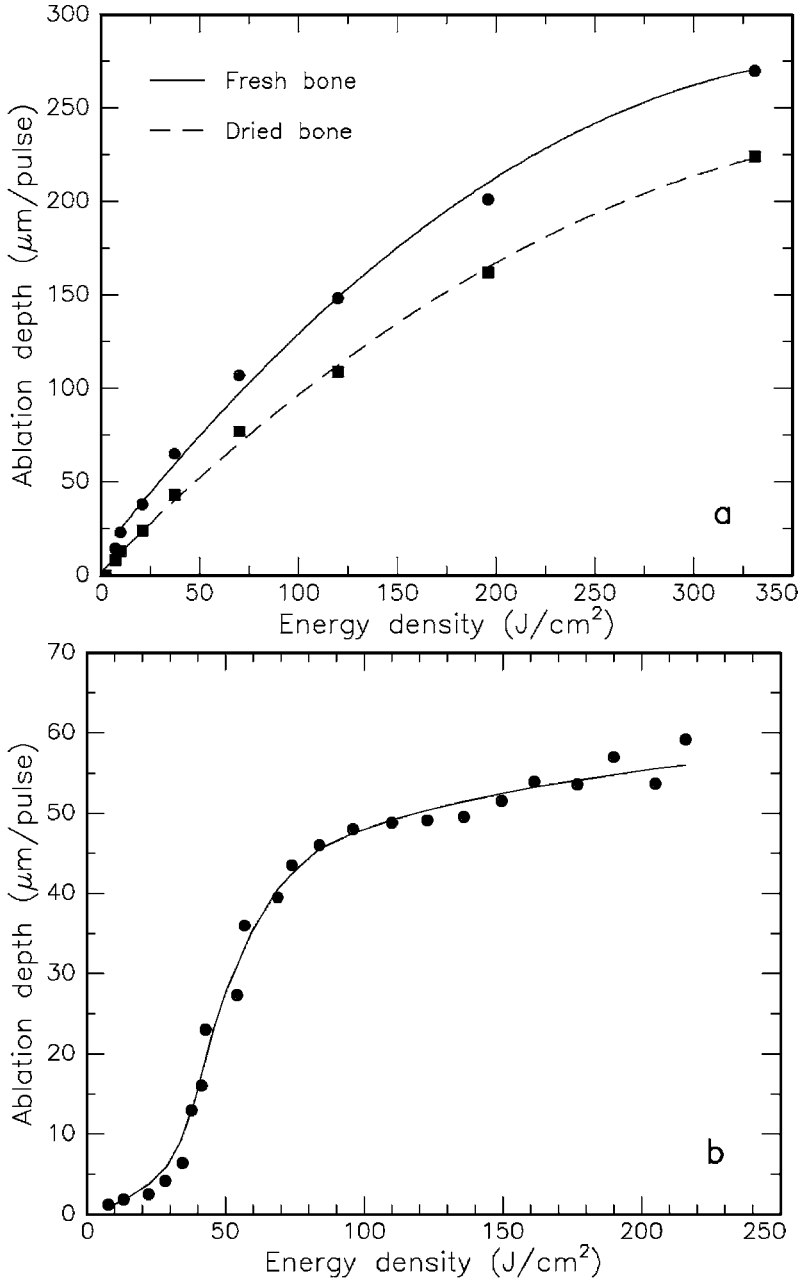
Fig. 4.64. (a) Ablation curves of fresh and dried bone obtained with a CO_2 laser (pulse duration: 250 μs, wavelength: 10.6 μm). Due to its higher water content, fresh bone is ablated more efficiently. Data according to Forrer et al. (1993). **(b)** Ablation curve of bone obtained with an Er:YAG laser (pulse duration: 180 μs, wavelength: 2.94 μm). Data according to Scholz and Grothves-Spork (1992)

In the 1980s, research focused on laser radiation at a wavelength of approximately 3 μm which is strongly absorbed by water. For instance, Wolbarsht (1984) compared the effects induced by CO_2 lasers at 10.6 μm and HF* lasers[10] at 2.9 μm with each other. From his observations, he concluded that the latter wavelength is better suited for orthopedic applications. Similar results were published by Izatt et al. (1990). Unfortunately, though, HF* lasers are very unwieldy machines. Walsh and Deutsch (1989), Nelson et al. (1989a), and Gonzales et al. (1990) reported on the application of compact Er:YAG lasers at a wavelength of 2.94 μm. They stated that this radiation efficiently ablates both bone and cartilage. The ablation curve of bone obtained with the Er:YAG laser is illustrated in Fig. 4.64b.

Another promising laser in orthopedics is the Ho:YAG laser which emits at a wavelength of 2.12 μm. Nuss et al. (1988), Charlton et al. (1990), and Stein et al. (1990) have investigated acute as well as chronic effects of bone ablation with this laser. Its major advantage is that its radiation can be efficiently transmitted through flexible fibers. However, thermal effects are significantly enhanced compared to those induced by Er:YAG lasers at a wavelength of 2.94 μm as observed by Romano et al. (1994). They found that thermal damage is extremely pronounced when applying 250 μs pulses from a Ho:YAG laser. At an incident energy density of 120 J/cm^2, a thermal damage zone of roughly 300 μm is determined. On the other hand, pulses from an Er:YAG laser are associated with very little thermal damage. At an energy density of 35 J/cm^2, a damage zone of only 12 μm is estimated. The corresponding histologic sections are shown in Fig. 4.65a–b. In the case of the Er:YAG laser, a lower energy density was chosen to obtain a similar ablation depth as with the Ho:YAG laser. One potential application field of erbium lasers is microsurgery of the stapes footplate in the inner ear. This treatment belongs to the discipline of otorhinolaryngology, and it will therefore be addressed in Sect. 4.10.

Due to their high precision in removing tissues, excimer lasers have also been proposed for the ablation of bone material, e.g. by Yow et al. (1989). However, it was soon observed that their efficiency is much too low to justify their clinical application. Moreover, osteotomies performed with XeCl lasers at 308 nm are associated with severe thermal damage as reported by Nelson et al. (1989b). As in the case of CO_2 laser radiation, these thermal effects are believed to be responsible for the manifest delay in healing of the laser-induced bone excisions.

An interesting approach to determine laser effects on bone has recently been reported by Barton et al. (1995) and Christ et al. (1995). By using a confocal laser scanning microscope, they were able to analyze ablation rate and morphology as a function of incident pulse energy from a Ho:YAG laser. They concluded that scattering is a dominant factor in the interaction of Ho:YAG laser radiation and bone.

---

[10] Hydrogen fluoride lasers.
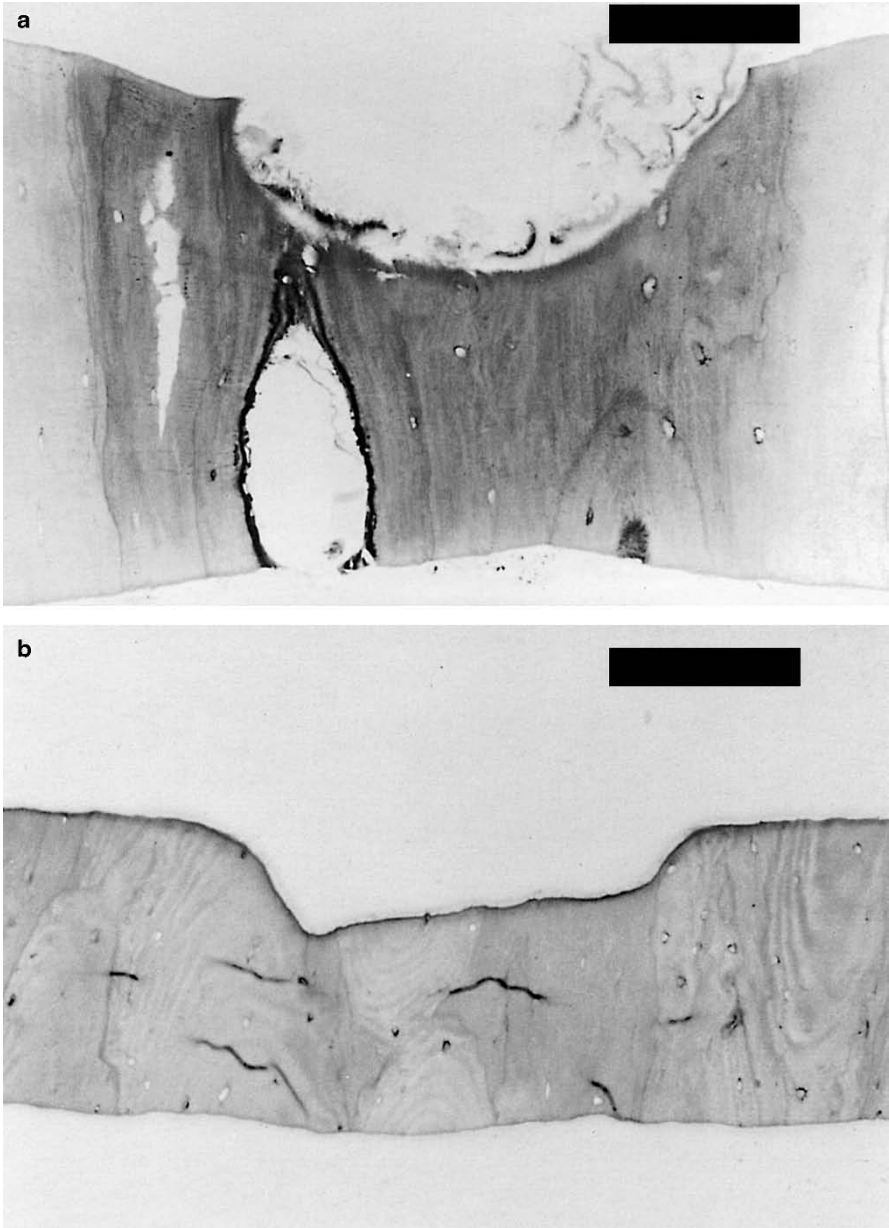
Fig. 4.65. (a) Histologic section of bone after exposure to a Ho:YAG laser (pulse duration: 250 μs, energy density: 120 J/cm², bar: 100 μm). (b) Histologic section of bone after exposure to an Er:YAG laser (pulse duration: 250 μs, energy density: 35 J/cm², bar: 200 μm). Photographs kindly provided by Dr. Romano (Bern)

Another discipline for laser applications within orthopedics is arthroscopy. Preliminary results regarding laser *meniscectomy*, i.e. the treatment of the meniscus, have already been reported by Glick (1981) and Whipple (1981) when using Nd:YAG and CO_2 lasers, respectively. At that time, though, suitable delivery systems were not available. Moreover, the CW mode of these lasers led to unacceptable thermal damage. Katsuyuki et al. (1983) and Bradrick et al. (1989) applied Nd:YAG lasers in arthroscopic treatment of the jaw joint. Significant improvements were not achieved until O'Brien and Miller (1990) made use of specially designed contact probes consisting of ceramics. Limbird (1990) pointed out the necessity of blood perfusion measurements after surgery. Major limitations for all infrared lasers in arthroscopic surgery arise from the optical delivery system. Transmission through flexible fibers can be regarded as a mandatory requirement for an efficient surgical procedure. Therefore, CO_2 lasers will never gain clinical relevance in arthroscopic treatments.

A new era of laser arthroscopy began with the application of holmium and erbium lasers. Trauner et a. (1990) reported promising results when using the Ho:YAG laser for the ablation of cartilage. Recently, Ith et al. (1994) have investigated the application of a fiber-delivered Er:YSGG laser emitting at a wavelength of $2.79\,\mu m$. The transmittance of novel zirconium fluoride (ZrF_4) fibers at this specific wavelength is satisfactory. Ith et al. (1994) have used fresh human meniscus from the knee joint which was obtained during surgery. They have observed a thermally damaged zone of $60\,\mu m$ when exposing the tissue in air to five laser pulses at a pulse energy of $53\,mJ$ and a pulse duration of $250\,\mu s$. On the other hand, when exposing the tissue through water at a slightly higher energy of $65\,mJ$, thermal damage extended to only $40\,\mu m$ close to surface and was even negligible elsewhere. In either case – whether exposed in air or through water – a crater depth of roughly $1\,mm$ was achieved. The surprising result of this study is that laser radiation at $2.79\,\mu m$ can be effectively used for tissue ablation, although it should be strongly absorbed by surrounding water. Thus, Ith et al. (1994) concluded that light – after exiting the fiber – is guided through a water-vapor channel created by the leading part of the laser pulse. The period during which this channel is open was found to be dependent on the duration of the laser pulse. For pulse durations of $250–350\,\mu s$, most of the laser energy is transmitted through the water-vapor channel to the target.

The experimental results mentioned above encourage the application of holmium and erbium lasers in arthroscopic surgery. Nevertheless, further investigations need to be performed regarding both thermal and mechanical side effects associated with laser exposure. From today's perspective, though, it is already obvious that arthroscopy belongs to those medical disciplines where minimally invasive techniques based on laser radiation will turn into unrenouncable surgical tools.

4.9 Lasers in Gastroenterology

Gastrointestinal diseases primarily include ulcers and tumors of the *esopha-gus*, *stomach*, *liver*, *gallbladder*, and *intestine*. The intestine further consists of the *jejunum*, *ileum*, *colon*, and *rectum*. According to the position of these organs, the gastrointestinal tract is subdivided into an upper and a lower tract. Both tracts are schematically illustrated in Fig. 4.66. Most intestinal tumors are reported to occur inside the colon or the rectum.
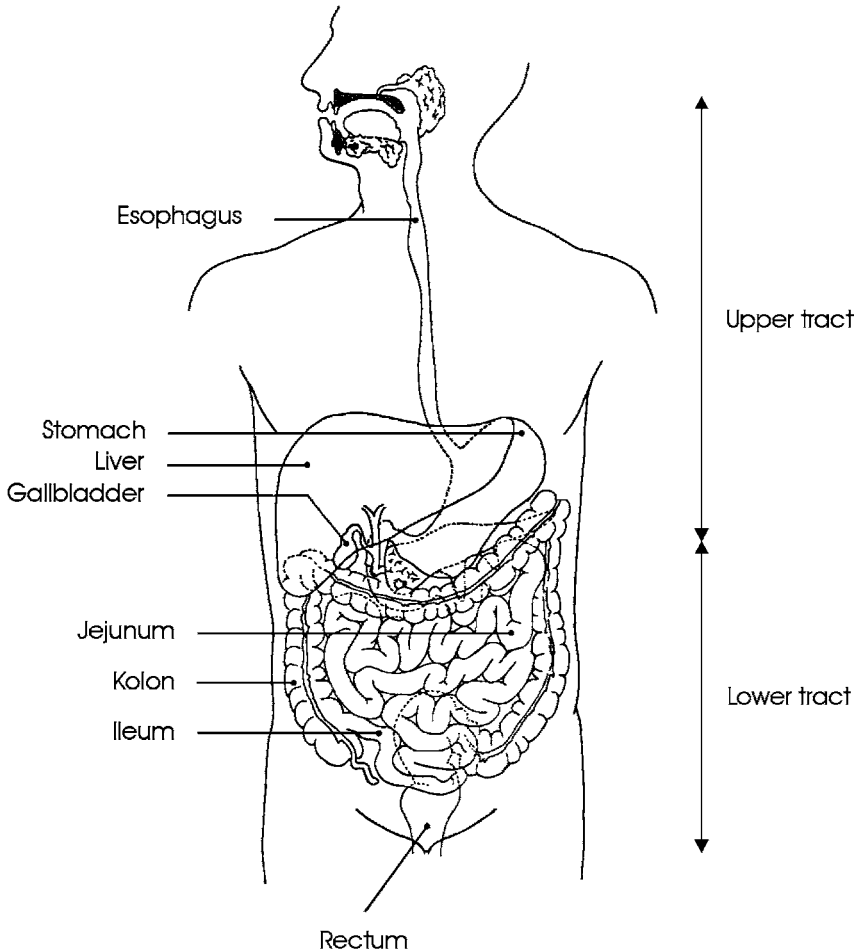
Fig. 4.66. Cross-section of the upper and lower gastrointestinal tracts. The upper tract includes esophagus, stomach, liver, and gallbladder, whereas the lower tract primarily consists of the intestine

In general, any kind of ulcer or tumor can be treated with lasers if it is accessible with endoscopic surgery. Ulcers and tumors tend to occupy additional space and are thus likely to induce severe stenoses. According to Sander et al. (1990), short and scarred stenoses of the lower tract are better suited for treatment than long and inflammable stenoses of the upper tract. If a tumor itself is no longer completely resectable due to its rather late detection – which unfortunately is quite often the case – laser application is restricted to a palliative treatment. The major concern of a palliative treatment is to provide an improved quality of the remaining life which also includes pain relief.

Gastroenterology is one of the major domains of the CW Nd:YAG laser. Only in photodynamic therapy are dye lasers applied. There exist mainly two indications for laser therapy: gastrointestinal hemorrhages and benign, malignant, or nonneoplastic[11] stenoses. Since the CW Nd:YAG laser is acting thermally, it can stop bleeding by means of coagulation. At higher power levels, i.e. in the vaporizing mode, it may serve in recanalization of stenoses. The application of other lasers was also investigated, e.g. the argon ion laser by Prauser et al. (1991), but was not associated with any significant advantages so far. The CO_2 laser is not suitable for clinical gastroenterology, since it is not transmitted through optical fibers which belong to the mandatory equipment of successful endoscopic surgery.

Stenoses of the esophagus are a common indication for laser treatment, since lasers can assist the surgeon in opening the stenosis. If even endoscopes cannot pass the stenosis, it must first be mechanically widened with specially designed dilatators. Afterwards, the stenotic tissue may be coagulated using a Nd:YAG laser and a flexible fiber. Frequently, quartz fibers with a diameter of 600 μm are used. The fiber is protected by a Teflon tube with diameters of 1.8–2.5 mm. CO_2 gas is provided to cool the fiber tip and to keep debris away from the tissue. During coagulation, the tissue significantly shrinks, thereby reducing the occupied lumen inside the esophagus. If the stenosis was induced by a tumor, the fiber should be placed inside the tumor – by endoscopic control – and the tumor is coagulated starting from its interior. Induced bleeding can be stopped by a temporary increase in laser power. Dilatation of the stenosis and coagulation of the tumor are usually performed during the same session. Up to 30 kJ may be necessary during one treatment as stated by Semler (1989). Remaining necrotic tissue is usually repelled during the next few days, resulting in a further widening of the available lumen of the esophagus.

Unfortunately, restenoses of the esophagus frequently occur after a few weeks. According to Bader et al. (1986), they can be efficiently prevented by a second treatment called *afterloading*. This treatment involves a radioactive source, e.g. ^{192}Ir, which is placed inside the esophagus for a few minutes by means of a computer-controlled probe. Between three and five of these

---

[11] Stenoses which are not related to tumor formation are called *nonneoplastic*.

afterloading treatments are normally performed starting approximately two weeks after laser coagulation. In malignant esophagus tumors, the mean survival rate is extremely low, since most of them are diagnosed at a very late stage. Treatment can then only be of a palliative character according to Fleischer and Sivak (1985), and *esophagectomy*, i.e. the complete or partial removal of the esophagus, must be performed. Afterwards, an artificial tube can be implanted.

Laser treatments of tumors belonging to the lower gastrointestinal tract were described by Hohenberger et al. (1986) and Kiefhaber et al. (1987). The conventional technique is called *cryotherapy*, since it induces tumor necrosis by freezing the tissue to temperatures of approximately $-180°$C. In contrast to laser and afterloading therapy, it can be performed only during a complete anesthetization of the patient. Especially among older patients, this is one of the major disadvantages of cryotherapy. On the other hand, laser therapy is associated with an enhanced formation of edema. However, such edema can be treated with proper medicamentation.

Nonneoplastic stenoses of the lower gastrointestinal tract are treated by applying 80–100 W of laser power to an optical quartz fiber and slowly moving this fiber backwards out of the stenosis. Thereby, 1–2 mm deep grooves along the stenosis are induced according to Sander et al. (1990). After 3–5 days the grooves have dilated to a permeable path, and endoscopic passage is possible without mechanical pressure. In extended and inflammated stenoses, several treatments may be necessary.

The first laser therapy in gastroenterology was performed in the case of a massive hemorrhage by Kiefhaber et al. (1977). Since then, several extensive studies have been reported, e.g. by Rutgeerts et al. (1982), Macleod et al. (1983), and Swain et al. (1986). In general, it can be summarized that all localized and acute hemorrhages are suitable for laser coagulation. Inside the rectum and stomach, powers of 50–70 W and 70–100 W, respectively, are applied. After a complete clearance of the bleeding source, the tissue is coagulated from a distance of 5–10 mm by performing circularly shaped movements of the laser beam. There is no time limit for this procedure. The operation is stopped by releasing a footpedal if the desired effect is achieved. Patients are normally supervised by intensive care for at least three days following laser treatment.

An improved technique for the laser treatment of ulcers or hemorrhages was developed by Sander et al. (1988). It is based on a combination of laser beam and water jet. The laser beam is guided through a water jet to the site of application. First results reported by Sander et al. (1989) have shown that – using this technique – the percentage of successful hemostatic treatments could be raised from 82 % to 93 %. Moreover, fewer emergency surgeries needed to be performed and less mortality was observed. Sander et al. (1990) added that this technique has proven to be useful for other kinds of tissue coagulation, as well.

Despite early expectations concerning the potential of lasers in gastroenterology, e.g. by Fleischer et al. (1982), they could only partially be fulfilled so far. It is not obvious that the Nd:YAG laser at a wavelength of $1.064\,\mu m$ provides the optimum radiation for gastrointestinal diseases. An extensive analysis of potential complications arising from the use of this laser was given by Mathus-Vliegen and Tytgat (1990). In the near future, alternative lasers with different wavelengths will certainly be investigated, as well. The surgical results obtained with these lasers must be compared to those achieved with the Nd:YAG laser. Most probably, not just one single laser will then prove to be best in the treatment of all diseases. There will rather be a variety of different lasers which – in combination with alternative treatments – should be used in specific cases.

One important branch of modern gastroenterologic treatment – which has not been addressed yet – is based on photodynamic therapy (PDT). The procedure of PDT has already been described in detail in Sect. 3.1. After injection of an appropriate photosensitizer and a time delay of approximately 48–72 hours, tumors of the gastrointestinal tract are exposed to a dye laser, e.g. a Rhodamine dye laser pumped with an argon ion laser. The clearance of the photosensitizer leads to a concentration gradient among benign and malignant tissue ranging from about 1:2 to 1:4. Meanwhile, several reports on PDT in gastroenterology have been published, e.g. by Barr et al. (1989), Barr et al. (1990), and Karanov et al. (1991). The success is inversely related to the tumor size at the time of treatment. According to Gossner and Ell (1993), tumors are curable only if their infiltration depths remain below 5–10 mm. Overholt et al. (1993) have shown that normal epithelium might then cover the interior of the esophagus again. The extent of a tumor is usually determined by ultrasound techniques. If a tumor is diagnosed at an early stage, more than 75 % of cases can be completely cured. In advanced cancer, the corresponding rate is less than 30 %. Tumors of the stomach are often more difficult to access for PDT due to wrinkles of the mucosa. Thus, treatments of the stomach are frequently associated with the application of higher energy doses. One major advantage of PDT is that fewer endoscopic sessions are usually required compared to treatments with the Nd:YAG laser. Hence, the overall duration of a PDT treatment is significantly shorter and easier to tolerate, as well.

In general, PDT is applied at early stages of cancer and in otherwise inoperable patients, e.g. if alternative methods are associated with a high risk for the patient. At advanced stages of esophagus cancer, PDT usually cannot provide a complete cure. However, it might significantly facilitate the act of swallowing. With the development of novel photosensitizers having a higher efficiency in the red and near infrared spectrum, additional applications of PDT might be indicated in the near future. Then, after careful evaluation of clinical studies, improved treatments characterized by even higher cure rates might be achievable.

4.10 Lasers in Otorhinolaryngology and Pulmology

Otorhinolaryngology is concerned with diseases of the *ear*, the *nose*, and the *throat*. So far, the most significant application of lasers in otorhinolaryngology aims at microsurgery of the *larynx*, e.g. in stenoses or laryngeal carcinoma. Stenoses of the larynx can be inherent or acquired. In either case, they are often associated with a severe impairment of the airway and should be treated immediately. Laryngeal carcinoma are the most frequent malignant tumors of the throat. The five major origins of these carcinoma are illustrated in Fig. 4.67. Diagnosis and treatment of laryngeal carcinoma are performed by means of a laryngoscope which consists of a rigid tube being connected to a surgical microscope. During treatment, the patient must be intubated as demonstrated in Fig. 4.68.
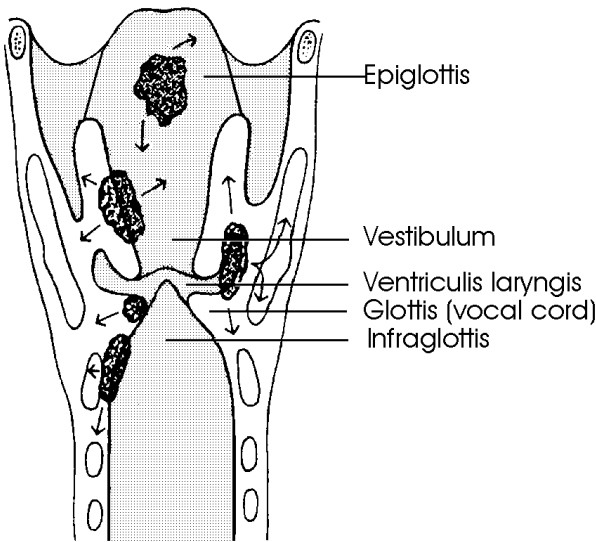
Fig. 4.67. Origins and directions of growth of laryngeal carcinoma

It has already been shown by Jako (1972) and Strong et al. (1976) that benign and malignant lesions of the glottis, i.e. the vocal cords, can be more saferly removed with the CO_2 laser rather than mechanically. In laryngeal carcinoma, a complete resection is ascertained if histopathology proves the absence of tumor cells in adjacent tissue. If the tumor is already at an advanced stage, however, laser therapy aims at a palliative treatment only. Complications arise when the laser treatment requires complete anesthetization of the patient, since the associated gases are inflammable. For a proper operation of the intubation tube, different materials are currently being investigated. Among these, metal tubes probably provide highest security.
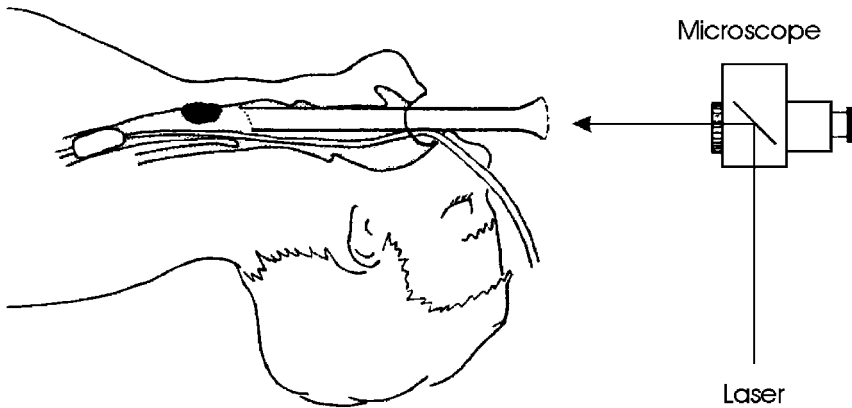
Fig. 4.68. Direct laryngoscopy with simultaneous intubation. Reproduced from Boenninghaus (1980) by permission. © 1980 Springer-Verlag

It was demonstrated by Holinger (1982) and Duncavage et al. (1985) that CO_2 lasers are superior to conventional therapy when treating laryngeal or subglottic stenoses. However, Steiner (1989) emphasizes that not all kinds of stenoses are equally indicated for laser treatment. In particular, large stenoses which extend over several centimeters in size should always be assigned to conventional surgery.

Major indications for laser treatment of the nose are highly vascularized tumors such as hemangiomas or premalignant alterations of the mucosa. The principal advantage of lasers is again their ability to simultaneously perform surgery and coagulate blood vessels. Lenz and Eichler (1984) and Parkin and Dixon (1985) have reported on argon ion laser treatments in vascular surgery of the nose. In proximal nose segments, Steiner (1989) suggests the application of a CO_2 laser which is connected to a surgical microscope. By means of tissue coagulation, even chronic nose-bleeding can be efficiently and safely treated.

Another very useful laser application in otolaryngology has been developed in the treatment of otosclerosis which is a bone disease of the inner ear. Otosclerosis usually affects the stapes shown in Fig. 4.69 and ultimately leads to its fixation. It is often associated with hearing impairment, because a movable stapes is necessary for the physiologic transport of sound to the cochlea. Two potential treatments are called *stapedectomy* and *stapedotomy*. In stapedectomy, the stapes footplate in the inner ear is mechanically removed and replaced by an artificial implant. In stapedotomy, a hole is drilled into the stapes to improve the propagation of sound to the oval window. Perforation of the stapes is achieved with either miniaturized mechanical drills or with suitable lasers and application units. Laser stapedotomy can be considered as a typical method of minimally invasive surgery (MIS).
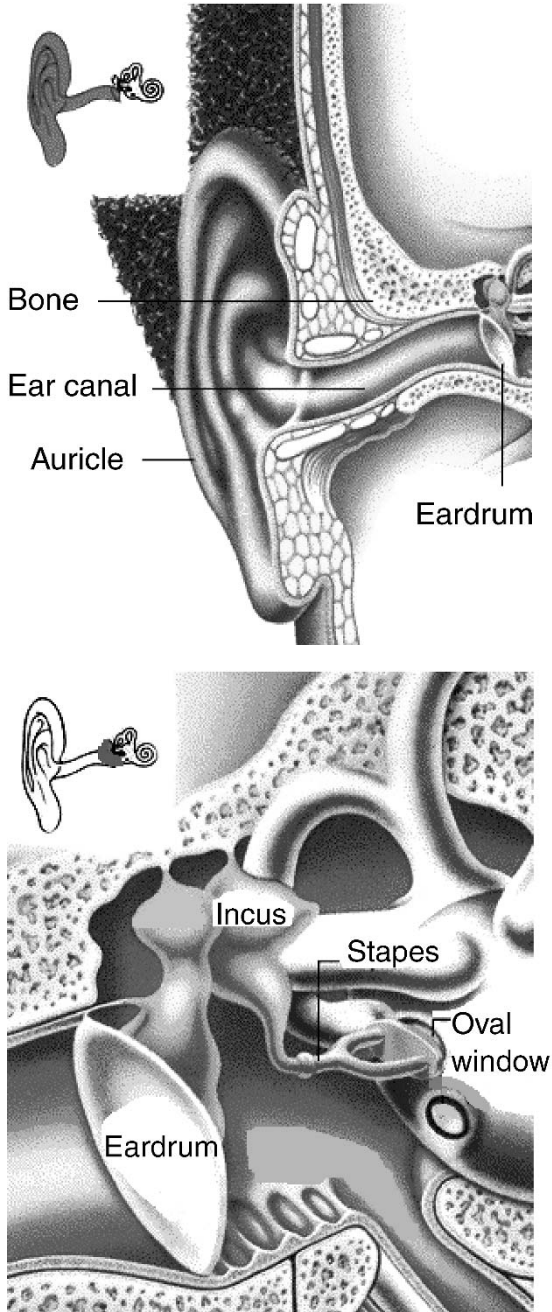
Fig. 4.69. Anatomy of outer and inner ear

Stapedotomy seems to be a predestined treatment for laser radiation, since it requires least mechanical damage. It is generally accepted that a noncontact method is certainly the best choice in preventing the inner ear structures from externally induced compression. Perkins (1980) and Gantz et al. (1982) performed the first stapedotomies with an argon ion laser. A few years later, Coker et al. (1986) investigated the application of a CO_2 laser for the same purpose. Finally, Lesinski and Palmer (1989) compared surgical results achieved with the CO_2 laser, argon ion laser, and a frequency-doubled Nd:YAG laser. The main disadvantage of radiation from the CO_2 laser is that it cannot be guided through optical fibers. On the other hand, radiation from argon ion or frequency-doubled Nd:YAG lasers is strongly absorbed only in highly pigmented tissue. The efficiency of these lasers in ablating cortical bone is thus rather weak. Due to the low absorption, their radiation might even induce severe lesions in adjacent tissue.

Recently, Frenz et al. (1994) and Pratisto et al. (1996) have studied stapedotomies performed with Er:YAG and Er:YSGG lasers, respectively. Radiation from erbium lasers combines the advantages of being strongly absorbed in bone and of being transmitted through zirconium fluoride (ZrF_4) fibers. In Figs. 4.70a–b, a perforation of the stapes is shown which was induced by only five pulses from an Er:YAG laser at a rather moderate fluence of only $10 \, \mathrm{J/cm^2}$. The edge of the perforation is very precise and does not indicate any mechanical damage. In Fig. 4.71, the ablation curve of cortical bone obtained with the Er:YSGG laser is shown. Due to the high ablation depths achieved with erbium lasers, only a few pulses are necessary to perforate the stapes. According to Pratisto et al. (1996), the ablation threshold was less than $5 \, \mathrm{J/cm^2}$.

Potential risks in laser-assisted stapedotomy evolve from either an excessive increase in temperature of the perilymph or too high pressures induced inside the cochlea of the inner ear. It was found by Frenz et al. (1994) that the temperature at the stapes increases by only less than $5\,^\circ\mathrm{C}$ if the power output of the Er:YAG laser is limited to $10 \, \mathrm{J/cm^2}$. In a specially designed ear model, the temperature increase in the perilymph was even negligible. The pressure inside the cochlea during the laser treatment is very important, since the ear is a very sensitive organ. Frenz et al. (1994) have measured pressure signals in their ear model using a PVDF foil as described in Sect. 3.5. The PVDF foil was located $3 \, \mathrm{mm}$ below the exposed area. The corresponding pressure data are presented in Fig. 4.72. Frenz et al. (1994) have compared these data with maximum tolerable sound pressures as published by Pfander (1975). They stated that erbium lasers permit a safe pressure level if their fluence is limited to $10 \, \mathrm{J/cm^2}$.

We conclude that laser-assisted stapedotomy has meanwhile become a considerable alternative to mechanical drills. Erbium lasers, e.g. Er:YAG or Er:YSGG lasers, are capable of performing safe and very precise stapedotomies with negligible thermal damage.
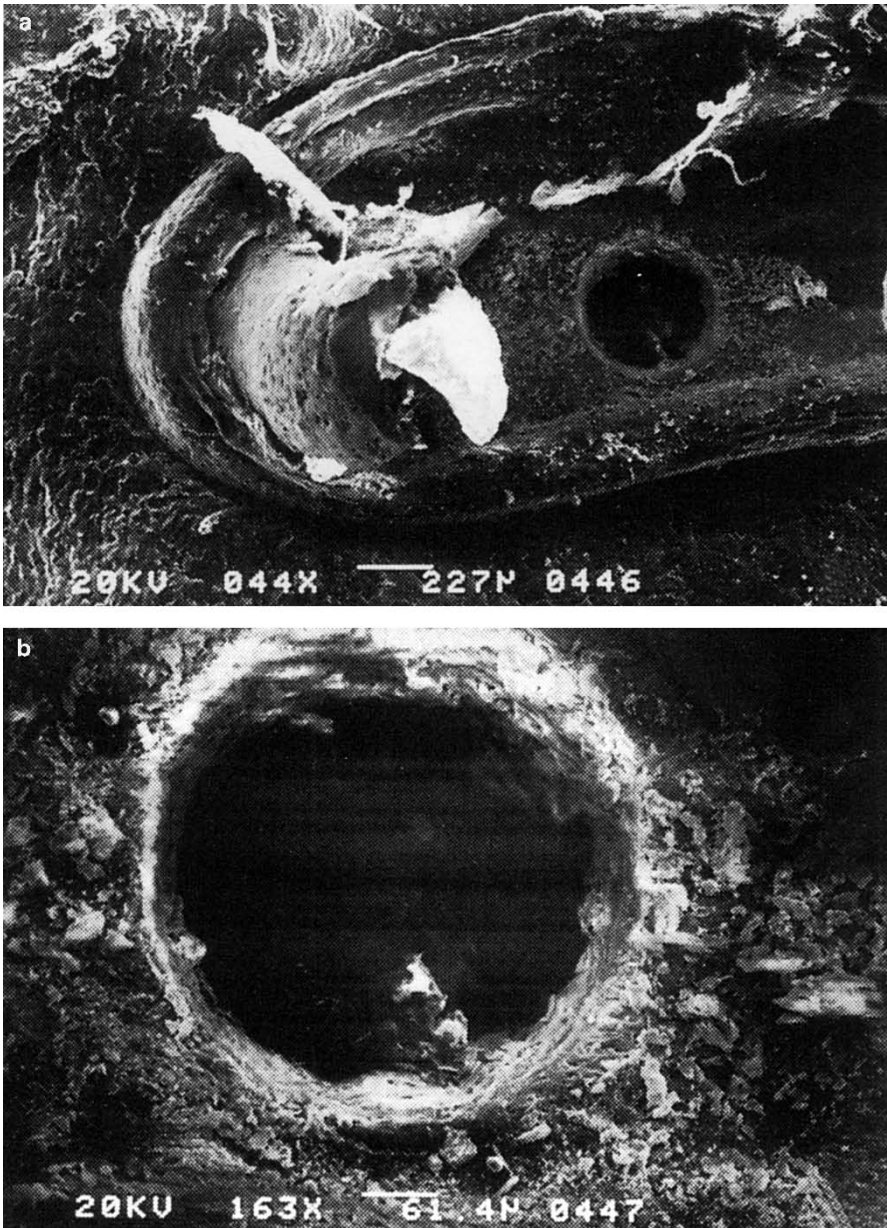
Fig. 4.70. (a) Stapedotomy performed with five pulses from an Er:YAG laser (pulse duration: 200 μs, fluence: 10 J/cm^2). **(b)** Enlargement of the perforation. Reproduced from Frenz et al. (1994) by permission. © 1994 Verlag Huber AG
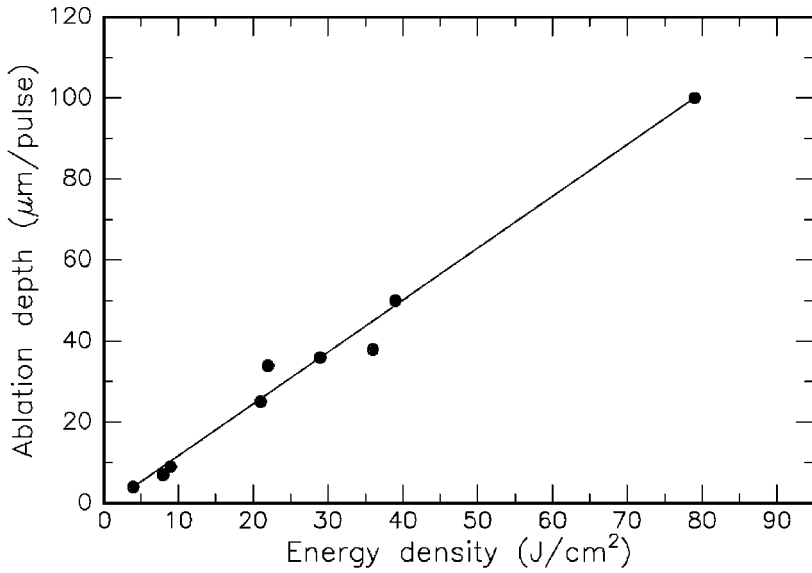
Fig. 4.71. Ablation curve of cortical bone obtained with an Er:YSGG laser (wavelength: 2.79 μm, pulse duration: 200 μs). Data according to Pratisto et al. (1996)
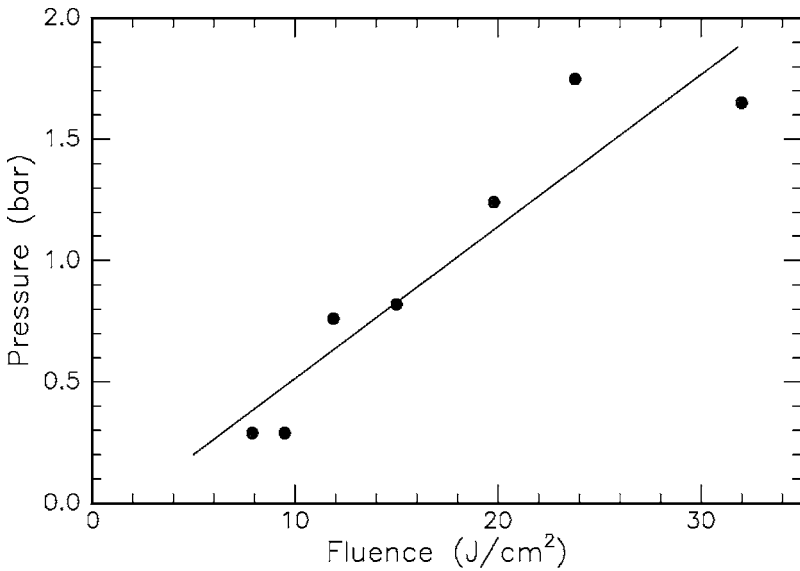
Fig. 4.72. Pressure in the perilymph of the inner ear during Er:YAG laser (wavelength: 2.94 μm, pulse duration: 200 μs) irradiation of the stapes footplate. Data according to Frenz et al. (1994)

   Pulmology is concerned with diseases of the lung. In the western civilized world, tracheobronchial tumors are the primary cause of death due to cancer. According to Macha (1991), only less than 6–8 % of patients survive the next five years after diagnosis, because the tumor is often diagnosed at a rather late stage. The resection of tracheobronchial tumors is conventionally performed with a rigid bronchoscope. Severe and life-threatening hemorrhage is often inevitable. Beside mechanical removal, electrocoagulation and cryotherapy are performed. Dumon et al. (1982) and Hetzel et al. (1985) have investigated the application of a Nd:YAG laser and a flexible fiber in the treatment of tracheobronchial lesions. Since the Nd:YAG laser provides the surgeon with the ability of immediate coagulation, the occurrence of severe hemorrhage can be significantly reduced. Moreover, Macha et al. (1987) have proposed a combined therapy of a radioactive source, e.g. ^{192}Ir, and laser radiation to improve the surgical result.

   In summary, the Nd:YAG laser is a valuable supplement in the therapy of tracheobronchial tumors, although it is usually limited to a palliative treatment. However, patients soon perceive pain relief during breathing. Further clinical studies with alternative lasers and sophisticated application units are badly needed. Preliminary results concerning photodynamic therapy in the treatment of lung cancer have already been published by Hayata et al. (1982). Meanwhile, this technique has been investigated in head and neck surgery, as well, e.g. by Feyh et al. (1990).

4.11 Questions to Chapter 4

Q4.1. During the treatment of hyperopia with PRK, the curvature of the anterior corneal surface must
A: be flattened.   B: remain unchanged.   C: be steepened.
Q4.2. Er:YAG lasers are not suitable for the treatment of caries because of
A: cytotoxicity.   B: low efficiency.   C: thermal effects.
Q4.3. Angioplasty with excimer lasers is likely to induce
A: atherosclerosis.   B: restenoses.   C: thermal injury.
Q4.4. In stapedotomy with Er:YAG lasers, the fluence should be limited to
A: $1\,\mathrm{J/cm^2}$.   B: $10\,\mathrm{J/cm^2}$.   C: $100\,\mathrm{J/cm^2}$.
Q4.5. The deepest layer of the skin is called
A: dermis.   B: epidermis.   C: subcutis.
Q4.6. Why is LASIK less sensitive to scattering effects than PRK?
Q4.7. Why is laser dentistry with picosecond or femtosecond pulses painfree?
Q4.8. What is the workhorse laser in gynecology?
Q4.9. How can BPH be treated optically?
Q4.10. What is the purpose of a stereotactic ring?